



Department of Neuroscience, Reproductive and Odontostomatologic Sciences

THESIS FOR DOCTORAL DEGREE (Ph.D.) IN NEUROSCIENCE

Re-arrangements of glutamatergic post-synaptic density transcripts after antipsychotics and add-on compounds administration in preclinical settings: translational implications for psychosis therapy and treatment resistance.

Dott.ssa Elisabetta Filomena Buonaguro, MD, Psychiatrist

Tutor: Prof. Andrea de Bartolomeis

SUMMARY

CHAPTER 1. Introduction

1. The rise and (partial) fall of the N-methyl-D-aspartate (NMDA) Receptor Hypofunction (NRH) hypothesis of schizophrenia pathophysiology
2. The dopamine-glutamate interplay and the Post-Synaptic Density (PSD) in psychosis
3. Current antipsychotic drugs and the challenge of non-response: translational implications from preclinical studies

CHAPTER 2. Aim of the Study

CHAPTER 3. Materials and Methods

CHAPTER 4. Re-arrangements of gene transcripts at glutamatergic synapses after chronic treatments by different doses of antipsychotics with distinct receptor profile

1. Rationale
2. Results

CHAPTER 5. Quantitative comparison of acute *versus* chronic antipsychotic treatments on the immediate early gene *Homer1a* expression profile

1. Rationale
2. Results

CHAPTER 6. Nicotine and caffeine modulate haloperidol-induced changes in postsynaptic density transcripts expression.

1. Rationale
2. Results

CHAPTER 7. Postsynaptic density protein transcripts are differentially modulated by minocycline alone or in add-on to haloperidol.

1. Rationale
2. Results

CHAPTER 8.

1. Discussion
2. Concluding remarks

Bibliography

LIST OF ABBREVIATIONS

AC, ACC	anterior cingulate cortex
AMPA receptor	α -amino-3-hydroxy-5-methyl-4-isoxazolepropionic acid receptors
ANOVA	Analysis of Variance
Arc	activity-regulated cytoskeleton-associated protein
ASE	asenapine
CAb	core of the nucleus accumbens
CAF	caffeine
cAMP	cyclic 3'-5' adenosine monophosphate
CP-DL	dorsolateral caudate-putamen
CP-DM	dorsomedial caudate-putamen
CP-VL	ventrolateral caudate-putamen
CP-VM	ventromedial caudate-putamen;
EVH1	Ena-VASP-homology domain
HAL	haloperidol
IC	insular cortex; MAC:
IP3	inositol trisphosphate
KET	ketamine
MAC, M2	medial agranular cortex
MAGUK	membrane-associated guanylyl kinase
MC, M1	motor cortex
MIN	minocycline
NIC	nicotine
NMDA receptor	N-methyl-D-aspartate receptor
NRH hypothesis	NMDA receptor hypofunction hypothesis
OLA	olanzapine
PCP	phencyclidine
PSD	post-synaptic density
ROIs	Regions of interest
SEM	standard error mean
SNK	Student-Newman-Keuls
SS	somatosensory cortex
SAb	shell of the nucleus
VEH	vehicle

CHAPTER 1

Introduction

Schizophrenia is a severe and chronic mental disorder with an incidence of about 0.3–1.0% in the human population (Howes and Kapur, 2009). Symptoms of schizophrenia include mainly positive symptoms (i.e. hallucinations and delusions), negative symptoms (i.e. blunted affect, poverty of speech, curbing of interest and social withdrawal), and cognitive deficits. The appearance of the disorder generally occurs during pubescence/young adulthood, and the time course of the disease is characterized by a series of repeated clinical deterioration periods (Weinberger and Harrison, 2011). Although the exact pathophysiology of the disease is still unknown, schizophrenia is believed to be a multifactorial disorder, with genetics, environmental, psychological, and social factors contributing to its etiology and clinical manifestations.

On the molecular level, in its more traditional postulation, the dopaminergic hypothesis of psychosis stated that putative subcortical hyperdopaminergy, stemming from over-activation of meso-striatal pathways, may cause productive psychotic symptoms, while a decreased function of the dopaminergic neurons belonging to the meso-cortico-limbic tract may explain the cognitive dysfunctions that are observed in schizophrenia (Kapur, 2004). The observation that early antipsychotic medications such as chlorpromazine and haloperidol shared a capacity to block dopamine D2 receptors corroborated this view. However, despite direct evidence supporting a dopaminergic dysfunction in schizophrenia, several neurotransmitter systems and functional networks within the brain have been found to be affected in this disorder, postulating that dopaminergic dysfunction may not necessarily be a primary phenomenon.

Indeed, abnormalities in glutamate neurotransmissions have nowadays been suggested as major,

albeit not unique, players in the pathophysiology of psychosis (de Bartolomeis et al., 2005; Iasevoli et al., 2014b; Javitt and Zukin, 1991; Konradi and Heckers, 2003; Laruelle et al., 2003; Seeman, 2009).

1.The rise and (partial) fall of the N-methyl-D-aspartate (NMDA) Receptor Hypofunction (NRH) hypothesis of schizophrenia pathophysiology

One of the first evidence of an altered glutamate system in schizophrenia was provided by a report of significantly reduced glutamate levels in schizophrenia patients' cerebrospinal fluid (Kim et al., 1981). Further attention to the glutamatergic system was given after the observation that phencyclidine (PCP; angel dust), which is a N-methyl-D-aspartate (NMDA) receptor non-competitive antagonist, could exacerbate psychotic symptoms in humans and generate a "schizophrenia-like" syndrome in PCP addicts (Javitt, 1987; Rosenbaum et al., 1959). Ketamine, another non-competitive NMDA receptor antagonist, was described to induce a psychotic-state in healthy volunteers particularly mimicking positive, negative and cognitive symptoms of schizophrenia (Javitt, 2010; Javitt and Zukin, 1991; Krystal et al., 2003; Krystal et al., 1994), and to exacerbate psychotic symptoms in both drug-free schizophrenia patients and in antipsychotic-responder patients (Lahti et al., 1995; Lahti et al., 2001; Malhotra et al., 1997). The occurrence of negative symptoms in healthy subjects had not been observed in other models of schizophrenia, rendering glutamatergic drugs-induced psychosis the best pharmacological model of the disease in all its psychopathological manifestations. Interestingly, animal studies showed that acute PCP administration increased both locomotor activity and stereotypic motor behaviors (Kesner et al., 1981), whereas sub-chronic PCP administration was reported to induce behavioral sensitization (Jentsch et al., 1998). Moreover, ketamine and other NMDA receptor non-competitive antagonists, such as MK-801, were also described to induce similar behavioral outcomes (Tricklebank et al., 1989). A part from the effects on the locomotor behavior, these compounds were also found to impair animal behaviors reminiscent of cognitive tasks in humans (Verma and Moghaddam, 1996). Altogether, the biochemical and behavioral studies quoted

above were the basis for the Olney and Farber model of psychosis, known as the NMDA receptor hypofunction (NRH) hypothesis (Olney et al., 1999). Thus, the administration of non-competitive NMDA receptor antagonists such as ketamine has been suggested as a powerful preclinical model of psychosis, with substantial heuristic properties to study both molecular targets in psychosis pathophysiology and novel therapeutic strategies (Lipska and Weinberger, 2000). Accordingly, the administration of antipsychotic agents in preclinical settings was found to revert behavioral alterations caused by non-competitive NMDA receptor antagonists (Corbett et al., 1995; Johansson et al., 1994).

Specifically, the NRH hypothesis implied that glutamatergic alterations in schizophrenia, starting from a reduced NMDA receptor activity, would perturb a number of glutamatergic and non-glutamatergic systems and NMDA receptor hypo-functionality became widely accepted as the primary lesion leading to a complex cortical-subcortical perturbation in several neurotransmitter systems (Olney and Farber, 1995; Olney et al., 1999). Many efforts were therefore spent in the search of molecular abnormalities primarily in the number and distribution of glutamate receptors in key brain regions of schizophrenia patients, but the results obtained are still contradictory (Beneyto et al., 2007; Beneyto and Meador-Woodruff, 2008; Clinton et al., 2003; Corti et al., 2007; Gupta et al., 2005; Lyddon et al., 2012; McCullumsmith et al., 2007; O'Connor and Hemby, 2007; O'Connor et al., 2007; Richardson-Burns et al., 2000; Weickert et al., 2013). Significant discrepancies remain over the role of glutamate receptor abnormalities in schizophrenia patients—discrepancies most likely due to methodological issues, like limited sample selection and biochemical techniques. Thus, the lack of consistent evidence has warranted further research to refine the role of the glutamatergic system, shifting the focus on abnormalities in glutamatergic post-receptor molecules implicated in neurotransmitter signaling (Coyle et al., 2012). Intriguingly, the post-receptor molecules that have been found involved in schizophrenia pathophysiology and responsive to antipsychotic drugs do contribute to glutamatergic signaling and promote the interplay between

glutamate receptors and other neurotransmitter systems, mainly the dopaminergic one. Therefore, perturbation of the dopamine-glutamate interplay at multiple levels has been proposed to play a pivotal role in psychosis pathophysiology.

2. The dopamine-glutamate interplay and the Post-Synaptic Density (PSD) in psychosis

At the subcellular level, the dopamine-glutamate interplay occurs within the Post-Synaptic Density (PSD), a specialized matrix that appears as an electron-dense thickening located at excitatory post-synaptic terminals of the glutamatergic synapse (Okabe, 2007). The PSD represents a complex protein network devoted to the fine-tuning of signal transduction that integrates synaptic signals from presynaptic neurons and different neurotransmitter systems (de Bartolomeis et al., 2005). It has been shown that up to four-hundred proteins can be regularly found by mass spectrometry fingerprinting in the PSD proteome, including: membrane receptors and channels, scaffold and anchoring proteins, signaling proteins, GTPases, kinases, phosphatases and cytoskeleton proteins (Collins et al., 2006; Gold, 2012; Sheng and Hoogenraad, 2007). Specifically, NMDA receptors are placed at the core of this protein mesh, with non-NMDA ionotropic and metabotropic glutamate receptors located at the edge of the ultrastructure (Sheng and Hoogenraad, 2007). In this molecular context, dopamine and glutamate signaling pathways cross-talk starting from the receptor level, since it has been found that the activation of NMDA receptors favors the recruitment of D1 receptors to the plasma membrane of neurons *in vitro* (Scott et al., 2002). In turns, the activation of dopamine D1 receptors has been found to modulate the rapid trafficking of NMDA receptor subunits (Hallett et al., 2006). Moreover, a physical interaction leading to the formation of an NMDA/D1 receptor hetero-oligomer has been reported (Lee et al., 2002). At the post-receptor level, many PSD proteins (such as the dopamine- and adenosine 3',5' monophosphate (cAMP)-regulated phosphoprotein pf 32 kD (DARPP-32), CaMKII, Neuronal Calcium Sensor-1 (NCS-1), and calycon have essential roles in controlling and routing both dopamine and glutamate neurotransmission. One relevant effector of dopamine-glutamate interplay within the PSD

is the activity-regulated cytoskeleton-associated protein (Arc), which is a highly expressed dendritic protein involved in synaptic plasticity (Shepherd and Bear, 2011). Arc has a spectrin homology sequence in the C-terminal region and binding sites for endophilin 3 and dynamin 2, interacts with proteins involved in clathrin-mediated endocytosis and facilitates the removal of α -amino-3-hydroxy-5-methyl-4-isoxazolepropionic acid (AMPA) receptors from the membrane ((Bloomer et al., 2007; Chowdhury et al., 2006) and is considered a marker for neuronal plastic changes relevant for learning and memory (McIntyre et al., 2005).

However, recent attention is focused on the scaffold proteins, which constitute a class of PSD proteins with multiple functions. Particularly, scaffolding proteins owe a particular role by linking the different components of glutamate receptor complexes and by regulating glutamate receptor trafficking and therefore modulating the signaling cascade starting from membrane receptors (Figure 1.) (Iasevoli et al., 2013b; Vessey and Karra, 2007).

The scaffold protein subsets mostly studied are: 1) the NMDA receptor and type I metabotropic glutamate receptor (mGluR1/5) scaffold members of the membrane-associated guanylyl kinase (MAGUK) family; 2) the Homer family of proteins; 3) and the ProSAP/Shank (SH3 domain and ankyrin repeat-containing protein) family of proteins (Bayes et al., 2011; Iasevoli et al., 2013b).

The MAGUKs, including PSD-95, SAP102 and PSD-93, contain the PSD-95/disc large/zonula occludens-1 (PDZ) domains, which are considered a hallmark of the PSD (Xu, 2011). PDZ domains are of fundamental importance since they are peptide-binding domains that allow the above-mentioned proteins to interact with a variety of binding partners within the PSD, such as NMDA receptors (Kim and Sheng, 2004). Moreover, PSD-95 has been shown to interact with dopamine and glutamate receptors and regulate their activation state through its binding domain (Zhang et al., 2009). Therefore, MAGUKs participate to the formation of protein multimers within the PSD, providing a physical bridge between receptors and intracellular molecules at the crossroad among glutamatergic and dopaminergic signaling pathways (de Bartolomeis et al., 2014)

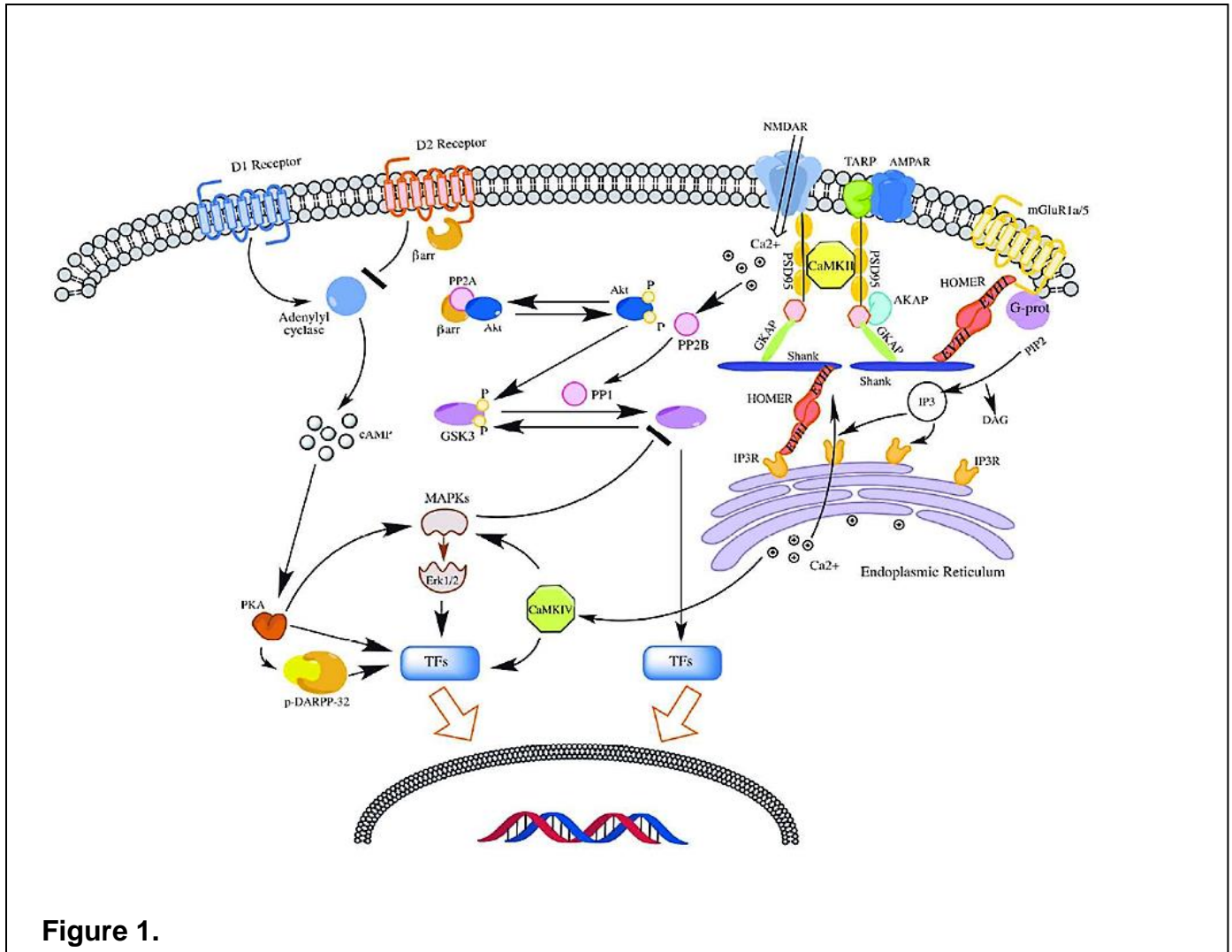


Figure 1.

Figure 1. Postsynaptic density (PSD) proteins elaborate and integrate multiple transductional pathways starting at main dopamine membrane receptors. Scaffolding proteins (Homer, Shank, PSD-95) physically connect receptors, linking them to intracellular calcium stores. NMDAR, N-methyl-D-aspartate glutamate receptor; AMPAR, α -amino-3-hydroxy-5-methyl-4-isoxazolepropionic acid glutamate metabotropic glutamate receptor type 1a/5; TARP, transmembrane AMPA receptors regulating protein or stargazin; PSD-95, postsynaptic density DISC1, disrupted in schizophrenia 1; GSK3, glycogen synthase kinase 3; PDE4, phosphodiesterase 4; GKAP, guanylate kinase associated protein; H1a, early inducible protein; PIP2, phosphatidylinositol biphosphate; DAG, diacylglycerol; IP3, inositol 1,4,5-trisphosphate; cAMP, cyclic monophosphate; ER, endoplasmic reticulum; PLC, phospholipase C; PKC, protein kinase C; PKA, protein kinase A; CAMK, calcium-calmodulin regulated kinase; activated protein kinases; Erk, extracellular signal-regulated kinase; MEK, MAPK/Erk kinase; and Rac1, Ras-related C3 botulinum toxin substrate 1.

The second most studied PSD scaffold family of proteins is the Homer one, whose products are encoded by three distinct genes (*Homer 1, 2, 3*), providing both constitutive (Homer1b/c, Homer2a/b, Homer3) and inducible (Homer1a and ania-3) isoforms (de Bartolomeis and Iasevoli, 2003; Shiraishi-Yamaguchi and Furuichi, 2007). Through a conserved N-terminal Ena-VASP-homology (EVH1) domain, Homer proteins interact with multiple PSD targets, whereas the C-terminus coiled-coil (CC) domain mediates homotypic interactions and is required for self-multimerization (Xiao et al., 1998), 1998 #166}. Homer long isoforms are constitutively expressed in neurons (Soloviev et al.,

2000), and have been described to physically bridge mGluRsI to inositol 1,4,5-trisphosphate receptors (IP3Rs) (Tu et al., 1998). Moreover, the multimeric Homer clusters may link NMDA receptors with mGluRsI via a Shank-guanylate kinase-associated protein (GKAP)- PSD95 complex (Tu et al., 1999). Through their EVH1 domain, long Homers may also bind to cytoskeletal components, such as filamentous actin and Drebrin, and the de-clustering of Homer complexes in response to synaptic activity has been demonstrated to anticipate the synaptic cytoskeletal rearrangements (Shiraishi et al., 2003). Moreover, recent evidence demonstrated the role of long Homers in forming a polymeric network with other PSD proteins, which is essential to maintain dendritic spine structure and to ensure synaptic function (Hayashi et al., 2009). On the other end, the short isoform Homer1a is induced in an immediate-early gene (IEG)-like fashion, lacks the CC motif and is unable to multimerize (Bottai et al., 2002). This truncated isoform is induced by several synaptic stimuli and act as ‘dominant negative’ by disrupting long Homers constitutive clusters (Xiao et al., 1998), thus regulating the scaffolding-process and function of long isoforms finally resulting in a modification of synaptic architecture (Sala et al., 2003). *Homer1a* induction by synaptic stimuli has been demonstrated also to impact Ca⁺⁺ intracellular oscillations, through the regulation of long Homers’ coupling with Transient Receptor Potential Channels, IP3Rs, and Ryanodine receptors (RyRs) (Worley et al., 2007).

Finally, the ProSAP/Shank family of proteins is composed by Shank 1, Shank 2, and Shank 3, which are considered key PSD scaffolds implicated in modulating glutamate neurotransmission (Boeckers et al., 2002; Vessey and Karra, 2007). Particularly, as mentioned before, Shank proteins allow the formation of polymeric network complexes that require the assembly of Homer tetramers and have been proposed to build functional platforms for other PSD proteins (Hayashi et al., 2009). Indeed, affinity-purified complexes obtained from PSD fractions have been described to include 2-amino-3-(3-hydroxy-5-methylisoxazol-4-yl) propanoic acid (AMPA) receptor subunits (GluR1, GluR2, GluR3, GluR4), subunits of the NMDA receptor (NR1, NR2A, NR2B), G protein regulators and scaffolds such as PSD-95, Shank 2, Shank 3, and Homers (Dosemeci et al., 2007).

Recent findings have demonstrated that PSD proteins contribute substantially to the interaction between dopamine and glutamate systems at receptors and post-receptors levels. Specifically, PSD scaffolds are thought to modulate dopamine and glutamate receptor trafficking and localization to the surface membrane and their reciprocal interaction. For instance, the scaffold PSD-95 has been found to be required for D1 dopamine receptors in order to modulate NMDA currents (Gu et al., 2007), as well as PSD-95 has been described to directly regulate NMDA functions by abolishing the NMDA-mediated inhibition of D1 receptors internalization (Zhang et al., 2009).

Intriguingly, stable or transient changes in the number and/or activity of PSD components have been suggested to be implicated in the pathophysiology of a number of neuropsychiatric diseases such as schizophrenia, but also developmental disorders that present similarities with some schizophrenia symptoms domains (Cheng et al., 2010; de Bartolomeis and Iasevoli, 2003; Gardoni et al., 2009; Szumlinski et al., 2006). Consequently, it could be speculated that the disruption of post-receptor clusters due to PSD dysfunctions may cause complex behavioral deficits (e.g. motor, cognitive deficits) that mirror a failure in synaptic plasticity, which has been considered central to schizophrenia pathophysiology (Moreau and Kullmann, 2013; Wiescholleck and Manahan-Vaughan, 2013). For example, knock-out mice for *Shank1* gene have been reported to exhibit impaired memory functions, weaker basal synaptic transmission, reduced number of dendritic spines, and diminished PSD density compared to wild-type littermates (Hung et al., 2008). Moreover, these animals have been shown to poorly perform in social communication tasks, regarded as animal behavioral correlates of the social and communicative impairments commonly associated with schizophrenia (Wohr et al., 2011). Consistently, a mutation in the promoter region of *Shank1* gene has been associated with working memory deficits in schizophrenia patients in subjects at risk for psychosis (Lennertz et al., 2012). Focusing on the MAGUKs family of scaffolds, the levels of *PSD-95* mRNA have been reported differentially altered in several brain areas of postmortem tissues from schizophrenia patients compared to healthy subjects (Clinton et al., 2003; Ohnuma et al., 2000) and some, although still conflicting, evidence is accumulating on associations between functional polymorphisms of the *DLG4* gene with a genetic susceptibility to

schizophrenia (Cheng et al., 2010; Tsai et al., 2007). Other genetic studies have observed a possible involvement also of Homer genes in the pathophysiology of schizophrenia. Indeed, an association between *Homer1* gene polymorphisms and clinical psychopathology assessments in schizophrenia has been demonstrated. Two *Homer1* polymorphisms (rs2290639 and rs4704560) have been associated with scores on Positive and Negative Syndrome Scale (PANSS, a common rating scale for symptoms severity assessment in schizophrenia) subscales at baseline (Spellmann et al., 2011). In preclinical settings, expression of *Homer1a* has been found significantly increased in the striatum in a condition modeling NRH, i.e. acute administration of neurotoxic and non-neurotoxic subanesthetic doses of ketamine (Iasevoli et al., 2007), and a series of abnormal behaviors have been observed in an experiment of *Homer1a* RNA interference (RNAi) in rats, which exhibited a significant decrease in *Homer1a* expression in the striatum and hippocampus (Hong et al., 2013). After *Homer1a* RNAi treatment, it has been observed: higher levels of vertical and horizontal activities at the Låt maze, indicating increased hyperactivity and non-selective attention; longer latencies before locating the platform and longer total swim distances in the Morris water maze (MWM), indicating that *Homer1a* down-regulation impaired attention, learning and memory abilities (Hong et al., 2013)as. Moreover, *Homer1* knock out mice exhibit attention deficits and hyperactivity-like behavior, which has been reversed by adeno-virus associated delivery of *Homer1a* in the prefrontal cortex (Lominac et al., 2005). Finally, also the other *IEG Arc* has been found implicated in schizophrenia pathophysiology (Manago et al., 2016), and its levels of expression have been demonstrated to be responsive to antipsychotic administration (de Bartolomeis et al., 2016; de Bartolomeis et al., 2013b).

Indeed, our group has observed that gene expression of PSD transcripts may be modulated by antipsychotic drugs, implying that the PSD may be centrally involved in the mechanism of action of these agents (Iasevoli et al., 2011a; Iasevoli et al., 2010b; Polese et al., 2002; Tomasetti et al., 2007). Indeed, through postsynaptic network modulation, antipsychotics may induce dopamine-glutamate synaptic remodeling, which is at the basis of their long-term physiologic effects.

Due to the studies conducted so far, showing that PSD components play a key role in synaptic plasticity processes, behavioral conducts, and are modulated by antipsychotics, these molecules are gaining relevant interest in order to unveil the final molecular rearrangements at the synapse-level possibly implied in old, current and future psychosis treatment strategies.

3 .Current antipsychotic drugs and the challenge of non-response: translational implications from preclinical studies

Dopamine D2 receptor blockade is still regarded as the main condition for antipsychotic activity of a compound (Kapur et al., 2000; Mamo et al., 2004; Meisenzahl et al., 2008). Nevertheless, current treatments with antipsychotics have been proven effective in curtailing particularly acute symptoms, while schizophrenia patients show a large number of unmet needs in terms of negative and cognitive symptoms control by available pharmacotherapy. Indeed, an estimated 30% of patients do not respond or respond poorly to current treatments (Lindenmayer and Khan, 2004), and only a small percentage of responding patients is able to have a normal working life. Indeed, multiple relapses still occur frequently (almost 80% of patients within 5 years after initial diagnosis) and even with appropriate intervention, treatment responses often wane over a longitudinal timeline (Yin et al., 2017). This worsening of illness severity in the context of continual antipsychotic exposure may be a sign of treatment resistance. Recently, the Treatment Response and Resistance in Psychosis (TRRIP) working group was formed to establish consensus criteria to standardize the definition of treatment resistant schizophrenia (TRS) (Howes et al., 2017). As expected, in these guidelines, dose, duration of treatment and cognitive impairment were highly considered to play a role in non-response to antipsychotics (Howes et al., 2017).

As stated above, antipsychotics act at different degrees as antagonists at postsynaptic D2 receptors, thereby reducing the activation of dopaminergic pathways in the mesostriatal and mesolimbic

circuitries. D2 receptors are under dynamic regulation from many kinases and trafficking enzymes and neurotransmission can undergo both desensitization and resensitization depending on the regulatory mechanisms in play (Beaulieu and Gainetdinov, 2011). Therefore, continual administration of antipsychotics may be one of the factors that alter the sensitivity of D2 receptors possibly ending in alterations of the signaling cascade. Animal studies have variously reported at the behavioral level the effects of chronic administered antipsychotics in rodents. For example, rats pretreated with chronic haloperidol and subsequently administered apomorphine several days after haloperidol withdrawal, had greater behavioral supersensitivity—as measured by locomotor tasks—compared to control rats (Montanaro et al., 1982). Chronic haloperidol pretreatment has also been shown to decrease dopamine release in preclinical settings (Lane and Blaha, 1987), whereas injections of exogenous dopamine into the nucleus accumbens of rats pretreated with haloperidol elicited hypersensitization effects (Halperin et al., 1983). Moreover, rats pretreated to a low (0.25 mg/kg) or high (0.75 mg/kg) dose of haloperidol through continuous infusion via osmotic minipump receiving injections of amphetamine at fixed time-points after the discontinuation of haloperidol, were found to show locomotor activity supersensitivity reminiscent of previous withdrawal studies (Samaha et al., 2007). In addition to behavioral tests, assays examining the receptor number and affinity of D2 receptors found increases in the high affinity state of D2 receptors for the high dose of haloperidol pretreatment (Samaha et al., 2007). Taken together, these findings demonstrate that the effectiveness of chronic administration of antipsychotics diminish during the period of receptor sensitization. While the mechanism that underlies the development of supersensitivity cannot be directly measured using behavioral tasks, it seems likely that post-synaptic signaling regulations of the dopamine pathways are affected by chronic antipsychotic administration. As an example, several genes linked to dopaminergic signaling were found to be downregulated in the presence of chronic antipsychotic treatment (Fatemi et al., 2006). In this context, the study of molecular adaptations that may occur in acute *versus* chronic administration of antipsychotic compounds can be particularly

interesting in order to shed a light on molecular adaptations to the administration of these drugs. Early studies from our group demonstrated that in rodents both first and second generation antipsychotics may directly impact several PSD molecules and scaffolding proteins via differentially inducing their expression pattern in both acute and chronic paradigms of administration (de Bartolomeis et al., 2002; Polese et al., 2002). Particularly, the specific perturbation of dopaminergic signaling may lead to concurrently specific differential topographical brain expressions of the Homer family of PSD genes directly depending on the receptor profile of the antipsychotic (Tomasetti et al., 2007). Therefore, studies on chronic paradigms of antipsychotic administration are warranted to model from a translational point of view the conditions of therapy in clinical populations and to investigate the plastic changes occurring in the PSD in these settings. Other real-world conditions that can have an impact on antipsychotic treatment in terms of clinical response by acting as confounding factors may be represented by substance misuse during antipsychotic treatment. Apart from alcohol, cocaine or other drugs, the abuse of coffee drinking and tobacco smoking is a common addictive conduct in schizophrenia patients, above all among those taking antipsychotics (Thoma and Daum, 2013). On the clinical side, the abuse of such legal substances in patients has been variously regarded to cause beneficial other negative effects on the clinical course of the disease and on the rate of antipsychotic response. Despite this body of evidence, however, little is known about the molecular changes induced in synaptic sites by these compounds when given in association to antipsychotics. Nevertheless, nicotine and caffeine have been included among possible therapeutic strategies for Parkinson's disease (PD) and may counteract the PD-like extrapyramidal side effects of antipsychotics (Oertel and Schulz, 2016). Moreover, both adenosine receptors (which are directly modulated by caffeine) and nicotine receptors have been suggested as potential targets of pharmacological strategies to address residual symptoms not responding or responding poorly to conventional antipsychotics (Marcus et al., 2016; Rial et al., 2014).. Intriguingly, several reports exist on the modulation exerted by these substances on PSD molecules.

Nicotine has been reported to increase protein levels of the PSD protein Homer1a in HEK-293 cells, most presumably as a consequence of reduced proteasome degradation (Rezvani et al., 2007).

According to these observation, nicotine exposure significantly increased stability and levels of ubiquitinated Homer1a compared with control (Rezvani et al., 2007). These effects may indicate a generalized strengthening of glutamatergic activation by nicotine, since they were associated to a nicotine-dependent increase of multiple glutamate receptors in mouse prefrontal cortex (Rezvani et al., 2007). Moreover, in an early study, acute injection of a high caffeine dose (i.e. 100 mg/kg) was reported to significantly increase *Arc* mRNA expression in the striatum (Dassesse et al., 1999), supporting the idea that this compound may have modulatory effects also upon the expression of other IEGs. Therefore, it appears appealing to better characterize the molecular and behavioral effects of caffeine and nicotine in addition to haloperidol on key molecules implied in synaptic plasticity processes such as the ones belonging to the PSD.

Finally, it is nowadays widely accepted that current pharmacotherapeutic strategies do not effectively treat the cognitive deficits of schizophrenia (Dunlop and Brandon, 2015; Karam et al., 2010).

Cognitive dysfunction has been increasingly recognized as a core feature of schizophrenia; 90% of patients show deficits in at least one cognitive domain, including working memory, attention, processing speed, problem solving, social cognition, visual learning and memory, and verbal learning and memory (O'Tuathaigh et al., 2017) . Despite considerable heterogeneity (Weinberg et al., 2016), the severity of these symptoms at the early stage of illness represents a significant prognostic indicator of clinical course and functional outcomes (de Bartolomeis et al., 2013a; Green, 2006). Moreover, cognitive dysfunctions may play a role in TRS occurrence or generally in poor responders (de Bartolomeis et al., 2013a).

Significant obstacles to developing effective and novel cognitive enhancing therapies have included lack of clarity regarding the neural circuitry and molecular/cellular changes underlying cognitive dysfunction in schizophrenia (Cope et al., 2016; Tandon et al., 2009). Despite the complexity of cognitive impairment pathophysiology, glutamatergic dysfunctions together with reduced dopamine neurotransmission in medial prefrontal cortex have been considered major causative abnormalities

(Abi-Dargham and Moore, 2003; Gaspar et al., 2012). Indeed, agents stimulating NMDA receptors together with mGluRI antagonists have received the most attention among potential compounds targeting glutamatergic dysfunction in the effort of impacting also cognitive symptoms of the disease (Alberati et al., 2012; Chaki and Hikichi, 2011; Satow et al., 2008).

The recent observation that PSD proteins are modulated by anti-dopaminergic compounds commonly used in schizophrenia therapy but also by agents that modulate glutamatergic neurotransmission (Iasevoli et al., 2007), has further reinforced interest in these molecules. The effects of antipsychotics on PSD molecules are so specific that the topographical pattern of PSD genes expression may vary with the dose of the antipsychotic administered: indeed, increasing doses of selected first or second generation antipsychotic may progressively recruit the expression of crucial PSD genes, such as *Zif268*, *Homer1a*, *Arc*, while gradually impacting selected brain areas (de Bartolomeis et al., 2015). Moreover, the common clinical practice of switching antipsychotic has been demonstrated to specifically perturb PSD molecules depending on the specific switch procedure (de Bartolomeis et al., 2016). On the other hand, ketamine, MK-801 and the non-competitive NMDA receptor antagonist memantine have been found to exert divergent effects on PSD transcripts, reinforcing the idea that compounds impacting glutamatergic signaling may also modulate differentially these plasticity linked molecules (de Bartolomeis et al., 2013c; de Bartolomeis et al., 2012).

Since PSD molecules may represent an intracellular hub where dopamine and glutamate modulate one another reciprocally, targeting these molecules may appear to be beneficial in schizophrenia therapy, especially in the treatment of resistant conditions where conventional antipsychotic therapies fail to fully control symptoms.

CHAPTER 2

Aim of the Research

The possibility to translate real-world practice treatment strategies in psychosis to preclinical settings gives the opportunity to dissect at a molecular level the putative modifications that occur and concur to synaptic plasticity rearrangements. As already pointed-out, dopamine-glutamate interplay dysfunctions have been suggested as key factors in psychosis pathophysiology and for the most part, synaptic interactions between dopamine and glutamate signaling pathways take part at the PSD. Therefore, the major goal of the present research was to focus on PSD adaptations to pharmacological manipulations mimicking common clinical situations.

According to these premises, here we provide a set of preclinical studies whose aim was to investigate: i) the postsynaptic molecular adaptations to prolonged pharmacological treatments with the specific scope of comparing novel multitargeting agents to first and second generation antipsychotics currently used in clinical practice; ii) the comparison of acute *versus* chronic plasticity-related genes differences in terms of expression as a molecular fingerprint of the two different treatment situations; iii) the molecular effects on key PSD molecules of the combined assumption of voluptuary substances such as caffeine and nicotine *plus* antipsychotics; iiiii) the adaptations of PSD transcripts to novel proposed add-on treatment options to antipsychotics, and particularly to the administration of minocycline.

With the first set of experiments, particular efforts were made at recreating current pharmacological strategies focusing on newly approved antipsychotic agents that may activate postsynaptic transcripts with a different topographic distribution from that elicited by standard therapies, and that may suggest better clinical efficacy or possibly some new adverse effects. This study was followed by the second set of experiments, with the specific aim of providing a direct head-to-head comparison of

the synaptic molecular changes caused by acute *versus* chronic administration of the same compounds focusing on the IEG *Homer1a*.

The third set of experiments, through topographic analyses and a behavioral study, was aimed at providing the differential region-specific brain gene expression changes that may occur when antipsychotics are taken with nicotine and caffeine, whose positive or negative additive effects are still a matter of debate at the clinical level.

Finally, since glutamatergic agents have been considered as potentially relevant add-on strategies to antipsychotics in order to reduce negative symptoms and improve cognition, the last set of experiments was aimed at dissecting the molecular effects of the synthetic second-generation tetracycline minocycline that has been recently suggested for the treatment of schizophrenia. Indeed, several lines of evidence suggest that this antibiotic may exert glutamatergic modulatory and anti-inflammatory effects, which are consistent with a potential implication of inflammatory and oxidative pathways in the pathophysiology of psychosis.

CHAPTER 3

Materials and Methods

Animals

Male Sprague-Dawley rats with a mean weight of 250 gr. were obtained from Charles-River Laboratories (Lecco, Italy). Animals were housed and allowed to adapt to human handling in a temperature and humidity controlled colony room with 12/12 h light–dark cycle (lights on from 06:00–18:00) with ad libitum access to chow and water. All procedures were conducted in accordance with the National Institute of Health (NIH) Guide for Care and Use of Laboratory Animals (NIH Publication No. 82-23, revised 1996) and were approved by local Animal Care and Use Committee. All efforts were made to minimize animal suffering.

Drugs

Asenapine powder (gently supplied by H. Lundbeck A/S, Copenhagen, Denmark) and olanzapine powder (Sigma-Aldrich, Milan, Italy) were dissolved in saline solution (NaCl 0.9%).

Haloperidol was provided as an injectable solution (Lusofarmaco, Milan, Italy) and then diluted at experimental doses.

Caffeine powder (Sigma-Aldrich, Milan, Italy), (-)-nicotine hydrogen tartrate salt powder (Sigma-Aldrich, Milan, Italy), and GBR-12909 dihydrochloride powder (Sigma-Aldrich, Milan, Italy) were dissolved in saline solution (NaCl 0.9%).

Minocycline and ketamine (Sigma-Aldrich, St. Louis, MS, USA) were supplied as a powder and dissolved in saline solution (NaCl 0.9%).

All solutions were adjusted to physiological pH value and injected i.p. at a final volume of 1 ml/kg, according to internationally approved protocols (Turner et al., 2011).

In situ hybridization

Radioactive in situ hybridization was performed according to previously published protocols (Ambesi-Impiombato et al., 2003). Animals were killed by decapitation and brains were quickly removed, frozen on powdered dry ice and stored at -70°C prior to sectioning. Serial brain coronal sections of 12µm were cut on a cryostat set at a temperature of -18°C from Bregma -1.20mm to -1.00mm, using the rat brain atlas of Paxinos and Watson as an anatomical reference (George Paxinos, 2001). Sections were thaw-mounted on to gelatin-coated slides and stored at -70°C for subsequent analysis. Probes used for radioactive in situ hybridization were oligodeoxyribonucleotides complementary to mRNA sequences of target genes (MWG Biotech, Firenze) and were designed from Gen-Bank sequences and checked with BLAST in order to avoid cross-hybridization. For each probe, a 50 µl labeling reaction mix was prepared on ice using DEPC-treated water, 1X tailing buffer, 7.5 pmol/µl of oligodeoxyribonucleotide, 125 units of terminal deoxynucleotidyl transferase (TdT) and 100 mCi 35 S-dATP. Unincorporated nucleotides were separated from radiolabeled DNA using ProbeQuant G-50 Micro Columns (Amersham- GE Healthcare Biosciences, Milano, Italy). Sections were fixed in 4% formaldehyde in 0.12 M PBS (pH 7.4), quickly rinsed three times with PBS, placed in 0.25% acetic anhydride in 0.1 M triethanolamine/0.9% NaCl, pH 8.0, for 10 min and then dehydrated in 70%, 80%, 95% , 100% ethanol, delipidated in chloroform for 5 min, rinsed again in 100% and 95% ethanol and finally air-dried. Sections were hybridized with 0.4-0.6x10⁶ cpm of radiolabeled oligonucleotide in a buffer containing 50% formamide, 600 mM NaCl, 80 mM Tris-HCl (pH 7.5), 4 mM EDTA, 0.1% pyrophosphate, 0.2 mg/ml heparin sulfate, and 10% dextran 5 sulfate. Slides were incubated at 37°C in a humidified chamber for 22-24 h. Section were subsequently washed in 2x SSC/50% formamide at 43-44°C, and then in 1X SSC at room temperature. Finally, sections were dried and exposed to a Kodak- 10 Biomax MR auto-radiographic film (Sigma), and a slide containing a scale of 16 known amounts of ¹⁴ C standards (ARC-146C, American Radiolabeled Chemical) was co-exposed. The auto-radiographic films were exposed in a

time range of 14-30 days. The optimal time of exposure was chosen to maximize signal-to-noise ratio but to prevent optical density from approaching the limits of saturation. Film development protocol included a 1.5-minute dip in the developer solution and 3 minutes in the fixer solution. The quantitation of the autoradiographic signal was performed using a computerized image analysis system, including: a transparency film scanner (Microtek Europe B. V., Rotterdam, The Netherlands), an Apple iMac and an ImageJ software (v. 1.50, Rasband, W.S., <http://rsb.info.nih.gov/ij/>). Brain sections on films were captured individually. Scanned images were showed in inverted look-up table (LUT) color, although all the other original characteristics (i.e. contrast, brightness, resolution) were preserved. All hybridized sections were exposed on the same sheet of X-ray film. Signal intensity analyses were carried out on digitized autoradiograms measuring mean optical density within the outlined regions of interest (ROIs) corresponding to rat brain subregions of the cortex, caudate-putamen, and nucleus accumbens (Figure 2.).

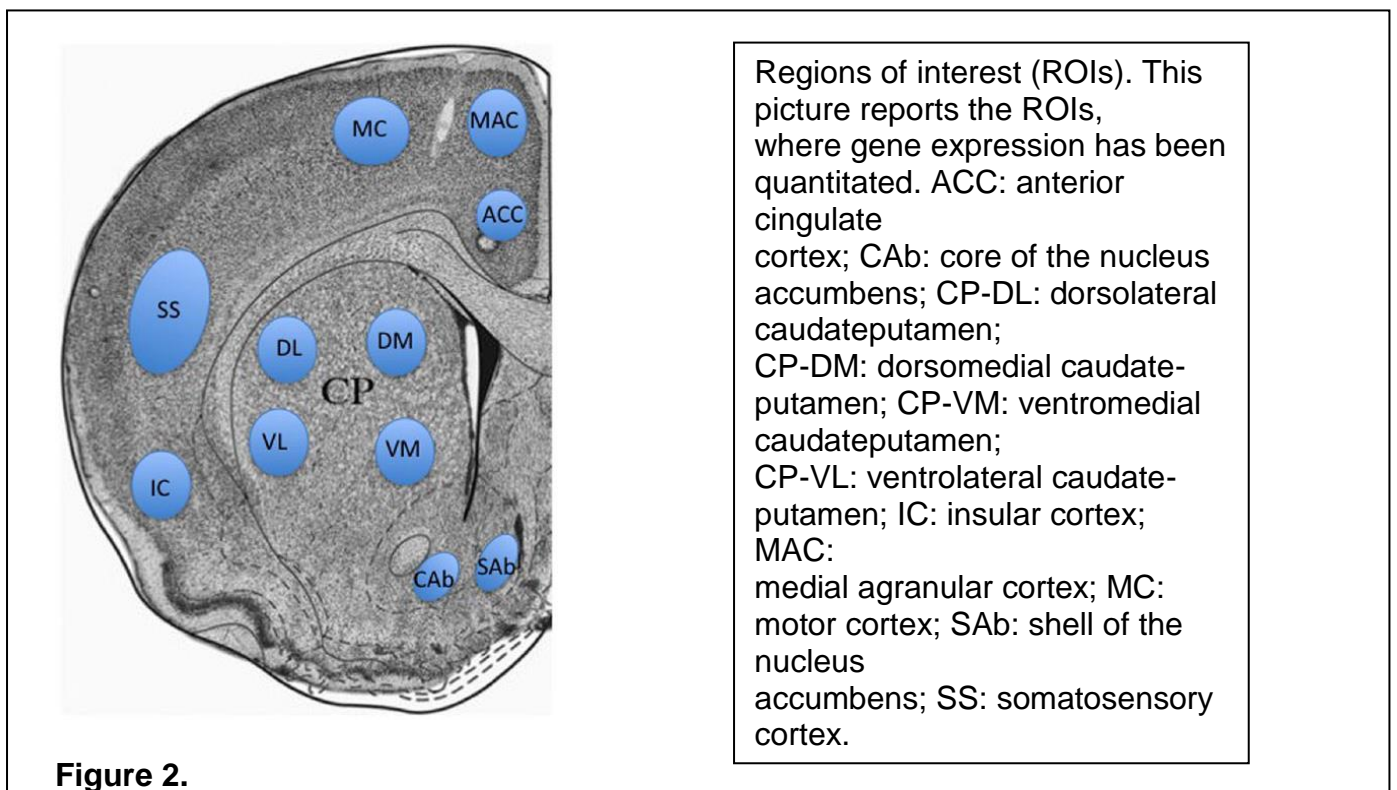


Figure 2. Regions of interest (ROIs). This picture reports the ROIs, where gene expression has been quantitated.

ROIs were selected based on data describing functional and anatomical correlation between cortical and striatal subregions (Willuhn et al., 2003).

Studies from our laboratory have demonstrated that these ROIs are key motor-related and limbic-related regions for evaluating gene expression, with putative translational value (Buonaguro et al., 2017b; Tomasetti et al., 2011). Measurements of optical density within ROIs were converted into “relative dpm” using a calibration curve based on the standard scale co-exposed to the sections. ¹⁴C standard values from 4 through 12 were previously cross-calibrated to 35 S brain paste standards. In order to obtain a calibration curve for each X-ray film, a “best fit” 3rd degree polynomial was used. For each animal, measurements from 4 adjacent sections were averaged and the final data reported in relative dpm as mean ± S.E.M. The whole in situ hybridization procedure was performed blinded with coded frozen brains. To test for inter-observer reliability, an independent quantitation was performed by a second investigator. Results were considered reliable only when the statistical significance of effects obtained by the second investigator was quantitatively consistent with the results obtained by the first investigator.

Western Blot

Rat brains stored at -70°C were dissected on ice to isolate the striatum, which was placed in 1.5ml tubes and treated with ThermoScientific SynPER Synaptic Protein Reagent™ (10ml per gram of tissue, protease inhibitors added immediately before use), and then homogenated in a dounce tissue grinder. The obtained homogenates were rapidly transferred to appropriate centrifuge tubes and centrifuged at 1200g for 10 minutes at 4°C. The supernatant was transferred to new tubes and centrifuged at 15000g for 20 minutes at 4°C. Protein amount was measured by Bradford sampling and then 2ml SynPER Reagent per gram of tissue was added for storage at -70°C in 5% (v/v) DMSO

for subsequent analyses. An amount of 4µg/µl protein *per* each experimental group was run in wells using Bio-Rad Mini-PROTEAN® system, mixed to equal amount v/v of Laemmli™ buffer for visualization and separated on SDS-PAGE 10% polyacrylamide gel. Proteins were transferred on nitrocellulose membranes (Amersham Hybond-ECL, GE Healthcare) and blocked in blocking buffer (5% nonfat dry milk in PBS and 0.1% Tween 20) for 1 h. The blots were incubated in primary rabbit polyclonal antibody for rat Homer1 (Merck Millipore) 1:2000, primary rabbit polyclonal antibody for rat Arc (Synaptic Systems) 1:2000 and primary monoclonal anti-actin antibody produced in mouse 1:1000 (Sigma-Aldrich) at 4°C overnight. This was followed by appropriate washes in TBS and 1 h incubation in a goat horseradish peroxidase-linked anti-rabbit and rabbit anti-mouse secondary antibodies respectively (Sigma-Aldrich). Blots were developed with LiteABlot® Extend chemiluminescent substrate (EuroClone) and exposed on Fujifilm® western blot films.

The quantitation of the signal was performed using a computerized image analysis system by ImageJ software. Signal intensity by each band was relativized by dividing *per* the corresponding standard band (the β-Actin band). Data were reported in relative intensity as means ± S.E.M.

Locomotor Activity

Activity for each animal was filmed in transparent plastic cages (210 square inches floor) with a computerized photo camera system (Apple computer™) and it was measured using a motion capture system that simultaneously labeled and tracked movements of each rat (Kinovea®). Three rats were placed in each cage and a cage corresponded to a specific treatment group. Motion was calculated using centimeters walked through in continuous shot considered as the dependent variable for total activity measurement. Locomotor activity following each treatment administration was measured for a period of 5 minutes, as in previous established protocols (de Bartolomeis et al., 2015). Distance walked through by each rat was averaged with the others belonging to the same treatment group and expressed as centimeters walked through ± S.E.M.

CHAPTER 4

Re-arrangements of gene transcripts at glutamatergic synapses after chronic treatments by different doses of antipsychotics with distinct receptor profile

1. Rationale

To reproduce chronic antipsychotic treatment paradigms in preclinical settings is considered of valuable translational meaning since they may more closely mimic real-world therapeutic approaches and are supposed to produce the synaptic changes occurring during prolonged treatments (Kontkanen et al., 2002). Indeed, putative brain structural changes after chronic antipsychotic treatments have not been completely described yet. In the context of chronic treatments, another common prescribing practice is to prescribe the same compound at different doses. This observation rises the issue of understanding how antipsychotics with different receptor profiles and at different doses may impact brain plasticity processes (Ho et al., 2011; Vita et al., 2015).

To do so, we evaluated the expression of key PSD transcripts, i.e. *Homer1a*, *Arc*, *Homer1b*, *PSD-95*, and *Shank* (details for oligodeoxyribonucleotide probes have been listed in Table 1.) in rat brain selected ROIs after chronic administration of: i) haloperidol, which is considered the prototype of first generation antipsychotics and has a relatively selective D2 receptor profile (Correll, 2010); ii) olanzapine, a second generation antipsychotic with a broad multi-receptor profile (Correll, 2010); and iii) asenapine, the novel multi-receptor targeting antipsychotic with dopamine D1 and D2 receptor blockade ratio of approximately 1 (Shahid et al., 2009).

Probe	cDNA length (bp)	cDNA position	mRNA	Gen-Bank#
Homer1a	48	2527–2574	<i>Homer1a</i>	U92079
Homer1b/c	48	1306–1353	<i>Homer1b/c</i>	AF093268
Arc	45	789–833	<i>Arc</i>	NM019361
Shank	48	2757–2804	<i>Shank1</i>	AF131951
PSD-95	48	225–269	<i>PSD-95</i>	M96853

Table 1.

Table 1. Probes for in situ hybridization histochemistry.

The rationale of comparing the above mentioned compounds comes from the observation that current antipsychotic development strategies have focused on compounds acting on multiple selected targets in order to mainly avoid motor side effects and produce increased efficacy in treating negative and cognitive symptoms (Roth et al., 2004).

The newly developed antipsychotic which responds to these “multitargeting” strategies is asenapine, which shows a binding affinity profile for all serotonergic receptors, equal affinity for D2 and D1 receptors, as well as for alpha adrenergic receptors, and no affinity for muscarinic receptors (Shahid et al., 2009). Thanks to its unique multi-receptor profile, asenapine may differentially impact dopaminergic, noradrenergic, serotonergic and glutamatergic neurotransmission: it specifically enhances the dopamine bursts from ventral tegmental area (VTA) to the medial prefrontal cortex and the nucleus accumbens; regulates noradrenaline signaling from locus coeruleus to the cortex; promotes serotonin release in the cortex; enhances glutamate NMDA-mediated currents in pyramidal cortical neurons, while it decreases NMDA receptor activity in caudate-putamen and nucleus accumbens (Franberg et al., 2009; Franberg et al., 2008; Tarazi et al., 2010). Finally, asenapine administered at different doses may exert brain region-specific differential effects on dopamine, serotonin and glutamate receptors (Tarazi et al., 2008, 2010).

Considering that PSD molecules represent crucial crossroads for multiple receptor signaling involved in the mechanisms of action of the most frequently used psychotropic drugs and that a direct head-to-head comparison of the molecular effects of first and second-generation antipsychotics at different doses in a chronic paradigm can be of translational value, we tried to address the following questions:

1. Do prototypical first, second generation antipsychotics and newly developed antipsychotics induce unique changes in the expression of PSD transcripts with respect to cortical/sub-cortical brain regions in a chronic paradigm of administration?

2. Are there different expression profiles of PSD transcripts in selected ROIs secondary to the dose of the antipsychotic chronically administered?
3. Is it possible that antipsychotics with different receptor profile or that different doses of the same antipsychotic may produce an imbalance of the Homer1 isomers (i.e. *Homer1a* and *Homer1b*) relative ratio of transcript expression, considering that those isoforms have been described to exert opposite molecular effects (Kammermeier, 2008)?

In the present study, rats were randomly assigned to one of the following treatment groups (n = 5 for each group): control group receiving vehicle (NaCl 0.9%, VEH); haloperidol 0.25 mg/kg (HAL0.25); haloperidol 0.5 mg/kg (HAL0.5); haloperidol 0.8 mg/kg (HAL0.8); asenapine 0.05 mg/kg (ASE0.05); asenapine 0.1 mg/kg (ASE0.1); asenapine 0.3 mg/kg (ASE0.3); olanzapine 2.5 mg/kg (OLA). All drugs were given at behaviorally active doses, based on previous works (Huang et al., 2008; Iasevoli et al., 2010a; Marston et al., 2009; Tomasetti et al., 2007). The above-listed drugs were administered once a day for twenty-one consecutive days. All animals received the drugs in one i.p. injection a day. Care was taken to carry out injections at the same hour of the day, every day. ANOVA (One-way Analysis of Variance) was used to analyze treatment effects. The Student-Newman-Keuls (SNK) post-hoc test with the Bonferroni correction was used for groups' comparison. In all tests, significance was set at $p < 0.05$. To calculate the *Homer1a/Homer1b* ratio, signal intensity of *Homer1a* and *Homer1b* mRNA expression by each antipsychotic compound was normalized on values of vehicle mRNA expression (de Bartolomeis et al., 2013c). The Student's t-test was then used to compare normalized *Homer1a* vs. *Homer1b* mRNA levels by each antipsychotic in each ROI. The statistical analyses were performed using JMP9.0.1 software.

2. Results

The main result of the present study was that chronic treatments with prototypical first and second generation antipsychotics compared to the newly developed drug asenapine triggered a complex,

antipsychotic- and dose-specific set of re-arrangements in PSD gene transcripts known to be key players in structural and functional plasticity processes (Representative autoradiograms of gene expression were shown in Figure3.).

Results are listed for each gene as the expression differences obtained comparing the antipsychotic taken into account *versus* the control group, followed by intragroup differences among the different doses of haloperidol and asenapine considered. Finally, the intergroup differences in the expression of each gene has been obtained comparing haloperidol *versus* asenapine, asenapine *versus* olanzapine and haloperidol *versus* olanzapine –administered groups.

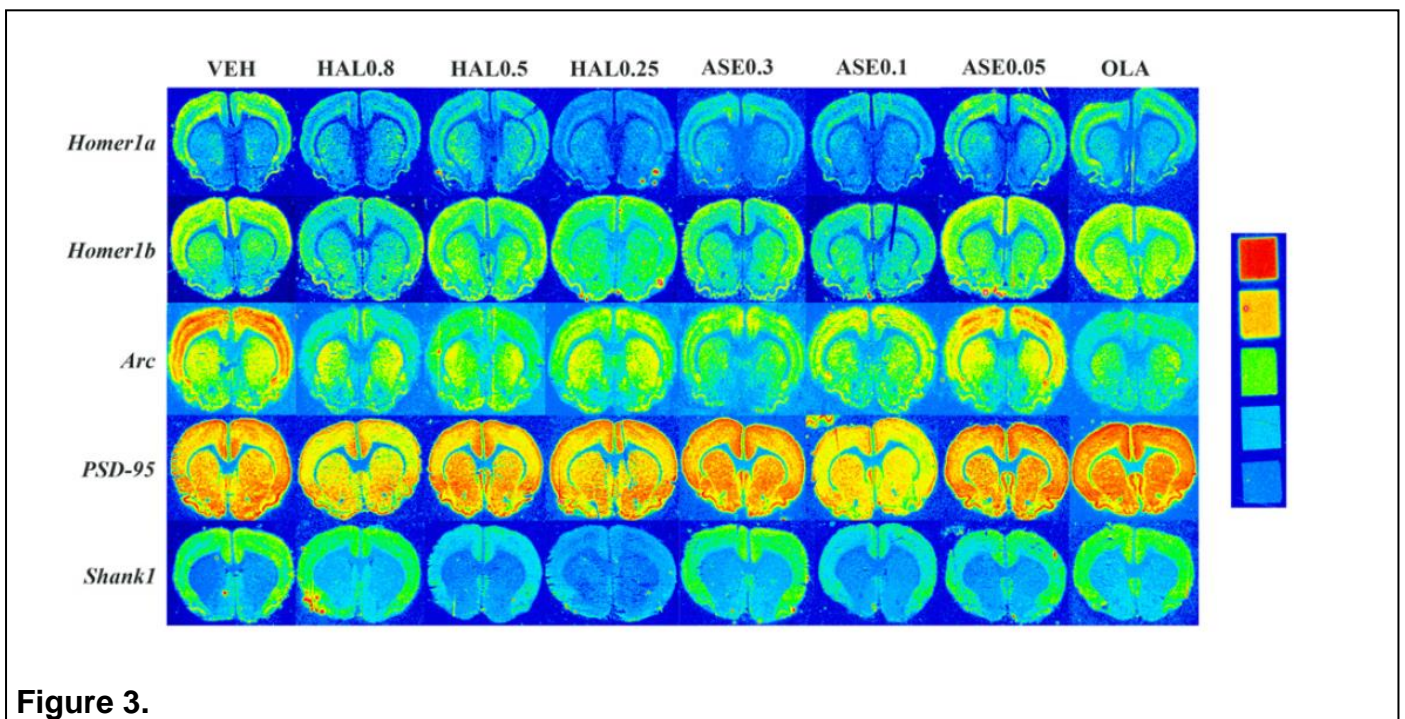


Figure 3. Autoradiographic film images of Homer1a, Homer1b, Arc, PSD-95 and Shank1mRNA detected by means of in situ hybridization histochemistry in coronal brain sections after chronic treatment with vehicle (NaCl 0.9%, VEH), haloperidol 0.8 mg/kg (HAL0.8), haloperidol 0.5 mg/kg (HAL0.5), haloperidol 0.25 mg/kg (HAL0.25), asenapine 0.3 mg/kg (ASE0.3), asenapine 0.1 mg/kg (ASE0.1), asenapine 0.05 mg/kg (ASE0.05), olanzapine 2.5 mg/kg (OLA). Blue to red labeling identifies increasing signal intensity levels.

2.1 Homer1a

2.1.1. Gene expression differences between antipsychotic-administered groups and control group.

In the cortex, *Homer1a* expression was significantly reduced by HAL0.8, HAL0.25 and by ASE0.1 administration (Figure 4., Table 2.). In the striatum, HAL0.5 and HAL0.8 significantly induced

Homer1a mainly in the dorsal and ventro-lateral caudate putamen (Figure 4., Table 2.). *Homer1a* mRNA levels were significantly induced only in the dorso-lateral caudate putamen by ASE0.05 administration. Olanzapine was found to affect gene expression only in the dorso-lateral region of the caudate putamen and in the shell of the nucleus accumbens (Figure 4.,Table 2.).

2.1.2. Haloperidol intragroup gene expression differences.

The different doses of haloperidol considered in this study affected *Homer1a* mRNA expression only in the MAC region of the cortex and in the shell of the nucleus accumbens (Figure 5.). Specifically, HAL0.5 induced significant higher levels of *Homer1a* gene compared to haloperidol administered at higher and lower doses (Figure 5.).

2.1.3. Asenapine intragroup gene expression differences.

In the MAC and SS cortical regions, *Homer1a* expression was significantly induced at a higher extent by ASE0.05 compared to ASE0.1 (Figure 5.).

2.1.4. Asenapine vs. Haloperidol gene expression differences.

Homer1a mRNA levels were found significantly affected in cortical regions mainly in the ASE0.05 treated group compared to haloperidol administered at high and low doses (Table 3.). Conversely, in the striatum, *Homer1a* expression levels were significantly higher in the haloperidol treated groups compared to asenapine treated groups (Table 3.).

2.1.5. Asenapine vs. Olanzapine gene expression differences.

Olanzapine was found to induce significantly higher levels of *Homer1a* mRNA compared to ASE0.1 in both cortical and striatal regions (Table 4.).

2.1.6. Haloperidol vs. Olanzapine gene expression differences.

Olanzapine was found to induce significantly higher levels of *Homer1a* mRNA compared to haloperidol treated groups only in cortical regions and mainly in the MAC region (Table 5.).

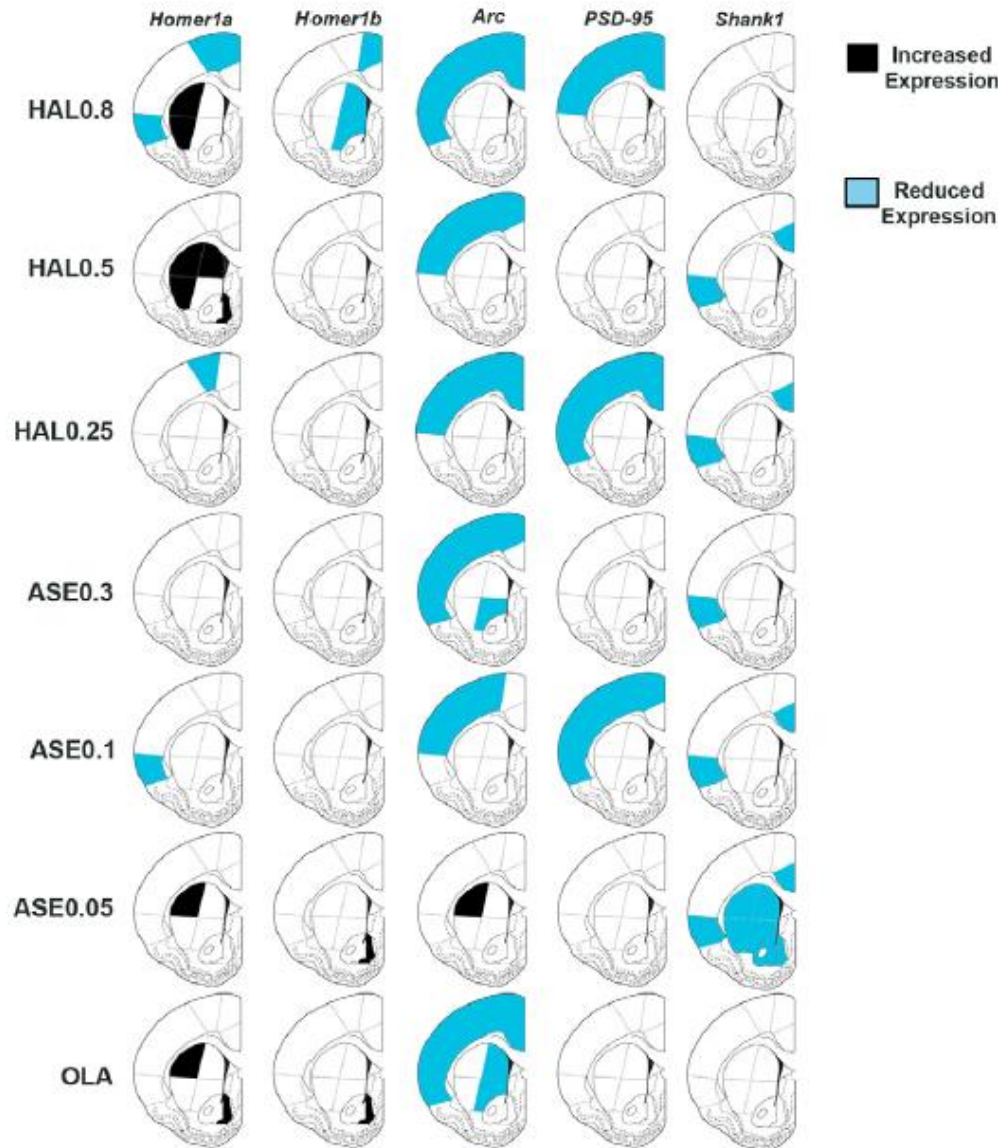


Figure 4.

Figure 4. *Homer1a*, *Homer1b*, *Arc*, *PSD-95* and *Shank1* gene expression patterns in cortical and subcortical regions by haloperidol 0.8 mg/kg (HAL0.8), haloperidol 0.5 mg/kg (HAL0.5), haloperidol 0.25 mg/kg (HAL0.25), asenapine 0.3 mg/kg (ASE0.3), asenapine 0.1 mg/kg (ASE0.1), asenapine 0.05 mg/kg (ASE0.05), olanzapine 2.5 mg/kg (OLA).

Black label: increased expression vs. VEH at the Student-Newman-Keuls (SNK) post-hoc test with Bonferroni correction ($p < 0.05$). Blue label: decreased expression vs. VEH at the Student-Newman-Keuls (SNK) post-hoc test with Bonferroni correction ($p < 0.05$).

		relative d.p.m. ± S.E.M.								ANOVA		
	ROIs	VEH	HAL0.8	HAL0.5	HAL0.25	ASE0.3	ASE0.1	ASE0.05	OLA	F	df	p
<i>Homer1a</i>	AC	73.72 ± 6.33	61.47 ± 2.66	78.99 ± 5.21	67.64 ± 3.11	80.91 ± 4.74	77.35 ± 2.92	84.52 ± 5.57	90.20 ± 4.80	4.09	7,22	0.0051
	M2	94.75 ± 6.39	69.18 ± 2.80	86.31 ± 1.61	81.16 ± 6.28	91.18 ± 2.29	90.53 ± 1.07	98.61 ± 1.16	102.38 ± 2.89	11.73	7,22	<.000
	M1	103.18 ± 7.63	83.71 ± 2.32	97.99 ± 2.82	84.88 ± 6.47	94.93 ± 1.72	87.86 ± 1.92	106.88 ± 2.50	107.99 ± 3.40	7.33	7,22	0.0001
	SS	95.27 ± 6.06	85.70 ± 4.73	95.65 ± 3.83	82.61 ± 6.46	90.49 ± 1.91	81.91 ± 3.16	97.61 ± 2.07	101.88 ± 1.09	3.93	7,22	0.0063
	I	97.29 ± 5.37	76.01 ± 5.48	86.08 ± 5.70	77.48 ± 9.46	79.78 ± 2.11	75.17 ± 4.62	92.18 ± 2.07	96.50 ± 3.00	3.54	7,22	0.0106
	dm	75.11 ± 6.57	79.81 ± 6.70	94.23 ± 3.75	84.18 ± 4.23	80.29 ± 2.95	74.75 ± 2.85	87.15 ± 2.05	87.61 ± 4.51	2.71	7,21	0.0358
	dl	75.72 ± 7.16	96.25 ± 7.45	102.88 ± 2.78	92.52 ± 0.78	87.59 ± 1.54	85.02 ± 3.46	100.95 ± 2.39	95.76 ± 5.76	4.27	7,21	0.0044
	vm	84.61 ± 7.70	87.39 ± 2.17	95.85 ± 5.33	83.45 ± 3.81	80.35 ± 2.38	82.38 ± 3.81	90.06 ± 1.53	87.23 ± 4.37		7,21	ns
	vl	78.68 ± 7.81	104.04 ± 5.35	104.89 ± 4.83	86.96 ± 3.17	84.62 ± 0.47	74.64 ± 5.12	87.17 ± 2.04	95.79 ± 4.55	6.23	7,21	0.0005
	core	66.68 ± 4.12	76.52 ± 4.05	82.59 ± 4.01	73.90 ± 7.94	72.09 ± 3.69	67.98 ± 1.35	74.77 ± 4.49	82.42 ± 4.52		7,21	ns
shell	56.33 ± 3.25	71.49 ± 1.54	87.45 ± 5.38	65.88 ± 4.54	67.29 ± 1.57	64.09 ± 3.32	70.59 ± 6.25	79.40 ± 6.12	4.29	7,21	0.0043	
<i>Homer1b</i>	AC	90.98 ± 2.73	85.09 ± 0.95	87.44 ± 4.70	87.28 ± 2.75	91.65 ± 1.98	88.18 ± 1.46	96.32 ± 2.18	93.41 ± 3.09		7,27	ns
	M2	91.60 ± 2.26	84.09 ± 0.66	93.76 ± 1.09	86.03 ± 2.19	89.18 ± 0.86	86.62 ± 0.71	95.91 ± 1.55	94.97 ± 2.49	7.51	7,27	<.0001
	M1	91.16 ± 2.96	84.74 ± 0.78	93.92 ± 1.76	88.61 ± 3.05	90.08 ± 1.11	87.71 ± 1.48	97.89 ± 1.45	93.63 ± 2.53	4.59	7,27	0.0017
	SS	89.88 ± 3.11	84.44 ± 1.61	87.34 ± 5.04	88.70 ± 2.71	92.37 ± 2.54	85.98 ± 2.12	97.44 ± 2.03	92.22 ± 2.28	2.52	7,27	0.0389
	I	91.15 ± 3.26	86.64 ± 1.39	90.33 ± 4.31	91.29 ± 2.871	93.94 ± 1.81	86.79 ± 2.57	98.14 ± 2.30	97.83 ± 1.77	3.17	7,27	0.0138
	dm	88.89 ± 0.64	80.60 ± 1.15	89.23 ± 1.04	84.47 ± 2.24	87.76 ± 1.36	83.20 ± 1.05	91.45 ± 0.98	92.49 ± 2.08	8.86	7,27	<.0001
	dl	90.89 ± 1.20	82.75 ± 1.14	89.71 ± 3.44	87.54 ± 2.48	91.60 ± 1.64	87.54 ± 1.85	96.64 ± 2.41	98.17 ± 2.21	6.03	7,27	0.0003
	vm	91.42 ± 0.37	82.02 ± 0.77	92.10 ± 0.85	87.16 ± 2.74	89.32 ± 1.01	86.15 ± 1.33	93.48 ± 1.39	95.08 ± 1.70	9.85	7,27	<.0001
	vl	93.69 ± 0.50	85.71 ± 1.68	93.46 ± 3.78	90.26 ± 3.22	93.04 ± 1.95	87.90 ± 1.50	97.49 ± 1.85	101.29 ± 1.96	5.66	7,27	0.0004
	core	89.08 ± 1.24	82.45 ± 0.72	90.21 ± 3.54	87.68 ± 2.48	89.46 ± 1.27	86.39 ± 1.92	95.12 ± 1.52	91.07 ± 4.12	2.53	7,27	0.0383
shell	87.82 ± 0.75	81.64 ± 1.02	93.74 ± 3.11	87.65 ± 2.15	88.19 ± 0.64	84.39 ± 2.14	95.12 ± 1.37	95.16 ± 0.77	10.37	7,27	<.0001	
<i>Arc</i>	AC	111.44 ± 10.33	78.47 ± 1.22	106.28 ± 4.06	70.99 ± 5.31	84.87 ± 11.09	94.82 ± 5.90	85.63 ± 12.79	56.46 ± 2.27	4.81	7,19	0.0029
	M2	192.34 ± 20.42	89.98 ± 3.76	123.79 ± 15.01	106.18 ± 12.72	130.34 ± 19.00	161.38 ± 15.40	151.82 ± 17.78	87.41 ± 4.07	5.97	7,19	0.0009
	M1	188.19 ± 14.67	83.44 ± 2.98	112.38 ± 10.62	98.07 ± 11.45	106.49 ± 10.17	133.72 ± 12.44	149.66 ± 21.15	83.68 ± 6.47	9.80	7,19	<.0001
	SS	188.06 ± 18.23	80.69 ± 2.62	102.37 ± 2.10	106.16 ± 21.86	100.12 ± 8.12	123.28 ± 11.66	147.78 ± 10.57	79.33 ± 7.13	9.89	7,19	<.0001
	I	131.12 ± 19.64	72.64 ± 1.78	87.88 ± 1.87	82.35 ± 16.24	80.46 ± 5.83	105.55 ± 14.28	120.15 ± 14.64	62.91 ± 7.22	3.97	7,19	0.0077
	dm	106.32 ± 8.76	104.08 ± 4.52	112.95 ± 11.37	95.43 ± 3.98	81.94 ± 5.53	97.35 ± 8.29	102.61 ± 5.41	74.04 ± 6.73	2.98	7,21	0.0243
	dl	116.84 ± 6.76	133.29 ± 3.50	130.67 ± 3.53	119.49 ± 6.69	103.56 ± 8.01	122.95 ± 13.94	158.27 ± 3.98	97.93 ± 4.98	6.94	7,22	0.0002
	vm	119.15 ± 9.49	107.30 ± 4.91	112.16 ± 8.19	93.85 ± 5.42	87.40 ± 7.69	105.41 ± 13.97	101.97 ± 6.48	68.27 ± 3.00	3.98	7,22	0.0059
vl	99.19 ±	111.91	120.70	100.11 ±	86.38 ±	105.57	110.47 ±	80.32	4.88	7,21	0.0021	

		5.87	± 3.46	± 7.04	4.87	6.41	± 8.81	3.50	± 6.83			
	core	71.26 ± 2.49	71.87 ± 4.16	94.06 ± 2.72	74.16 ± 3.95	67.73 ± 9.10	72.90 ± 3.48	83.69 ± 9.61	62.88 ± 1.51	3.21	7,20	0.0189
	shell	82.51 ± 9.31	86.76 ± 7.92	93.78 ± 2.14	72.20 ± 4.68	64.91 ± 12.07	87.68 ± 3.85	90.42 ± 13.70	67.65 ± 4.70		7,22	ns
PSD-95												
	AC	117.15 ± 3.49	101.35 ± 2.26	106.01 ± 1.93	99.42 ± 3.82	121.20 ± 3.16	105.00 ± 1.62	121.62 ± 3.91	127.65 ± 3.02	13.87	7,25	<.0001
	M2	107.05 ± 3.72	95.57 ± 3.13	100.65 ± 2.46	90.69 ± 2.60	110.58 ± 2.51	95.67 ± 1.69	110.03 ± 0.73	117.13 ± 2.17	13.85	7,25	<.0001
	M1	106.27 ± 3.50	94.11 ± 2.03	102.38 ± 2.67	92.89 ± 3.46	110.45 ± 2.53	94.15 ± 1.95	108.28 ± 1.71	115.88 ± 2.18	12.53	7,25	<.0001
	SS	101.82 ± 1.93	90.22 ± 1.57	97.38 ± 1.37	89.56 ± 2.90	107.96 ± 3.23	90.22 ± 1.86	103.96 ± 4.10	109.85 ± 2.66	10.70	7,25	<.0001
	I	116.18 ± 6.31	106.23 ± 1.50	111.79 ± 2.23	99.78 ± 3.78	121.48 ± 4.28	101.51 ± 1.54	119.05 ± 2.22	129.86 ± 3.29	11.68	7,25	<.0001
	dm	105.35 ± 5.04	94.17 ± 1.68	101.94 ± 3.74	93.52 ± 2.47	110.11 ± 4.46	95.14 ± 2.01	104.90 ± 2.69	112.77 ± 3.43	5.79	7,25	0.0005
	dl	104.23 ± 3.24	91.95 ± 1.81	101.10 ± 4.78	93.70 ± 3.17	113.40 ± 2.89	95.99 ± 1.80	107.00 ± 4.82	113.51 ± 3.13	6.99	7,25	0.0001
	vm	107.05 ± 6.27	98.89 ± 1.88	106.31 ± 4.38	95.83 ± 3.12	115.65 ± 3.20	101.29 ± 2.01	112.93 ± 4.34	121.14 ± 3.55	6.43	7,25	0.0002
	vl	110.04 ± 3.56	100.75 ± 2.45	107.82 ± 3.99	100.67 ± 4.13	122.13 ± 4.11	102.53 ± 2.61	115.26 ± 6.34	125.65 ± 4.34	5.98	7,25	0.0004
	core	111.16 ± 2.81	100.44 ± 1.72	109.61 ± 3.41	98.08 ± 4.80	118.16 ± 5.68	100.76 ± 1.85	119.63 ± 5.13	123.69 ± 5.37	6.16	7,25	0.0003
	shell	108.72 ± 4.37	99.40 ± 1.74	110.65 ± 3.07	97.47 ± 4.70	112.39 ± 4.81	98.91 ± 2.11	112.65 ± 2.41	121.38 ± 5.33	5.65	7,25	0.0005
Shank1												
	AC	127.37 ± 5.51	116.32 ± 3.09	114.32 ± 1.21	113.00 ± 0.69	116.27 ± 3.84	113.67 ± 1.11	111.44 ± 1.57	122.23 ± 2.63	3.57	7,21	0.0109
	M2	117.92 ± 0.37	114.03 ± 2.16	115.17 ± 2.11	112.71 ± 1.08	116.54 ± 3.95	113.44 ± 1.70	113.26 ± 2.17	122.38 ± 4.06		7,20	ns
	M1	114.27 ± 1.55	111.67 ± 2.07	112.32 ± 1.43	109.69 ± 0.95	112.23 ± 3.10	110.04 ± 1.71	108.76 ± 1.44	117.91 ± 2.64		7,20	ns
	SS	116.60 ± 3.75	111.55 ± 1.98	110.93 ± 1.41	109.09 ± 1.46	108.98 ± 2.95	109.95 ± 2.00	107.17 ± 2.12	114.49 ± 2.52		7,20	ns
	I	125.31 ± 3.03	118.68 ± 3.56	115.09 ± 1.29	111.62 ± 1.58	114.12 ± 2.78	111.64 ± 1.19	111.99 ± 2.24	123.01 ± 2.70	5.53	7,22	0.0009
	dm	99.79 ± 1.25	102.02 ± 1.66	99.38 ± 0.97	100.22 ± 0.82	100.84 ± 0.65	99.60 ± 0.95	94.86 ± 1.01	99.89 ± 0.08	5.10	7,20	0.0019
	dl	98.27 ± 1.23	101.99 ± 1.72	99.19 ± 0.66	97.96 ± 1.24	100.06 ± 1.18	99.43 ± 0.77	93.94 ± 0.53	98.65 ± 0.23	5.33	7,21	0.0013
	vm	101.66 ± 0.66	104.10 ± 2.26	100.54 ± 0.99	100.07 ± 1.24	103.26 ± 0.93	101.56 ± 0.97	95.96 ± 1.06	102.02 ± 0.90	4.69	7,21	0.0027
	vl	100.22 ± 1.05	103.23 ± 1.86	100.28 ± 0.85	99.22 ± 0.93	101.45 ± 1.30	100.53 ± 0.96	95.12 ± 1.34	100.80 ± 0.59	3.74	7,20	0.0094
	core	104.18 ± 1.22	106.93 ± 2.12	100.00 ± 1.13	98.80 ± 0.55	103.19 ± 1.61	100.58 ± 1.63	98.04 ± 0.97	103.33 ± 1.04	5.24	7,20	0.0016
	shell	104.95 ± 0.84	106.41 ± 1.80	99.51 ± 0.74	101.69 ± 1.61	103.06 ± 1.59	101.98 ± 1.04	96.29 ± 1.68	104.57 ± 0.77	5.83	7,19	0.0010

Table 2.

Table 2. The table summarizes values of mRNA expression in relative d.p.m.mean value±S.E.M. for *Homer1a*, *Homer1b*, *Arc*, *PSD-95*, and *Shank1* transcripts, and significant values (P) and effect sizes (F) along with degrees of freedom of one-way ANOVA. Data are listed by brain regions analyzed. AC= anterior cingulate cortex; M2= medial agranular cortex; M1= motor cortex; SS= somatosensory cortex; I= insular cortex; dmCP = dorso-medial caudate putamen; dlCP = dorso-lateral caudate putamen; vlCP = ventro-lateral caudate putamen; vmCP = ventro-medial caudate putamen; core = core of the nucleus accumbens; shell= shell of the nucleus accumbens. Vehicle (NaCl 0.9%, VEH), haloperidol 0.8 mg/kg (HAL0.8), haloperidol 0.5 mg/kg (HAL0.5), haloperidol 0.25 mg/kg (HAL0.25), asenapine 0.3 mg/kg (ASE0.3), asenapine 0.1 mg/kg (ASE0.1), asenapine 0.05 mg/kg (ASE0.05), olanzapine 2.5 mg/kg (OLA).

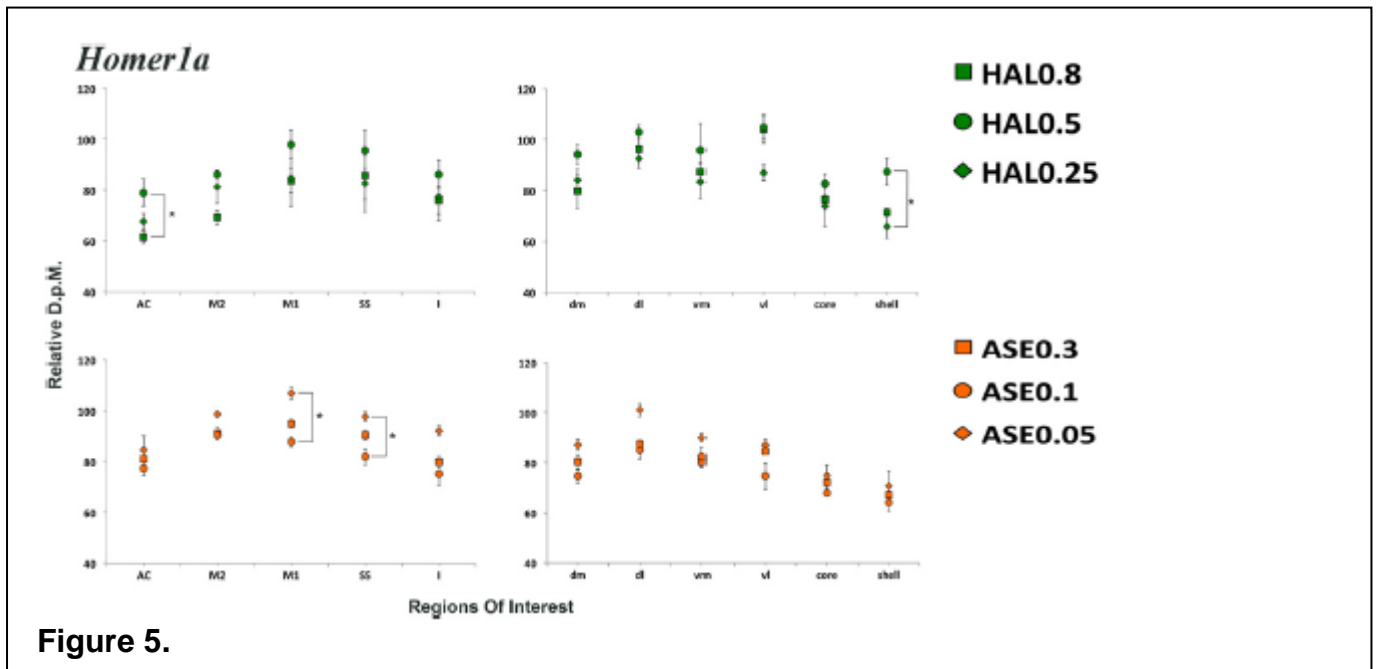


Figure 5.

Figure 5. Intragroup differences in *Homer1a* mRNA expression among haloperidol doses (upper panel), i.e. haloperidol 0.8 mg/kg (HAL0.8), haloperidol 0.5mg/kg (HAL0.5), and haloperidol 0.25mg/kg (HAL0.25); and among asenapine doses (lower panel), i.e. asenapine 0.3mg/kg (ASE0.3), asenapine 0.1 mg/kg (ASE0.1), asenapine 0.05mg/kg (ASE0.05). Data are reported in relative d.p.m. as mean ± S.E.M. * = significant difference at the Student-Newman-Keuls (SNK) post-hoc test with Bonferroni correction (p < 0.05). Lines connect groups whose mean mRNA expression is significantly different. AC= anterior cingulate cortex; M2= medial agranular cortex; M1= motor cortex; SS= somatosensory cortex; I = insular cortex; dmCP = dorso-medial caudate putamen; dlCP = dorso-lateral caudate putamen; vlCP = ventro-lateral caudate putamen; vmCP = ventro-medial caudate putamen; core = core of the nucleus accumbens; shell= shell of the nucleus accumbens.

	<i>Homer1a</i>	<i>Homer1b</i>	<i>Arc</i>	<i>PSD-95</i>	<i>Shank1</i>
AC	ASE 0.05 > HAL 0.8 ASE 0.3 > HAL 0.8			ASE0.05>HAL0.25 ASE0.3>HAL0.25 ASE0.05>HAL0.8 ASE0.3>HAL0.8 ASE0.05>HAL0.5 ASE0.3>HAL0.5	
M2	ASE 0.05 > HAL 0.8 ASE 0.3 > HAL 0.8 ASE 0.1 > HAL 0.8 ASE 0.05 > HAL 0.25	ASE0.05>HAL0.8 ASE0.05>HAL0.25	ASE0.1 > HAL0.8	ASE0.3>HAL0.25 ASE0.3>HAL0.8 ASE0.05>HAL0.25 ASE0.05>HAL0.8	
M1	ASE 0.05 > HAL 0.8 ASE 0.05 > HAL0.25	ASE0.05>HAL0.8 ASE0.05>HAL0.25	ASE0.05 > HAL0.8	ASE0.3>HAL0.25 ASE0.3>HAL0.8 ASE0.05>HAL0.25 ASE0.05>HAL0.8	
SS		ASE0.05>HAL0.8	ASE0.05 > HAL0.8	ASE0.3>HAL0.25 ASE0.3>HAL0.8 ASE0.05>HAL0.25 ASE0.05>HAL0.8	
I		ASE0.05>HAL0.8		ASE0.3>HAL0.25 ASE0.05>HAL0.25 ASE0.3>HAL0.8 ASE0.05>HAL0.8	
CPdm	HAL0.5>ASE0.1	ASE0.05>HAL0.8 ASE0.3>HAL0.8 ASE0.05>HAL0.25	HAL 0.5>ASE0.3	ASE0.3>HAL0.25 ASE0.3>HAL0.8	HAL0.8>ASE0.05 HAL0.25>ASE0.05 HAL0.5>ASE0.05
CPdl	HAL0.5>ASE0.1	ASE0.05>HAL0.8 ASE0.05>HAL0.25 ASE0.3>HAL0.8	ASE0.05 > HAL0.25 HAL0.8 > ASE0.3 HAL0.5 > ASE0.3	ASE0.3>HAL0.8 ASE0.3>HAL0.25 ASE0.05>HAL0.8	HAL0.8>ASE0.05 HAL0.5>ASE0.05
CPvm		ASE0.05>HAL0.8 ASE0.3>HAL0.8 ASE0.05>HAL0.25		ASE0.3>HAL0.25 ASE0.05>HAL0.25 ASE0.3>HAL0.8 ASE0.05>HAL0.8	HAL0.8>ASE0.05
CPvl	HAL0.5>ASE0.1 HAL0.8>ASE0.1 HAL0.5>ASE0.3 HAL0.8>ASE0.3	ASE0.05>HAL0.8	HAL0.5>ASE0.3 HAL0.8>ASE0.3	ASE0.3>HAL0.25 ASE0.3>HAL0.8	HAL0.8>ASE0.05 HAL0.5>ASE0.05
core		ASE0.05>HAL0.8	HAL0.5>ASE0.3	ASE0.05>HAL0.25 ASE0.3>HAL0.25 ASE0.05>HAL0.8 ASE0.3>HAL0.8	HAL0.8>ASE0.05 HAL0.8>ASE0.1
shell					

	HAL0.5>ASE0.1 HAL0.5>ASE0.3	ASE0.05>HAL0.8 HAL0.5>ASE0.1 ASE0.05>HAL0.25		ASE0.05>HAL0.25	HAL0.8>ASE0.05
--	--	--	--	-----------------	--------------------------

Table 3.

Table 3. Intergroup differences in genes expression by asenapine vs. haloperidol administration at the Student-Newman-Keuls (SNK) post-hoc test with Bonferroni correction (p < 0.05) within each ROI. In bold are reported those significant differences in which at least one of the two groups was also significantly different vs. vehicle. ASE0.3= Asenapine 0.3 mg/kg; ASE0.1 = Asenapine 0.1mg/kg; ASE0.05=Asenapine 0.05mg/kg;HAL0.8=Haloperidol 0.8mg/kg;HAL0.5=Haloperidol 0.5mg/kg;HAL0.25=Haloperidol 0.25 mg/kg. AC=anterior cingulated cortex; M2=medial agranular cortex; M1=motor cortex; SS =somatosensory cortex; I=insular cortex; dmCP=dorso-medial caudate putamen; dlCP=dorso-lateral caudate putamen; vlCP= ventro-lateral caudate putamen; vmCP= ventro-medial caudate putamen; core= core of the nucleus accumbens; shell = shell of the nucleus accumbens.

	<i>Homer1a</i>	<i>Homer1b</i>	<i>Arc</i>	<i>PSD-95</i>	<i>Shank1</i>
AC			ASE0.1 > OLA	OLA>ASE0.1	
M2		OLA>ASE0.1	ASE0.1 > OLA	OLA>ASE0.1	
M1	OLA > ASE 0.1		ASE0.05 > OLA	OLA>ASE0.1	
SS	OLA > ASE 0.1		ASE0.05 > OLA	OLA>ASE0.1	
I	OLA > ASE 0.1	OLA>ASE0.1	ASE 0.05 > OLA	OLA>ASE0.1	OLA>ASE0.1 OLA>ASE0.05
CPdm		OLA>ASE0.1		OLA>ASE0.1	OLA>ASE0.05
CPdl		OLA>ASE0.1	ASE0.05 > OLA	OLA>ASE0.1	OLA>ASE0.05
CPvm		OLA>ASE0.1	ASE 0.1 > OLA	OLA>ASE0.1	OLA>ASE0.05
CPvl	OLA>ASE0.1	OLA>ASE0.1	ASE 0.05 > OLA	OLA>ASE0.1	OLA>ASE0.05
core				OLA>ASE0.1	OLA>ASE0.05
shell		OLA>ASE0.1 OLA>ASE0.3		OLA>ASE0.1	OLA>ASE0.05

Table 4.

Table 4. Intergroup differences in gene expression by asenapine vs. olanzapine administration at the Student-Newman-Keuls (SNK) post-hoc test with Bonferroni correction (p < 0.05) within each ROI. In bold are reported those significant differences in which at least one of the two groups was also significantly different vs. vehicle. AC=anterior cingulated cortex; M2=medial agranular cortex; M1=motor cortex; SS =somatosensory cortex; I=insular cortex; dmCP=dorso-medial caudate putamen; dlCP=dorso-lateral caudate putamen; vlCP= ventro-lateral caudate putamen; vmCP= ventro-medial caudate putamen; core= core of the nucleus accumbens; shell = shell of the nucleus accumbens. Vehicle (NaCl 0.9%, VEH), haloperidol 0.8 mg/kg (HAL0.8), haloperidol 0.5 mg/kg (HAL0.5), haloperidol 0.25 mg/kg (HAL0.25), asenapine 0.3 mg/kg (ASE0.3), asenapine 0.1 mg/kg (ASE0.1), asenapine 0.05 mg/kg (ASE0.05), olanzapine 2.5 mg/kg (OLA).

	<i>Homer1a</i>	<i>Homer1b</i>	<i>Arc</i>	<i>PSD-95</i>	<i>Shank1</i>
AC	OLA>HAL0.8 OLA>HAL0.25		HAL0.5 > OLA	OLA>HAL0.25 OLA>HAL0.8 OLA>HAL0.5	
M2	OLA>HAL0.8 OLA>HAL0.25 OLA>HAL0.5	OLA>HAL0.8 OLA>HAL0.25		OLA>HAL0.25 OLA>HAL0.8 OLA>HAL0.5	
M1	OLA>HAL0.8 OLA>HAL0.25	OLA>HAL0.8		OLA>HAL0.25 OLA>HAL0.8 OLA>HAL0.5	
SS	OLA>HAL0.25 OLA>HAL0.8			OLA>HAL0.25 OLA>HAL0.8 OLA>HAL0.5	
I		OLA>HAL0.8		OLA>HAL0.25	OLA>HAL0.25

	OLA>HAL0.8			OLA>HAL0.8 OLA>HAL0.5	
CPdm	OLA>HAL0.8 OLA>HAL0.25	HAL0.5>OLA		OLA>HAL0.25 OLA>HAL0.8	
CPdl	OLA>HAL0.8 OLA>HAL0.25	HAL0.8 > OLA HAL0.5 > OLA		OLA>HAL0.8 OLA>HAL0.25	
CPvm	OLA>HAL0.8 OLA>HAL0.25	HAL0.5>OLA HAL0.8>OLA		OLA>HAL0.25 OLA>HAL0.8 OLA>HAL0.5	
CPvl	OLA>HAL0.8 OLA>HAL0.25	HAL0.5>OLA HAL0.8>OLA		OLA>HAL0.8 OLA>HAL0.25 OLA>HAL0.5	
core			HAL0.5>OLA	OLA>HAL0.25 OLA>HAL0.8	
shell	OLA>HAL0.8 OLA>HAL0.25			OLA>HAL0.25 OLA>HAL0.8	

Table 5.

Table 5. Intergroup differences in genes expression by haloperidol vs. olanzapine administration at the Student-Newman-Keuls (SNK) post-hoc test with Bonferroni correction (p b 0.05) within each ROI. In bold are reported those significant differences in which at least one of the two groups was also significantly different vs. vehicle. AC=anterior cingulated cortex; M2=medial agranular cortex; M1=motor cortex; SS =somatosensory cortex; I=insular cortex; dmCP=dorso-medial caudate putamen; dlCP=dorso-lateral caudate putamen; vlCP= ventro-lateral caudate putamen; vmCP= ventro-medial caudate putamen; core= core of the nucleus accumbens; shell = shell of the nucleus accumbens. Vehicle (NaCl 0.9%, VEH), haloperidol 0.8 mg/kg (HAL0.8), haloperidol 0.5 mg/kg (HAL0.5), haloperidol 0.25 mg/kg (HAL0.25), asenapine 0.3 mg/kg (ASE0.3), asenapine 0.1 mg/kg (ASE0.1), asenapine 0.05 mg/kg (ASE0.05), olanzapine 2.5 mg/kg (OLA).

2.2.Homer1b

2.2.1. Gene expression differences between antipsychotic-administered groups and control group.

Homer1b expression was significantly decreased mostly by HAL0.8 in few cortical and striatal regions. ASE0.05 and olanzapine significantly increased gene expression levels limitedly to the shell of the nucleus accumbens (Figure 4., Table 2.).

2.2.2. Haloperidol intragroup gene expression differences.

Homer1b expression was poorly affected by the different doses of haloperidol considered in this study (Figure 6.). The major differences were found between HAL0.5 and HAL0.8, with the first treatment significantly increasing *Homer1b* mRNA compared to the latter treatment in cortical and striatal regions.

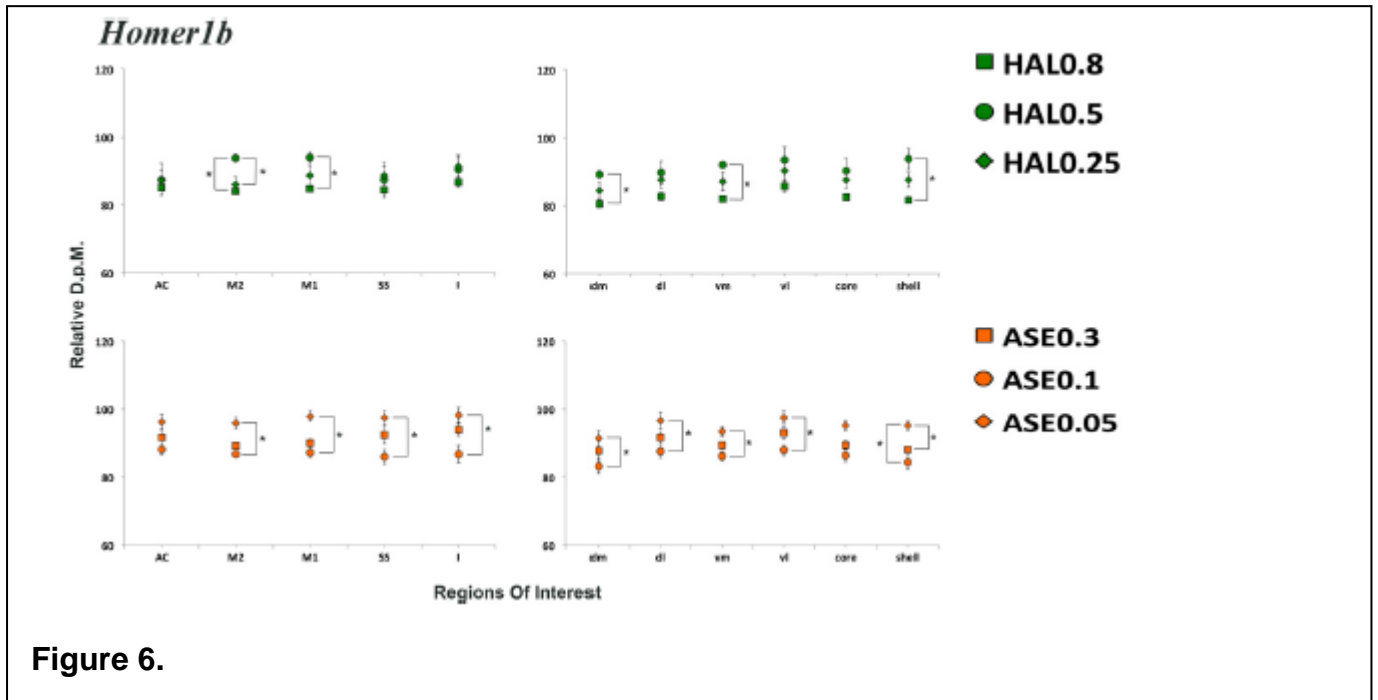


Figure 6.

Figure 6. Intragroup differences in *Homer1b* mRNA expression among haloperidol doses (upper panel), i.e. haloperidol 0.8mg/kg (HAL0.8), haloperidol 0.5mg/kg (HAL0.5), and haloperidol 0.25mg/kg (HAL0.25); and among asenapine doses (lower panel), i.e. asenapine 0.3mg/kg (ASE0.3), asenapine 0.1 mg/kg (ASE0.1), asenapine 0.05mg/kg (ASE0.05). Data are reported in relative d.p.m. as mean \pm S.E.M. * = significant difference at the Student-Newman-Keuls (SNK) post-hoc test with Bonferroni correction ($p < 0.05$). Lines connect groups whose mean mRNA expression is significantly different. AC=anterior cingulate cortex; M2=medial agranular cortex; M1=motor cortex; SS=somatosensory cortex; I=insular cortex; dmCP=dorso-medial caudate putamen; dlCP=dorso-lateral caudate putamen; vlCP=ventro-lateral caudate putamen; vmCP=ventro-medial caudate putamen; core=core of the nucleus accumbens; shell=shell of the nucleus accumbens.

2.2.3. Asenapine intragroup gene expression differences.

The different doses of asenapine administered affected *Homer1b* in both cortical and striatal regions (Figure 6.). Specifically, the low dose of asenapine significantly increased gene expression levels compared mostly to ASE0.1 administration in the ROIs considered.

2.2.4. Asenapine vs. Haloperidol gene expression differences.

In the ASE0.05 treated group, *Homer1b* mRNA levels in the cortex and in the striatum were significantly higher mainly compared to HAL0.8 and HAL0.25 (Table 3.). In the striatum, also ASE0.3 showed to significantly trigger gene expression at a higher extent compared to HAL0.8, while HAL0.5 increased *Homer1b* compared to ASE0.1 only in the shell of the nucleus accumbens (Table 3.).

2.2.5. Asenapine vs. Olanzapine gene expression differences.

Homer1b mRNA were significantly increased by olanzapine compared to ASE0.1 in both cortex and striatum regions (Table 4.).

2.2.6. Haloperidol vs. Olanzapine gene expression differences.

Olanzapine induced *Homer1b* gene levels in both cortical and striatal regions at a higher extent compared to HAL0.8 and HAL0.25 (Table 5.).

2.3. Relative Ratio of *Homer1a*/*Homer1b* expression

2.3.1. Haloperidol treatments

In the cortex, HAL0.8 administration significantly shifted the ratio toward *Homer1b* in ACC, MAC, MC and IC, HAL0.5 significantly shifted the ratio toward *Homer1b* in only one cortical region, while HAL0.25 chronic administration did not impact the isoforms relative ratio (Figure 7.). In the striatum, HAL0.8 shifted the ratio significantly toward *Homer1a* in the ventral caudate putamen, in the dorsolateral caudate putamen and in the nucleus accumbens. HAL0.25 and HAL0.5 were found to shift the ratio significantly toward *Homer1a* expression in the dorsal and ventro-lateral caudate putamen, and HAL0.5 administration produced the same effect also in the nucleus accumbens. (Figure 7.)

2.3.2. Asenapine treatments

In the IC region of the cortex, the administration of all the three doses of asenapine significantly shifted the ratio toward *Homer1b* expression (Figure 7.). ASE0.1 and ASE0.3 treatments produced the same effect also in MC, while only ASE0.1 shifted the ratio toward *Homer1b* in the SS region. In the striatum, the ratio toward *Homer1a* expression was shifted in the dorsolateral caudate putamen by all the three doses of asenapine (Figure 7.). ASE0.05 and ASE0.3 administration produced the same effect also in the dorso-medial and in the ventro-lateral caudate putamen, respectively. Finally, ASE0.1 and ASE0.3 shifted the ratio significantly toward *Homer1a* in the shell of the nucleus accumbens (Figure 7.)

2.3.3. Olanzapine treatment

In the cortex, olanzapine administration did not impact the relative ratio of *Homer1a*/*Homer1b* (Figure 7.)

In the striatum, olanzapine shifted the relative ratio significantly toward *Homer1a* in the lateral caudate putamen and in the nucleus accumbens (Figure 7.).

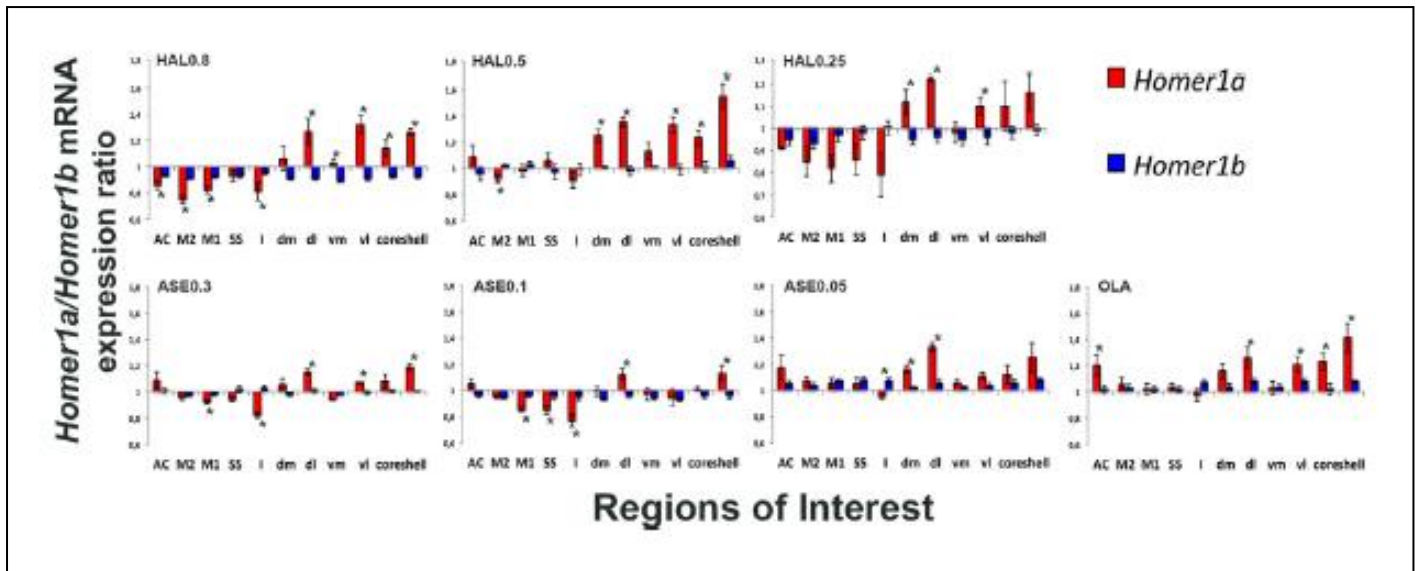


Figure 7.

Figure 7. Homer1a/Homer1b ratio by haloperidol 0.8mg/kg (HAL0.8), haloperidol 0.5mg/kg (HAL0.5), haloperidol 0.25mg/kg (HAL0.25), asenapine 0.3mg/kg (ASE0.3), asenapine 0.1mg/kg (ASE0.1), asenapine 0.05 mg/kg (ASE0.05), olanzapine 2.5 mg/kg (OLA) within each ROI; *=significant difference at the Student's t-test (p < 0.05). AC=anterior cingulate cortex; M2= medial agranular cortex; M1= motor cortex; SS = somatosensory cortex; I= insular cortex; dmCP= dorso-medial caudate putamen; dlCP= dorso-lateral caudate putamen; vlCP= vventro-lateral caudate putamen; vmCP= ventro-medial caudate putamen; core= core of the nucleus accumbens; shell = shell of the nucleus accumbens.

2.4.Arc

2.4.1. Gene expression differences between antipsychotic-administered groups and control group.

In the cortex, *Arc* expression levels were significantly reduced by all haloperidol doses. Also ASE0.1 and ASE0.3 and olanzapine exerted the same effects on the transcript levels of expression (Figure 4., Table 2.).

In the striatum, *Arc* mRNA levels were mostly reduced by olanzapine administration (Figure 4., Table 2.).

2.4.2. Haloperidol intragroup gene expression differences.

The comparison among the different doses of haloperidol did not produce many significant *Arc* expression differences (Figure 8.). The major differences were found in the shell of the nucleus accumbens, where HAL0.5 triggered significantly higher expression of *Arc* compared to HAL0.8 (Figure 8.).

2.4.3. Asenapine intragroup gene expression differences.

The main differences in *Arc* expression were observed in the dorso-lateral caudate putamen, where the transcript was significantly induced at a higher extent by ASE0.05 compared to ASE0.3 and ASE0.1 only (Figure 8.).

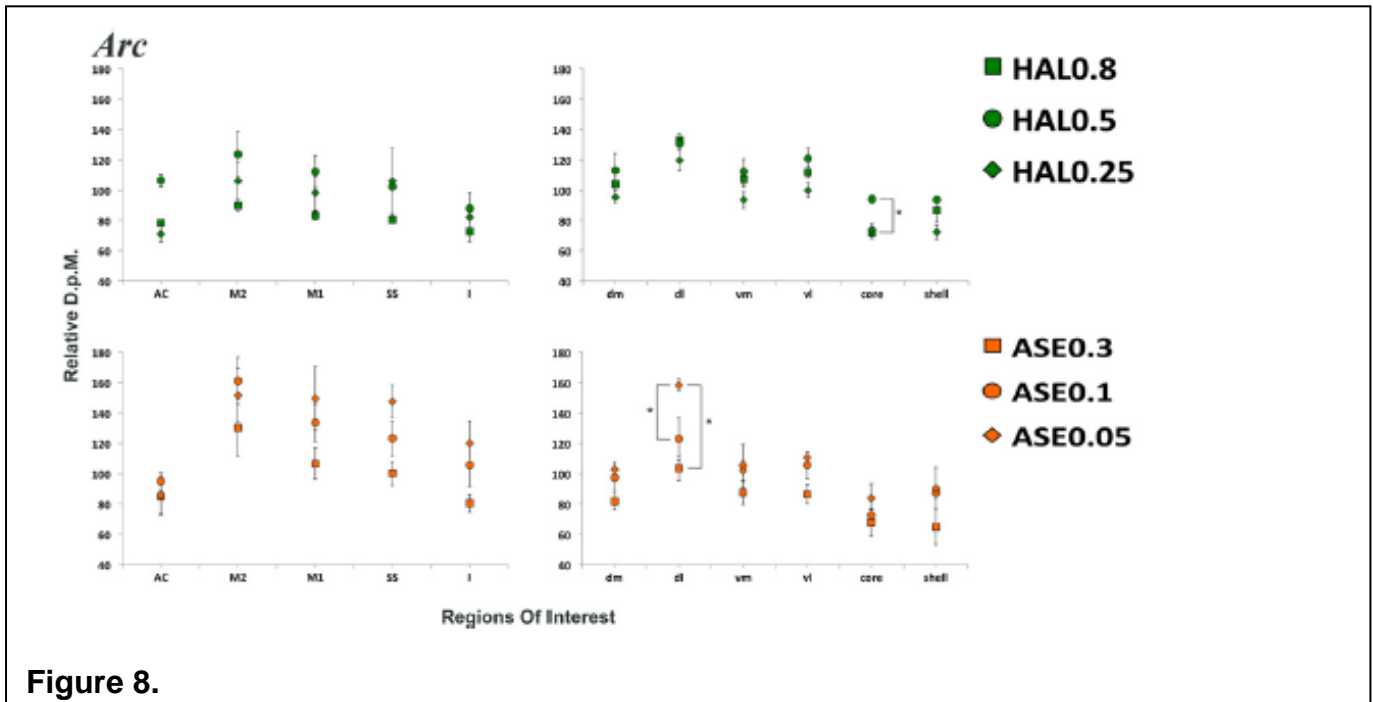


Figure 8. Intragroup differences in *Arc* mRNA expression among haloperidol doses (upper panel), i.e. haloperidol 0.8 mg/kg (HAL0.8), haloperidol 0.5 mg/kg (HAL0.5), and haloperidol 0.25 mg/kg (HAL0.25); and among asenapine doses (lower panel), i.e. asenapine 0.3 mg/kg (ASE0.3), asenapine 0.1 mg/kg (ASE0.1), asenapine 0.05 mg/kg (ASE0.05). Data are reported in relative d.p.m. as mean \pm S.E.M. * = significant difference at the Student-Newman-Keuls (SNK) post-hoc test with Bonferroni correction ($p < 0.05$). Lines connect groups whose mean mRNA expression is significantly different

2.4.4. Asenapine vs. Haloperidol gene expression differences.

In the cortex, *Arc* expression was found significantly higher in the ASE0.05 and ASE0.1 treated groups compared to HAL0.8 (Table 3).

In the majority of the striatal regions considered, *Arc* mRNA levels were found significantly higher in the HAL0.5 and HAL0.8 treated groups compared to ASE0.3 treated group (Table 3.). To note, only in the dorso-lateral caudate putamen ASE0.05 induced higher levels of the transcript compared to the low dose of haloperidol (Table 3.).

2.4.5. Asenapine vs. Olanzapine gene expression differences.

In both cortical and striatal regions, ASE0.05 and ASE0.1 induced significantly higher levels of *Arc* mRNA when compared to olanzapine treated group (Table 4.).

2.4.6. Haloperidol vs. Olanzapine gene expression differences.

The main significant differences in gene expression were found in the striatum, where haloperidol induced *Arc* mRNA levels at a higher extent compared to olanzapine (Table 5.)

2.5.PSD-95

2.5.1. Gene expression differences between antipsychotic-administered groups and control group.

In cortical regions, *PSD-95* expression was significantly decreased by HAL0.8, HAL0.25 and by ASE0.1 (Figure 4., Table 2.).

In the striatum, gene expression levels were not affected by the antipsychotics chronically administered in this study when compared to the control group (Figure 4., Table 2.).

2.5.2. Haloperidol intragroup gene expression differences.

The different doses of haloperidol did not affect *PSD-95* expression levels differentially in the cortical and striatal regions considered herein (Figure 9.).

2.5.3. Asenapine intragroup gene expression differences.

In both cortical and striatal regions, *PSD-95* expression was affected mainly by ASE0.05 and ASE0.3 that significantly increased gene expression compared to ASE0.1 (Figure 9.).

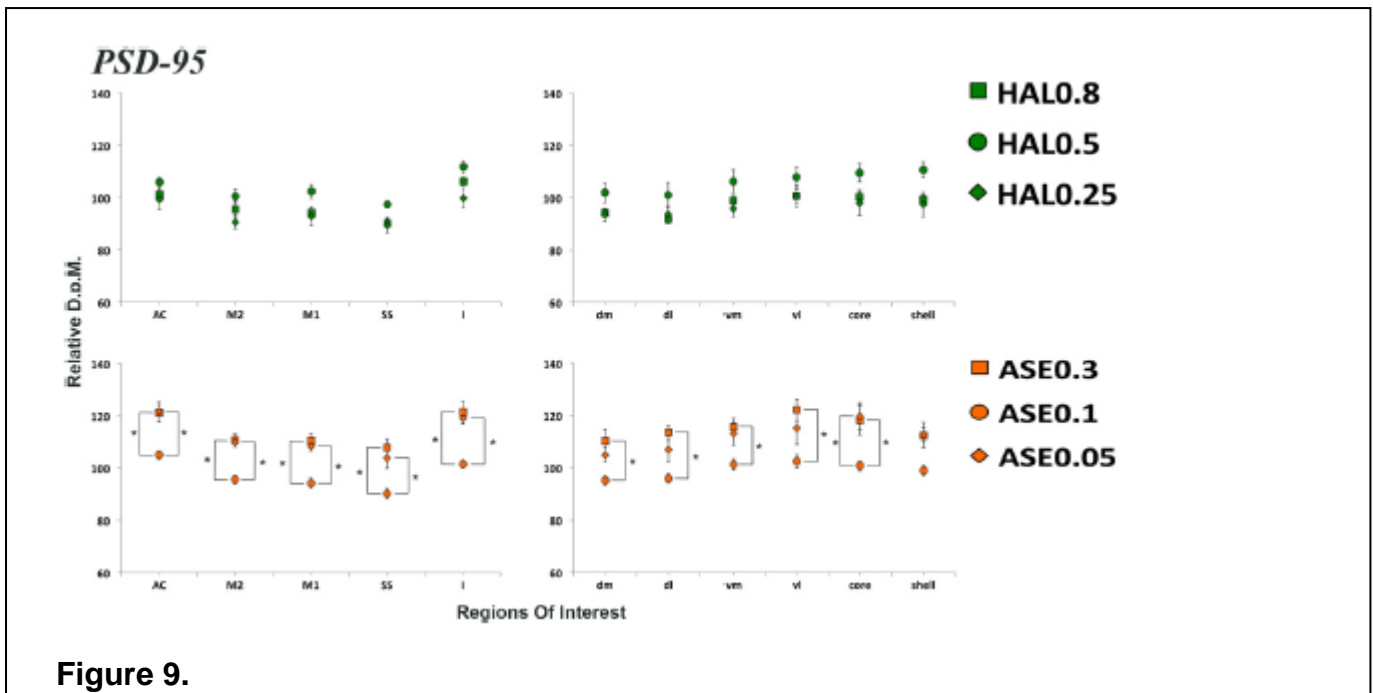


Figure 9.

Figure 9. Intragroup differences in PSD-95 mRNA expression among haloperidol doses (upper panel), i.e. haloperidol 0.8 mg/kg (HAL0.8), haloperidol 0.5 mg/kg (HAL0.5), and haloperidol 0.25mg/kg (HAL0.25); and among asenapine doses (lower panel), i.e. asenapine 0.3mg/kg (ASE0.3), asenapine 0.1 mg/kg (ASE0.1), asenapine 0.05mg/kg (ASE0.05). Data are reported in relative d.p.m. as mean \pm S.E.M. * = significant difference at the Student-Newman-Keuls (SNK) post-hoc test with Bonferroni correction ($p < 0.05$). Lines connect groups whose mean mRNA expression is significantly different.

2.5.4. Asenapine vs. Haloperidol gene expression differences.

In cortical ROIs, *PSD-95* transcript was found significantly higher mainly in the ASE0.05 and ASE0.3 treated groups compared to all haloperidol treated groups (Table 3.).

In the majority of the striatal regions, ASE0.05 and ASE0.3 increased gene expression mainly compared to the HAL0.25 and HAL0.8 (Table 3.).

2.5.5. Asenapine vs. Olanzapine gene expression differences.

In both cortex and striatum, olanzapine was found to significantly increase *PSD-95* expression compared to ASE0.1 (Table 4.).

2.5.6. Haloperidol vs. Olanzapine gene expression differences.

In the cortex, olanzapine significantly induced higher levels of *PSD-95* mRNA compared to all doses of haloperidol administered.

In the striatum, olanzapine was found to significantly induce the transcript when compared to HAL0.8 and HAL0.25 (Table 5.).

2.6. Shank1

2.6.1. Gene expression differences between antipsychotic-administered groups and control group.

In the cortex, *Shank1* mRNA levels were found decreased only in the ACC and IC regions by HAL0.25, HAL0.5, ASE0.05 and ASE0.1 (Figure 4., Table 2.).

In the striatum, ASE0.05 significantly decreased *Shank1* transcript levels in all the regions considered herein (Figure 4., Table 2.).

2.6.2. Haloperidol intragroup gene expression differences.

Shank1 mRNA expression was found affected only in the striatum. Particularly, HAL0.8 increased significantly the gene expression compared to the intermediate and low dose of haloperidol considered herein in the nucleus accumbens (Figure 10.).

2.6.3. Asenapine intragroup gene expression differences.

As observed within the haloperidol treated groups, *Shank1* mRNA expression was found affected only in the striatum by the different doses of asenapine considered in this study (Figure 9). Indeed, the ASE0.05 significantly decreased gene expression compared to ASE0.1 and ASE0.3 in almost all caudate putamen regions and in the shell of the nucleus accumbens (Figure 10.).

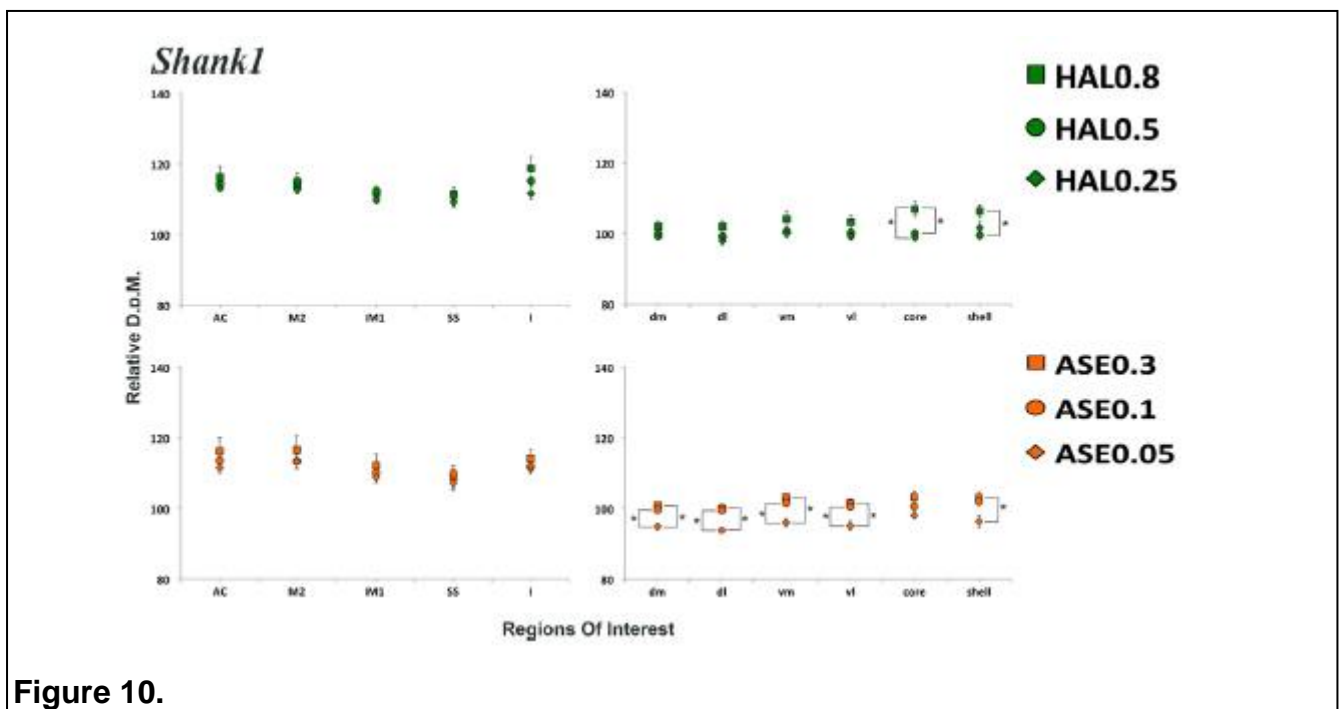


Figure 10. Intragroup differences in *Shank1* mRNA expression among haloperidol doses (upper panel), i.e. haloperidol 0.8 mg/kg (HAL0.8), haloperidol 0.5 mg/kg (HAL0.5), and haloperidol 0.25mg/kg (HAL0.25); and among asenapine doses (lower panel), i.e. asenapine 0.3mg/kg (ASE0.3), asenapine 0.1 mg/kg (ASE0.1), asenapine 0.05mg/kg (ASE0.05). Data are reported in relative d.p.m. as mean \pm S.E.M. * = significant difference at the

Student-Newman-Keuls (SNK) post-hoc test with Bonferroni correction ($p < 0.05$). Lines connect groups whose mean mRNA expression is significantly different.

2.6.4. Asepinone vs. Haloperidol gene expression differences.

In the striatum, *Shank1* mRNA levels were significantly lower in the ASE0.05 treated group when compared to HAL0.8 and HAL0.5 treated groups (Table 3.).

2.6.5. Asepinone vs. Olanzapine gene expression differences.

In both cortical and striatal regions, *Shank1* mRNA levels were found significantly increased by olanzapine when compared to ASE0.05 (Table 4.).

2.6.6. Haloperidol vs. Olanzapine gene expression differences.

Olanzapine triggered *Shank1* expression at a significant higher extent compared to HAL0.25 only in the IC region of the cortex (Table 5.).

CHAPTER 5

Quantitative comparison of acute versus chronic antipsychotic treatments on the immediate early gene *Homer1a* expression profile

1.Rationale

Molecular effects of antipsychotics may dramatically change according to the timing of administration (de Bartolomeis et al., 2015). Antipsychotic agents significantly modulate the expression and topography of PSD transcripts after acute treatments in animal studies (de Bartolomeis et al., 2013b; Fumagalli et al., 2008). Indeed, in a previous acute paradigm of administration, increasing doses of haloperidol, olanzapine and asenapine have been reported to induce a progressive recruitment of cortical/sub-cortical regions in rat brains (de Bartolomeis et al., 2015). Specifically, the administration of the above mentioned compounds at each dose produced a significant increase in the expression of early and constitutive genes in cortical and sub-cortical ROIs, with the exception of *Arc* mRNA expression in the cortex (de Bartolomeis et al., 2015).

Following the observations made in the previous chapter, we therefore aimed at investigating the molecular effects of acute *versus* chronic administration of the same compounds (haloperidol, olanzapine and asenapine) at different doses, in order to obtain an head-to-head comparison of the two paradigms of treatment on the expression pattern of the IEG *Homer1a*. Indeed, our goal was to use *Homer1a* expression as a molecular tool to assess putative plastic PSD rearrangements after acute treatments *versus* chronic ones.

To do so, we co-exposed slides corresponding to the treatment groups of both acute and chronic paradigms (namely: VEH; HAL0.25; HAL0.5; HAL0.8; ASE0.05; ASE0.1; ASE0.3; OLA) on the same auto-radiographic sheet. Mean values obtained by quantitation of the signal intensity for each treatment were normalized by subdividing them with vehicle's mean values obtained in the corresponding ROI. Therefore, results were given as a percentage of vehicle mRNA expression.

The Student's t-test was used to compare acute *versus* chronic normalized *Homer1a* mRNA levels by each antipsychotic in each ROI. In all tests, significance was set at $p < 0.05$. The statistical analyses were performed using JMP9.0.1 software.

2.Results

The main result obtained by this comparison was that *Homer1a* expression resulted significantly lower in chronic paradigms of treatment compared to acute ones. These observations were reported comparing the same compound and the same dose administered acutely or chronically. Finally, the pattern of expression of the IEG tested was affected both in cortical and sub-cortical ROIs, particularly depending on the compound tested (Table 6.).

2.1 Haloperidol induced Homer1a gene expression

The comparison of acute *versus* chronic haloperidol administration on *Homer1a* mRNA transcript resulted in significantly higher expression levels of the gene in the acute treated group of animals with respect to the chronically treated ones in striatal ROIs (Figure 11.). Moreover, the HAL0.8 group showed significant differences in gene expression also in the MC, SS and IC regions of the cortex.

2.2 Asenapine induced Homer1a gene expression

The comparison of acute *versus* chronic asenapine administration on *Homer1a* mRNA transcript resulted in significantly higher expression levels of the gene in the acute treated group of animals in respect of the chronically treated ones in several cortical and striatal ROIs (Figure 12.). Moreover, with increasing doses of the compound, the expression of the gene become significantly different in more striatal regions.

2.3 Olanzapine induced *Homer1a* gene expression

The comparison of acute *versus* chronic olanzapine administration on *Homer1a* mRNA transcript resulted in significantly higher expression levels of the gene in the acute treated group of animals in respect of the chronically treated ones in several cortical and striatal ROIs (Figure 13.).

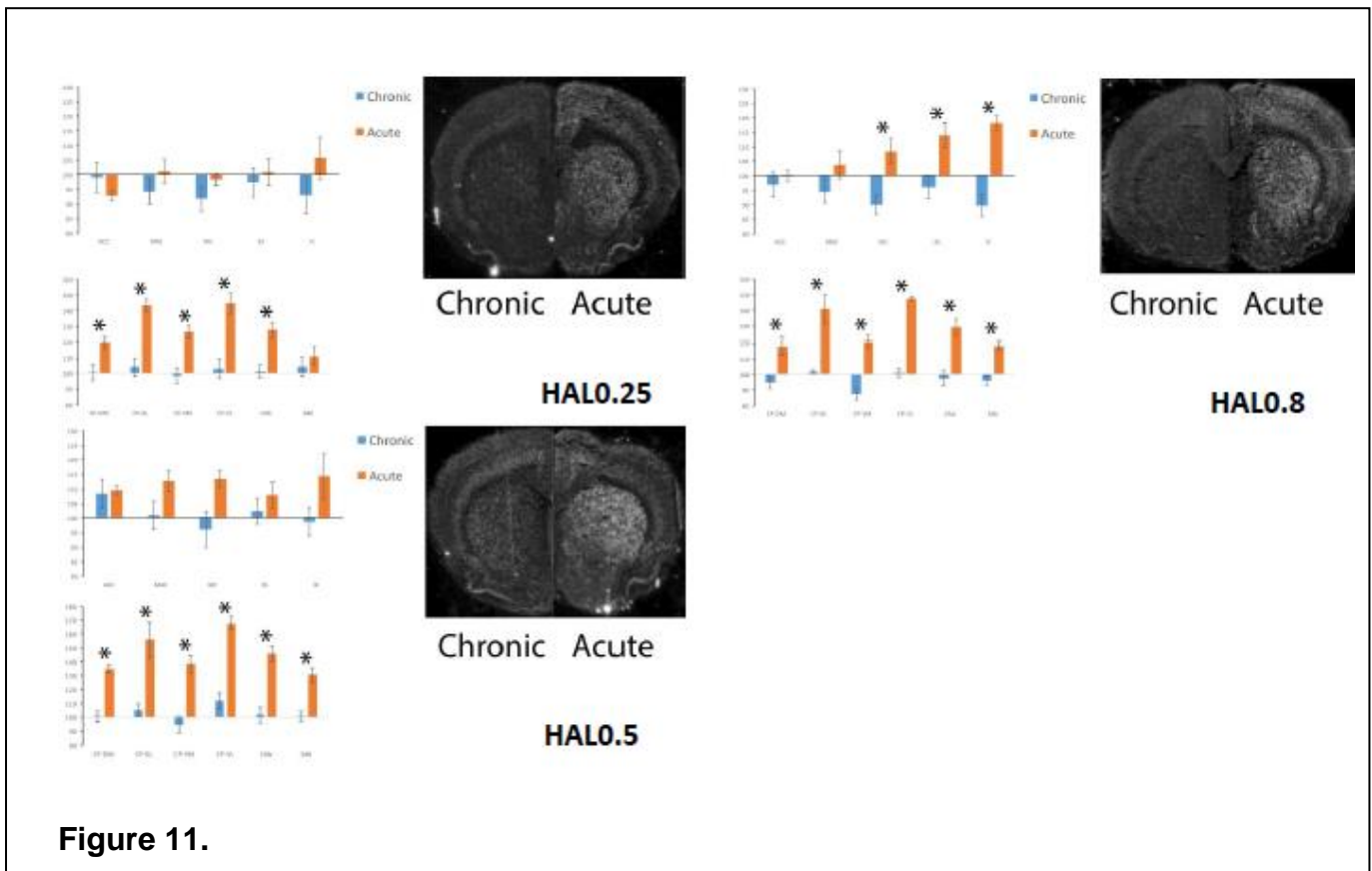


Figure 11. Normalized *Homer1a* mRNA levels after acute (blue bars) *versus* chronic (orange bars) haloperidol administration at different doses. Data are given as a percentage vehicle mRNA expression. * significant difference at the Student's t test ($p < .05$). Haloperidol 0.8 mg/kg (HAL0.8), haloperidol 0.5 mg/kg (HAL0.5), and haloperidol 0.25mg/kg (HAL0.25).

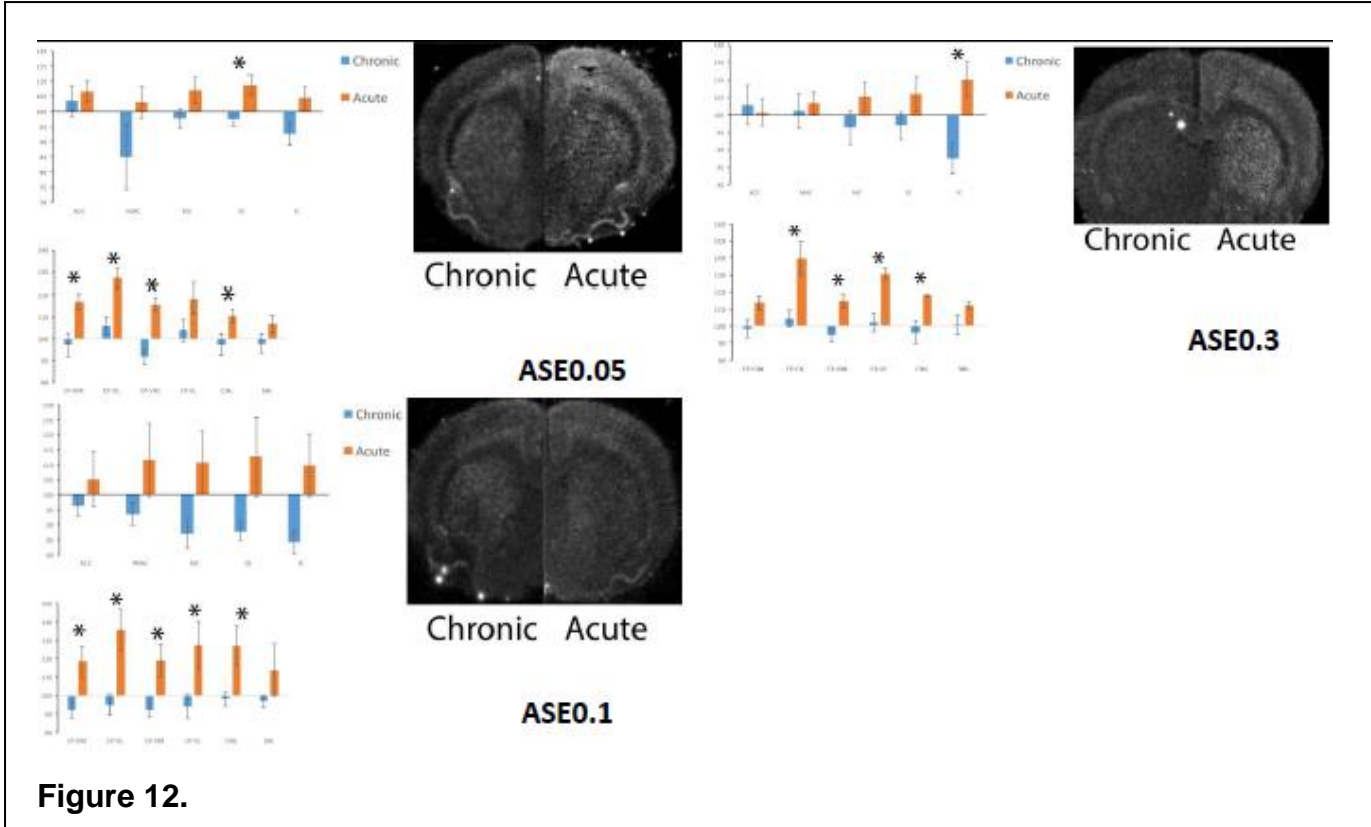


Figure 12.

Figure 12. Normalized *Homer1a* mRNA levels after acute (blue bars) versus chronic (orange bars) asenapine administration at different doses. Data are given as a percentage vehicle mRNA expression. * significant difference at the Student's t test ($p < .05$). Asenapine 0.3mg/kg (ASE0.3), asenapine 0.1 mg/kg (ASE0.1), asenapine 0.05mg/kg (ASE0.05).

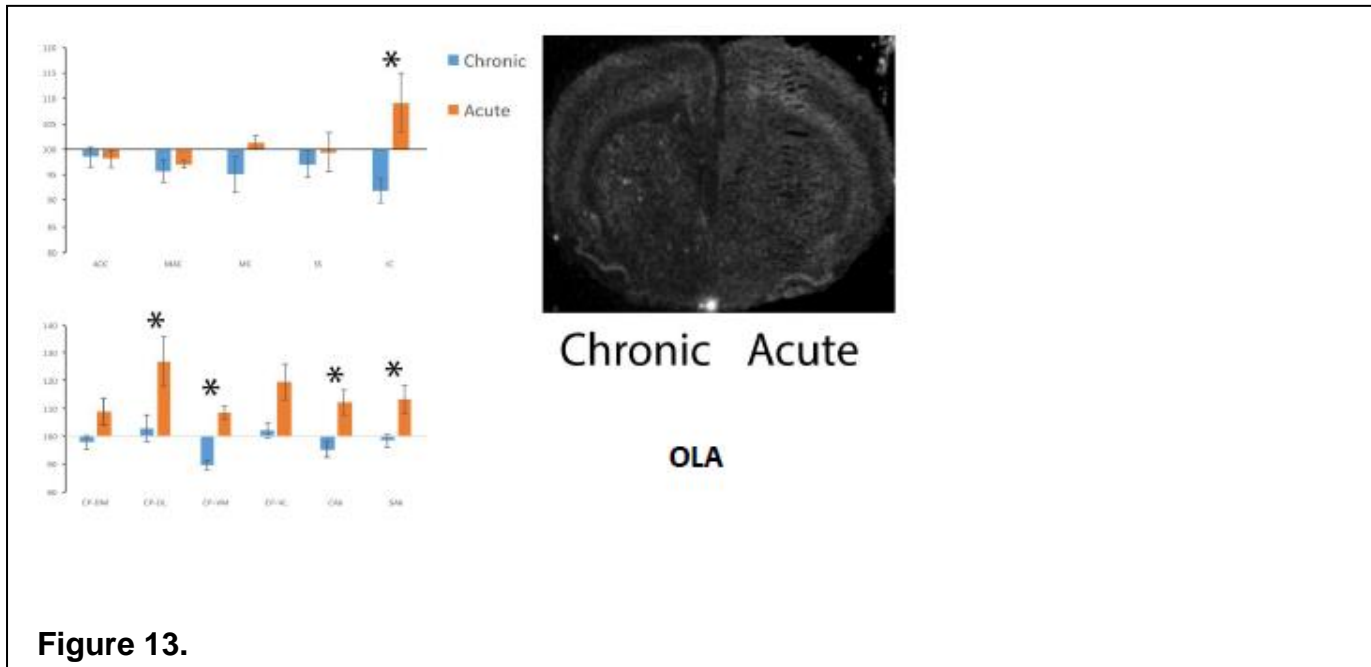


Figure 13.

Figure 13. Normalized *Homer1a* mRNA levels after acute (blue bars) versus chronic (orange bars) olanzapine administration. Data are given as a percentage vehicle mRNA expression. * significant difference at the Student's t test ($p < .05$). Olanzapine (OLA).

Treatment	ROI	Student's t			
		p	df	F	
OLA	ACC	>.05	1,4	0,0168	
	MAC	>.05	1,4	0,3945	
	MC	>.05	1,4	2,9746	
	SS	>.05	1,4	0,2723	
	I	.0497	1,4	7,7406	Acute>Chronic
	CP-DM	>.05	1,4	4,3766	
	CP-DL	.0147	1,4	16,9410	Acute>Chronic
	CP-VL	>.05	1,4	6,0657	
	CP-VM	.0033	1,4	39,4520	Acute>Chronic
	CAb	.0327	1,4	10,2759	Acute>Chronic
	SAb	>.05	1,4	6,8605	
ASE 0.05	ACC	>.05	1,6	0,2336	
	MAC	>.05	1,6	0,7224	
	MC	>.05	1,6	3,0382	
	SS	.0337	1,6	7,5119	Acute>Chronic
	I	>.05	1,6	4,7885	
	CP-DM	.0238	1,6	9,0373	Acute>Chronic
	CP-DL	.0111	1,6	13,0899	Acute>Chronic
	CP-VL	>.05	1,6	2,8961	
	CP-VM	.0026	1,6	24,3438	Acute>Chronic
	CAb	>.05	1,6	5,3797	
	SAb	>.05	1,6	2,2209	
ASE 0.1	ACC	>.05	1,6	0,7625	
	MAC	>.05	1,6	1,9828	
	MC	>.05	1,6	4,4781	
	SS	>.05	1,6	3,3458	
	I	>.05	1,6	4,7971	
	CP-DM	.0284	1,6	8,2339	Acute>Chronic
	CP-DL	.0181	1,6	10,3792	Acute>Chronic
	CP-VL	>.05	1,6	5,4368	
	CP-VM	.0340	1,6	7,4771	Acute>Chronic
	CAb	.0452	1,6	6,3562	Acute>Chronic
	SAb	>.05	1,6	1,3358	
ASE 0.3	ACC	>.05	1,5	0,0839	
	MAC	>.05	1,5	0,1139	
	MC	>.05	1,5	1,7002	
	SS	>.05	1,5	2,0861	
	I	.0188	1,5	11,7140	Acute>Chronic
	CP-DM	>.05	1,5	3,9544	
	CP-DL	.0024	1,5	32,1173	Acute>Chronic
	CP-VL	.0093	1,5	16,8715	Acute>Chronic

	CP-VM	.0216	1,5	10,8585	Acute>Chronic
	CAb	.0422	1,5	7,3534	Acute>Chronic
	SAb	>.05	1,5	2,4902	
HAL 0.25	ACC	>.05	1,6	1,2759	
	MAC	>.05	1,6	1,2917	
	MC	>.05	1,6	1,9612	
	SS	>.05	1,6	0,2658	
	I	>.05	1,6	1,7308	
	CP-DM	.0258	1,6	8,6707	Acute>Chronic
	CP-DL	.0012	1,6	33,4286	Acute>Chronic
	CP-VL	.0037	1,6	21,0306	Acute>Chronic
	CP-VM	.0046	1,6	19,3126	Acute>Chronic
	CAb	.0058	1,6	17,4517	Acute>Chronic
	SAb	>.05	1,6	0,6564	
HAL 0.5	ACC	>.05	1,5	0,0363	
	MAC	>.05	1,5	3,4733	
	MC	>.05	1,5	5,0683	
	SS	>.05	1,5	0,7583	
	I	>.05	1,5	3,1577	
	CP-DM	.0013	1,5	41,9684	Acute>Chronic
	CP-DL	.0086	1,5	17,4832	Acute>Chronic
	CP-VL	.0008	1,5	51,2822	Acute>Chronic
	CP-VM	.0040	1,5	25,3290	Acute>Chronic
	CAb	.0025	1,5	31,4600	Acute>Chronic
	SAb	.0048	1,5	23,1624	Acute>Chronic
HAL 0.8	ACC	>.05	1,6	0,4230	
	MAC	>.05	1,6	2,0622	
	MC	.0135	1,6	11,9538	Acute>Chronic
	SS	.0207	1,6	9,7079	Acute>Chronic
	I	.0007	1,6	40,9548	Acute>Chronic
	CP-DM	.0124	1,6	12,4444	Acute>Chronic
	CP-DL	.0062	1,6	17,0013	Acute>Chronic
	CP-VL	.0253	1,6	8,7540	Acute>Chronic
	CP-VM	.0007	1,6	40,5462	Acute>Chronic
	CAb	.0039	1,6	20,6230	Acute>Chronic
	SAb	.0014	1,6	31,6224	Acute>Chronic

Table 6.

Table 6. The table summarizes the P values and effect sizes (F) along with degrees of freedom of Student's t test. Data are listed by brain regions analyzed for each treatment. Haloperidol 0.8 mg/kg (HAL0.8), haloperidol 0.5 mg/kg (HAL0.5), and haloperidol 0.25mg/kg (HAL0.25); asenapine 0.3mg/kg (ASE0.3), asenapine 0.1 mg/kg (ASE0.1), asenapine 0.05mg/kg (ASE0.05); olanzapine (OLA).

CHAPTER 6

Nicotine and caffeine modulate haloperidol-induced changes in postsynaptic density transcripts expression.

1.Rationale

In clinical practice, antipsychotic therapy may be complicated by the exposure to substances such as caffeine and nicotine, which are among the most used ones by schizophrenia patients (Thoma and Daum, 2013). Intriguingly, these abuse-conducts may be functional for schizophrenia patients to alleviate antipsychotic side effects and/or psychotic symptoms (Acuna-Lizama et al., 2013; Featherstone and Siegel, 2015; Iasevoli et al., 2013a; Misiak et al., 2015). Indeed, caffeine and nicotine may counteract extrapyramidal side effects of antipsychotics (Oertel and Schulz, 2016) and both adenosine receptors (which are directly modulated by caffeine) and nicotine receptors modulation has been considered a potential pharmacological strategy to address residual symptoms not responding or responding poorly to conventional antipsychotics (Marcus et al., 2016; Rial et al., 2014). On the contrary, several studies have demonstrated that tobacco smoking and caffeine intake may impair neurocognitive outcomes, negative symptoms and social performances in schizophrenia patients (Iasevoli et al., 2013a; Nunez et al., 2015). Therefore, the final effect of caffeine or nicotine assumption in schizophrenia patients is still matter of debate.

Caffeine exerts an antagonist action on adenosine A1 receptor and A2A receptor (Chen et al., 2001), with the latter forming heteromers with postsynaptic D2 receptors in striatum (Ferre, 2016) . This observation can be of particular value, since the antagonistic action of caffeine on A2A receptors may modulate D2 receptors-mediated neurotransmission and therefore modify antipsychotics molecular action. For what concerns nicotine, it acts as an agonist at nicotinic acetylcholine (nACh) receptors, and this binding affinity particularly on receptors located on midbrain dopamine and GABAergic neurons has a final effect on dopamine firing (Dani and Bertrand, 2007; Pidoplichko et

al., 1997). To date, little is known about the molecular changes induced on brain plasticity processes by these compounds when given in association to antipsychotics. Considering the translational value of the research, we aimed at evaluating whether and to what extent PSD gene expression (Oligodeoxyribonucleotides complementary to bases sequence of *Homer1a*, *Homer1b* and *Arc* genes mRNAs are listed in Table 7.) and protein levels were affected by acute systemic administration of caffeine or nicotine alone or in association with the prototype first generation antipsychotic haloperidol or the indirect dopamine agonist GBR-12909.

Finally, behavioral (i.e. open field locomotor activity) testing was also carried out.

Rats were randomly assigned to one of the following treatment groups (n=8 for each group): 1) the control group receiving vehicle + vehicle injections (VEH); 2) vehicle + haloperidol 0.8 mg/kg (HAL); 3) vehicle + GBR-12909 30 mg/kg (GBR); 4) vehicle + caffeine 40 mg/kg (CAF); 5) vehicle + nicotine 1.5 mg/kg (NIC); 6) caffeine 40 mg/kg + haloperidol 0.8 mg/kg (CAF+HAL); 7) nicotine 1.5 mg/kg + haloperidol 0.8 mg/kg (NIC+HAL). The two subsequent injections were spaced by 20 minutes and were performed i.p.. All drugs were given at behaviorally active doses and caffeine and nicotine were administered at doses mimicking an intermediate-to-high caffeine/nicotine intake in humans (Cohen and George, 2013; Iasevoli et al., 2010b; Pechlivanova et al., 2010). Locomotor activity monitoring was assessed 20 minutes after the last injection.

For in situ hybridization histochemistry, animals were killed 90 minutes after the last injection.

For western blotting analysis, killing was performed 150 minutes after the last injection.

One-Way ANOVAs were used to compare groups and analyze treatment effects. The SNK *post-hoc* test with the Bonferroni correction was used to determine the locus of effects for significant ANOVA results. In all tests, significance was set at $p < 0.05$. The statistical analyses were performed using JMP9.0.1 software.

Probe	cDNA length (bp)	cDNA position	mRNA	Gen-Bank#
Homer1a	48	2527–2574	<i>Homer1a</i>	U92079
Homer1b/c	48	1306–1353	<i>Homer1b/c</i>	AF093268
Arc	45	789-833	<i>Arc</i>	NM019361

Table 7.

Table 7. Probes for in situ hybridization histochemistry.

2.Results

The major findings of the present study was that caffeine and nicotine *per se* were found to exert minor molecular effects on PSD molecules implicated in synaptic plasticity and antipsychotic induced molecular adaptations. However, these substances strongly affected haloperidol-mediated effects on *Homer1a* and *Arc* transcripts and, on the behavioral level, the locomotor activity appeared significantly different in groups receiving those substances *plus* haloperidol compared to the control group.

Results are listed as gene expression results obtained for each gene taken into account, followed by protein levels analyses at the level of the striatum. Finally, locomotor activity results are provided.

2.1.Gene Expression Analyses

2.1.1.Homer1a

In the cortex, only in the ACC region *Homer1a* expression was significantly reduced by caffeine plus haloperidol as compared to vehicle as well as to haloperidol alone.

In the striatum, *Homer1a* mRNA was significantly increased by HAL in all caudate putamen and nucleus accumbens regions compared to the control group. Nicotine alone only induced a significant *Homer1a* gene expression in the core of the nucleus accumbens, but the combination of NIC+HAL strongly enhanced *Homer1a* expression in dorso-medial and dorso-lateral striatum and in the nucleus accumbens. Caffeine administration alone provoked scarce modifications in striatal *Homer1a*

expression, while CAF+HAL provoked a peculiar decrease in the signal of the gene in medial caudate putamen and in the nucleus accumbens core as compared to VEH.

GBR-12909 induced *Homer1a* mRNA expression in ventro-medial caudate putamen and in the shell of the nucleus accumbens.

All statistically significant results are detailed in Table 8. Significant differences as compared to vehicle are depicted in Figure 14, intergroup differences are graphed in Figure 15.

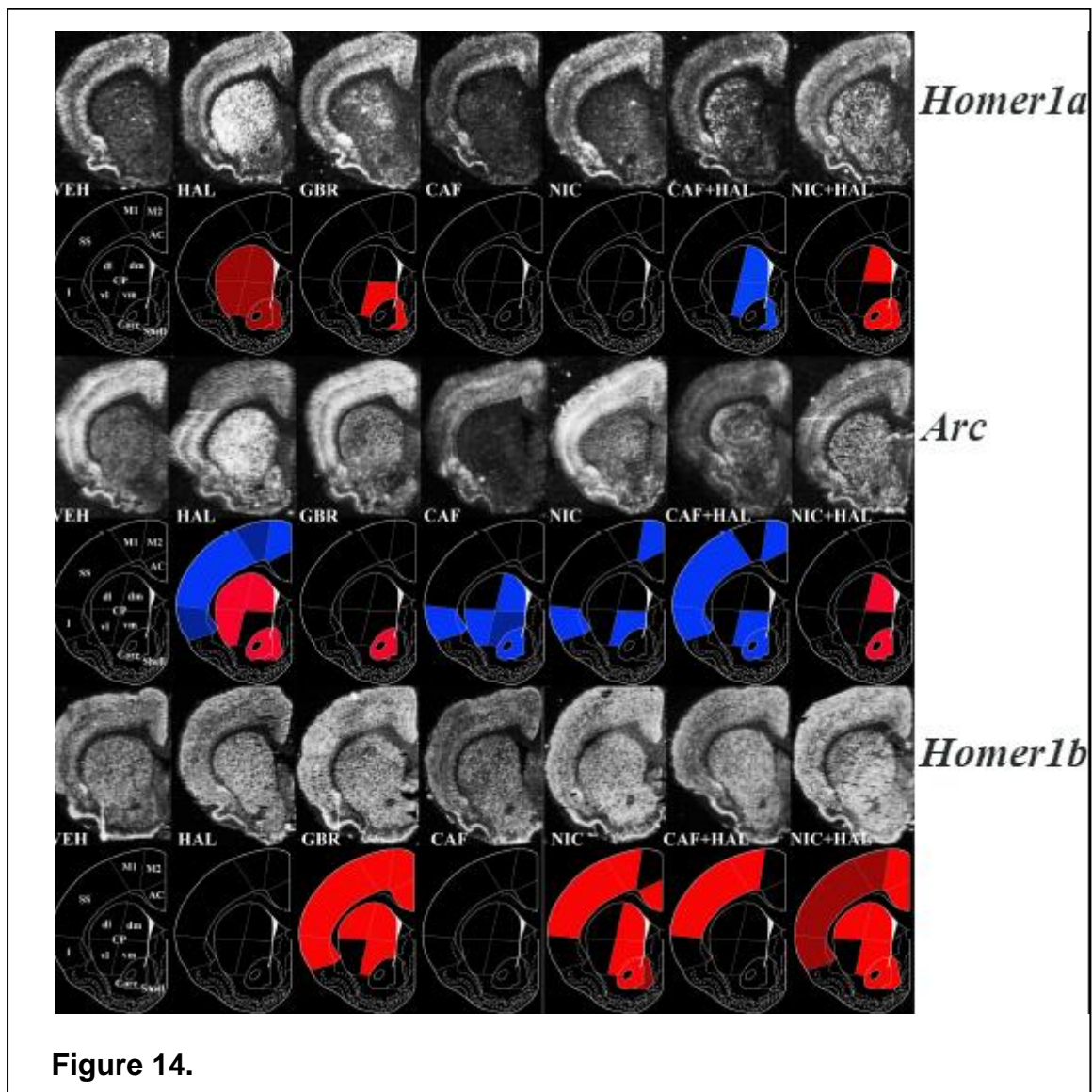


Figure 14.

Figure 14. Exemplificative autoradiographic film images of *Homer1a*, *Arc*, *Homer1b* mRNA expression detected by means of *in situ* hybridization histochemistry in coronal brain sections after acute treatment by vehicle+vehicle (NaCl 0.9%, VEH); vehicle+haloperidol 0.8mg/kg (HAL); vehicle+GBR-12909 30mg/kg (GBR); vehicle+caffeine 40mg/kg (CAF); vehicle+nicotine 1.5mg/kg (NIC); caffeine 40mg/kg+haloperidol 0.8mg/kg (CAF+HAL); nicotine 1.5mg/kg+haloperidol 0.8mg/kg (NIC+HAL). In the row below each gene-related series of exemplificative autoradiogram images, diagrams of regions of interest (ROIs) in which gene expression was measured were depicted. ROI-delimited color marks depict significant changes of mRNA expression compared to controls (i.e. VEH-treated rats) at the Student-Newman-Keuls post-hoc test (ANOVA, $p < 0.05$). Dark red: significant increase ($p < 0.001$); light red: significant increase ($p < 0.05$); dark blue: significant decrease ($p < 0.001$); light blue: significant decrease ($p < 0.05$); no color mark: no significant differences. AC=anterior cingulate cortex; M2=medial agranular cortex; M1=motor cortex; SS=somatosensory cortex; I=insular cortex; dm=dorso-medial caudate putamen; dl=dorso-lateral caudate putamen; vl= ventro-lateral caudate putamen; vm=ventro-medial caudate putamen; core=core of the nucleus accumbens; shell=shell of the nucleus accumbens. Modified from Paxinos and Watson (Paxinos and Watson, 1997)

	ANOVA		Post-hoc Test	
	F _(df)	p	Student-Newman-Keuls	Bonferroni
ACC	2.79 _{6,17}	0.04	CAF+HAL < VEH p=0.002 CAF+HAL < HAL p=0.006	CAF+HAL < VEH p=0.01 CAF+HAL < HAL p=0.04
MAC		ns		
MC		ns		
SS		ns		
IC		ns		
CP-DM	11.86 _{6,17}	<0.0001	HAL > VEH p=0.0004 CAF+HAL < VEH p=0.03 NIC+HAL > VEH p=0.03 CAF < GBR p=0.01 CAF < HAL p<0.0001 CAF+HAL < HAL p<0.0001 NIC < HAL p=0.0008 NIC+HAL < HAL p=0.04	HAL > VEH p=0.002 CAF < HAL p<0.0001 CAF+HAL < HAL p<0.0001 NIC < HAL p=0.005
CP-DL	6.38 _{6,17}	0.001	HAL > VEH p=0.0004 CAF < HAL p<0.0001 CAF+HAL < HAL p=0.001 NIC < HAL p=0.0002 NIC+HAL > VEH p=0.005	HAL > VEH p=0.002 CAF < HAL p<0.0001 NIC < HAL p=0.001 CAF+HAL < HAL p=0.007 NIC+HAL > VEH p=0.03
CP-VM	16.09 _{6,17}	<0.0001	HAL > VEH p=0.001 GBR > VEH p=0.03 CAF+HAL < VEH p=0.01 CAF < GBR p=0.0003 CAF < HAL p<0.0001 CAF+HAL < HAL p<0.0001 NIC < HAL p<0.0001 NIC+HAL < HAL p=0.001	HAL > VEH p=0.007 CAF < GBR p=0.002 CAF+HAL < HAL p<0.0001 CAF < HAL p<0.0001 NIC < HAL p<0.0001 NIC+HAL < HAL p=0.007
CP-VL	10.55 _{6,17}	<0.0001	HAL > VEH p<0.0001 CAF < HAL p<0.0001 CAF+HAL < HAL p<0.0001 NIC < HAL p<0.0001 NIC+HAL < HAL p=0.0004	HAL > VEH p<0.0001 CAF < HAL p<0.0001 CAF+HAL < HAL p<0.0001 NIC < HAL p<0.0001 NIC+HAL < HAL p=0.003
CAb	22.26 _{6,18}	<0.0001	HAL > VEH p<0.0001 CAF+HAL < VEH p=0.03 NIC+HAL > VEH p=0.02 CAF < GBR p=0.001 CAF < HAL p<0.0001 CAF+HAL < HAL p<0.0001 NIC < HAL p<0.0001 NIC+HAL < HAL p=0.0001	HAL > VEH p<0.0001 CAF < GBR p=0.007 CAF < HAL p<0.0001 CAF+HAL < HAL p<0.0001 NIC < HAL p<0.0001 NIC+HAL < HAL p=0.001

SAb	10.32 _{6,18}	<0.0001	<i>HAL > VEH p<0.0001</i>	<i>HAL > VEH p<0.0001</i>
			<i>GBR > VEH p=0.009</i>	<i>GBR > VEH p=0.05</i>
			<i>NIC > VEH p=0.05</i>	<i>NIC > VEH p=0.003</i>
			<i>NIC+HAL > VEH p=0.0005</i>	
			CAF < GBR p=0.01	CAF < HAL p<0.0001
			CAF < HAL p<0.0001	CAF+HAL < HAL p<0.0001
			CAF+HAL < HAL p<0.0001	CAF+HAL < HAL p<0.0001
			NIC < HAL p=0.008	NIC < HAL p=0.05
			NIC+HAL < HAL p=0.03	

Table 8.

Table 8. Summarization of statistical data for *Homer1a* mRNA expression analysis. In this table, we provided statistical data outputs after quantification of relativized signal intensity of *Homer1a* mRNA expression in ISHH. Data have been listed for Regions of Interest as effect size (F), degrees of freedom (df), and two-tailed p level. In case of significant ANOVA, results of group pair's comparisons at the Student-Newman-Keuls post-hoc test have been reported. Despite being an over-conservative test, we also included results after Bonferroni's correction. Only significant differences surviving after correction were reported. Significant differences vs. vehicle have been given in italics, for clarity.

Vehicle+vehicle (NaCl 0.9%, VEH); vehicle+haloperidol 0.8mg/kg (HAL); vehicle+GBR-12909 30mg/kg (GBR); vehicle+caffeine 40mg/kg (CAF); vehicle+nicotine 1.5mg/kg (NIC); caffeine 40mg/kg+haloperidol 0.8mg/kg (CAF+HAL); nicotine 1.5mg/kg+haloperidol 0.8mg/kg (NIC+HAL).

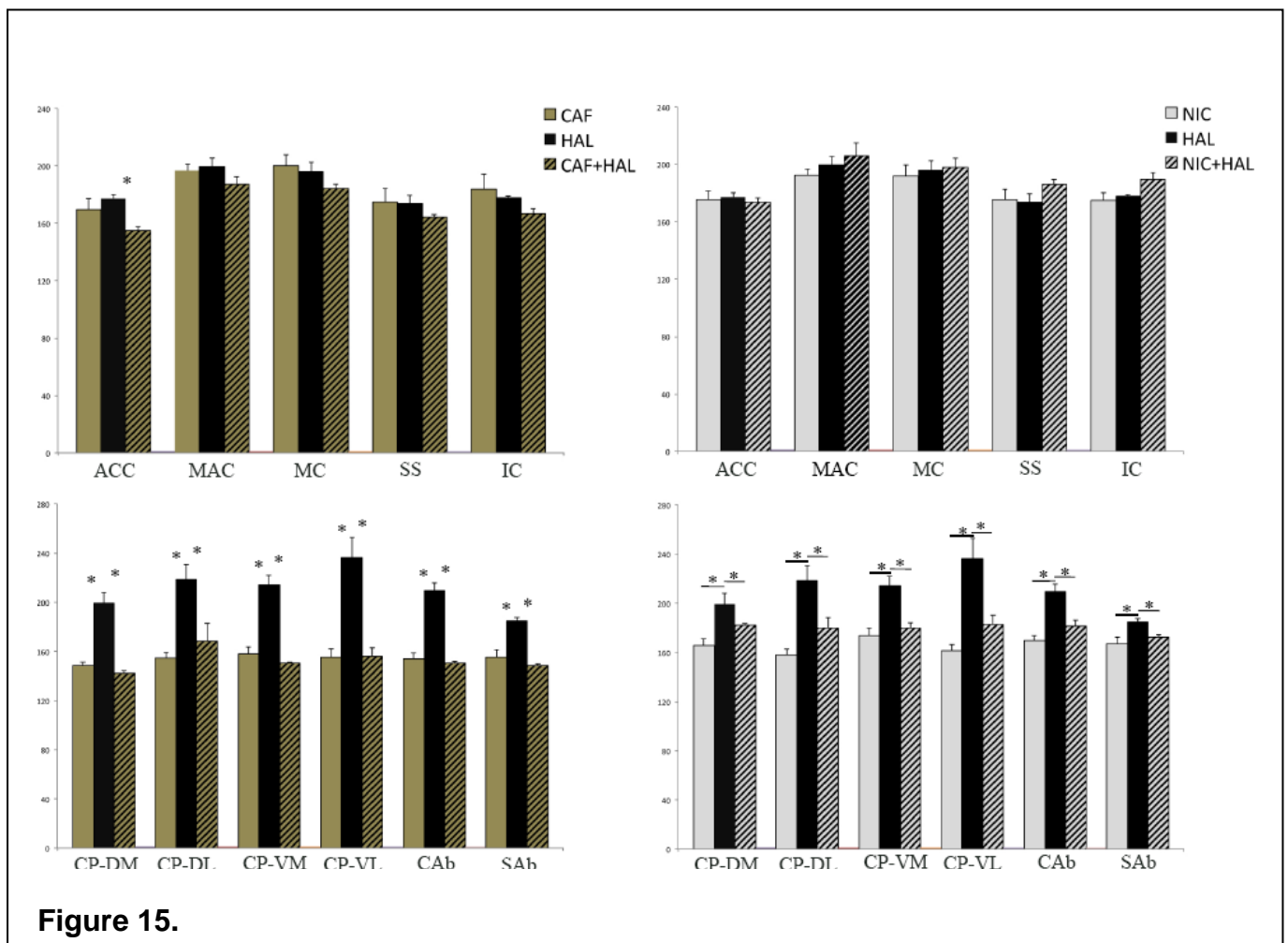


Figure 15.

Figure 15. Intergroup differences in *Homer1a* mRNA expression among haloperidol, caffeine, and caffeine+haloperidol (left side) and among haloperidol, nicotine, nicotine+haloperidol (right side) in cortical (upper side) and striatal (lower side) ROIs. Data were reported in relative d.p.m. as

mean±S.E.M. Lines connected groups whose mean mRNA expression was significantly different. * = significant difference at the Student-Newman-Keuls post-hoc test (p<0.05).

2.1.2. *Arc*

In the cortex, *Arc* transcript levels were significantly lower in HAL as compared to VEH. Nicotine treatment significantly decreased *Arc* expression in MC and IC regions compared to the control group, whereas caffeine provoked the same results only in the IC. CAF+HAL significantly reduced *Arc* mRNA expression in MC, SS and IC. To note, NIC+HAL, although not reaching statistical significance as compared to vehicle, was found to induce a slight, but significant, increase in *Arc* expression as compared to haloperidol.

In the striatum, *Arc* mRNA expression was significantly higher in the haloperidol treated group compared to the controls. Oppositely, CAF significantly reduced gene expression in almost all subcortical regions. Notably, CAF+HAL only induced significant decrease in *Arc* expression in ventro-medial caudate putamen and in the core region of the nucleus accumbens. Nicotine, when administered alone, resulted in no significant modifications of *Arc* gene expression, while NIC+HAL significantly increased *Arc* mRNA signal in medial striatal regions and in the nucleus accumbens. GBR-12909 specifically induced *Arc* gene expression in the nucleus accumbens core compared to the control group.

All statistically significant results are detailed in Table 9. Significant differences as compared to vehicle are depicted in Figure 14., intergroup differences are graphed in Figure 16.

	ANOVA		Post-hoc Test	
	F _(df)	p ns	Student-Newman-Keuls	Bonferroni
ACC				
MAC	2.92 _{6,18}	0.03	<i>HAL < VEH p=0.02</i> GBR > NIC p=0.02 NIC+HAL > HAL p=0.03	
MC	7.41 _{6,18}	0.0004	<i>HAL < VEH p=0.002</i> <i>NIC < VEH p=0.01</i> <i>CAF+HAL < VEH p=0.006</i> CAF < GBR p=0.001 NIC < GBR p=0.0002 NIC+HAL > HAL p=0.02	<i>HAL < VEH p=0.02</i> <i>CAF+HAL < VEH p=0.04</i> CAF < GBR p=0.007 NIC < GBR p=0.001
SS	2.77 _{6,18}	0.04	<i>HAL < VEH p=0.008</i> <i>CAF+HAL < VEH p=0.04</i> NIC+HAL > HAL p=0.02	<i>HAL < VEH p=0.05</i>
IC	3.19 _{6,18}	0.02	<i>HAL < VEH p=0.002</i> <i>CAF < VEH p=0.04</i> <i>NIC < VEH p=0.007</i> <i>CAF+HAL < VEH p=0.01</i> NIC+HAL > HAL p=0.02	<i>HAL < VEH p=0.01</i> <i>NIC < VEH p=0.05</i>
CP-DM	12.29 _{6,18}	<0.0001	<i>HAL > VEH p=0.02</i> <i>CAF < VEH p=0.006</i> <i>NIC+HAL > VEH p=0.007</i> CAF < GBR p=0.0001 NIC < GBR p=0.01 CAF < HAL p<0.0001 CAF+HAL < HAL p=0.0002 NIC < HAL p=0.002 NIC < NIC+HAL p=0.0005	<i>CAF < VEH p=0.04</i> <i>NIC+HAL > VEH p=0.05</i> CAF < GBR p=0.0007 CAF < HAL p<0.0001 CAF+HAL < HAL p=0.001 NIC < HAL p=0.01 NIC < NIC+HAL p=0.003
CP-DL	5.11 _{6,18}	0.003	<i>HAL > VEH p=0.04</i> CAF < GBR p=0.007 NIC < GBR p=0.03 CAF < HAL p=0.0003 CAF < CAF+HAL p=0.04 CAF+HAL < HAL p=0.04 NIC < HAL p=0.003 NIC < NIC+HAL p=0.006	CAF < GBR p=0.05 CAF < HAL p=0.002 NIC < HAL p=0.02 NIC < NIC+HAL p=0.04
CP-VM	12.61 _{6,18}	<0.0001	<i>CAF < VEH p<0.0001</i> <i>CAF+HAL < VEH p=0.01</i> <i>NIC+HAL > VEH p=0.03</i> CAF < GBR p<0.0001 NIC < GBR p=0.002 CAF < HAL p<0.0001	<i>CAF < VEH p<0.0001</i> CAF < GBR p<0.0001 NIC < GBR p=0.01 CAF < HAL p<0.0001

			CAF+HAL < HAL p=0.0006 NIC < HAL p=0.008 NIC < NIC+HAL p=0.0009	CAF+HAL < HAL p=0.004 NIC < HAL p=0.05 NIC < NIC+HAL p=0.006
CP-VL	8.82 _{6,18}	0.0001	<i>HAL > VEH p=0.005</i> <i>CAF < VEH p=0.02</i> CAF < GBR p=0.007 NIC < GBR p=0.04 CAF < HAL p<0.0001 CAF < CAF+HAL p=0.04 CAF+HAL < HAL p=0.0009 NIC < HAL p<0.0001 NIC < NIC+HAL p=0.001	<i>HAL > VEH p=0.03</i> CAF < GBR p=0.05 CAF < HAL p<0.0001 CAF+HAL < HAL p=0.006 NIC < HAL p<0.0001 NIC < NIC+HAL p=0.007
CAb	14.71 _{6,18}	<0.0001	<i>HAL > VEH p=0.002</i> <i>GBR > VEH p=0.03</i> <i>CAF < VEH p=0.006</i> <i>CAF+HAL < VEH p=0.04</i> <i>NIC+HAL > VEH p=0.02</i> CAF < GBR p<0.0001 NIC < GBR p=0.004 CAF < HAL p<0.0001 CAF+HAL < HAL p<0.0001 NIC < HAL p=0.0002 NIC < NIC+HAL p=0.001	<i>HAL > VEH p=0.01</i> <i>CAF < VEH p=0.04</i> CAF < GBR p<0.0001 NIC < GBR p=0.03 CAF < HAL p<0.0001 CAF+HAL < HAL p<0.0001 NIC < HAL p=0.001 NIC < NIC+HAL p=0.007
SAb	5.79 _{6,18}	0.002	<i>HAL > VEH p=0.008</i> <i>NIC+HAL > VEH p=0.007</i> CAF < GBR p=0.03 CAF < HAL p=0.0005 CAF+HAL < HAL p=0.002 NIC < HAL p=0.04 NIC < NIC+HAL p=0.04	<i>HAL > VEH p=0.05</i> <i>NIC+HAL > VEH p=0.05</i> CAF < HAL p=0.003 CAF+HAL < HAL p=0.01

Table 9.

Table 9. Summarization of statistical data for *Arc* mRNA expression analysis. In this table, we provided statistical data outputs after quantification of relativized signal intensity of *Arc* mRNA expression in ISHH. Data have been listed for Regions of Interest as effect size (F), degrees of freedom (df), and two-tailed p level. In case of significant ANOVA, results of group pair's comparisons at the Student-Newman-Keuls post-hoc test have been reported. Also, significant differences surviving Bonferroni's correction were reported. Significant differences vs. vehicle have been given in italics, for clarity.

Vehicle+vehicle (NaCl 0.9%, VEH); vehicle+haloperidol 0.8mg/kg (HAL); vehicle+GBR-12909 30mg/kg (GBR); vehicle+caffeine 40mg/kg (CAF); vehicle+nicotine 1.5mg/kg (NIC); caffeine 40mg/kg+haloperidol 0.8mg/kg (CAF+HAL); nicotine 1.5mg/kg+haloperidol 0.8mg/kg (NIC+HAL).

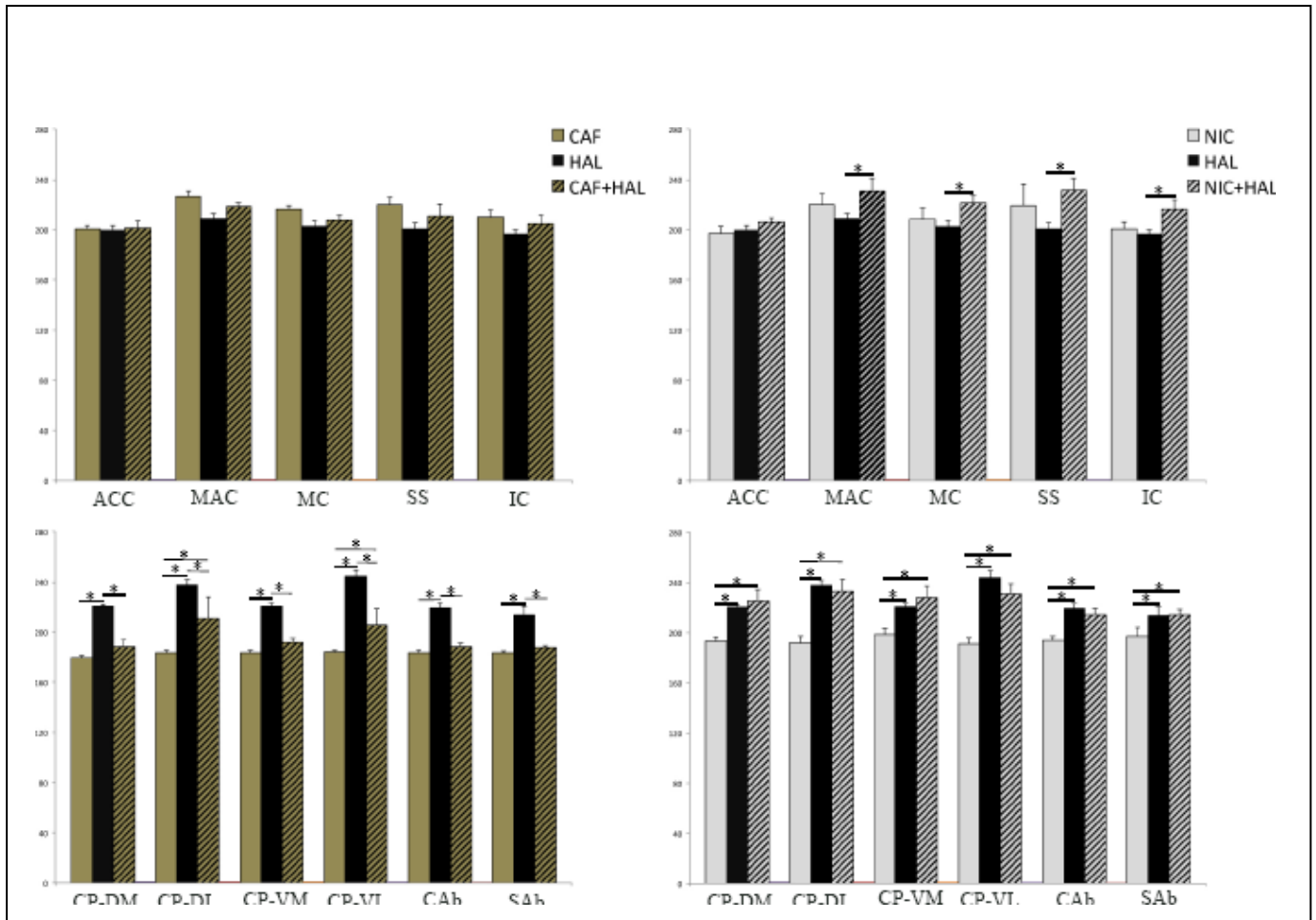


Figure 16.

Figure 16. Intergroup differences in *Arc* mRNA expression among haloperidol, caffeine, and caffeine+haloperidol (left side) and among haloperidol, nicotine, nicotine+haloperidol (right side) in cortical (upper side) and striatal (lower side) ROIs. Data were reported in relative d.p.m. as mean±S.E.M. Lines connected groups whose mean mRNA expression was significantly different. * = significant difference at the Student-Newman-Keuls post-hoc test ($p < 0.05$).

2.1.3. *Homer1b*

In the cortex, *Homer1b* mRNA expression was significantly increased by GBR-12909 administration as compared to vehicle. Nicotine significantly induced *Homer1b* expression as compared to vehicle in ACC, MC and SS, but NIC+HAL provoked a broader significant overexpression of *Homer1b* in all cortical subregions, similarly to GBR-12909. No cortical impact was found by caffeine on *Homer1b* when administered alone, while CAF+HAL strongly induced the expression of the constitutive gene specifically in the MC region. NIC+HAL produced an elevation of *Homer1b* mRNA levels at a greater extent than the sole haloperidol throughout the cortex, whereas in SS and IC nicotine reduced the gene expression as compared to NIC+HAL.

IC	5.62 6,19	0.001	<i>GBR > VEH p=0.008</i> <i>NIC+HAL > VEH p<0.0001</i> CAF < GBR p=0.03 NIC < NIC+HAL p=0.01 <i>NIC+HAL > HAL p=0.0007</i>	<i>GBR > VEH p=0.05</i> <i>NIC+HAL > VEH p<0.0001</i> <i>NIC+HAL > HAL p=0.005</i>
CP-DM	3.98 6,19	0.009	<i>GBR > VEH p=0.01</i> <i>NIC > VEH p=0.02</i> <i>NIC+HAL > VEH p=0.004</i> CAF < GBR p=0.006 <i>NIC+HAL > HAL p=0.02</i>	<i>NIC+HAL > VEH p=0.03</i> CAF < GBR p=0.05
CP-DL	2.82 6,19	0.04	<i>GBR > VEH p=0.01</i> <i>NIC+HAL > VEH p=0.04</i> CAF < GBR p=0.003 CAF < CAF+HAL p=0.05	CAF < GBR p=0.02
CP-VM	3.93 6,19	0.01	<i>GBR > VEH p=0.01</i> <i>NIC > VEH p=0.04</i> <i>NIC+HAL > VEH p=0.003</i> CAF < GBR p=0.008 <i>NIC+HAL > HAL p=0.009</i>	<i>NIC+HAL > VEH p=0.02</i> CAF < GBR p=0.05 <i>NIC+HAL > HAL p=0.05</i>
CP-VL	2.61 6,19	0.05	<i>GBR > VEH p=0.01</i> CAF < GBR p=0.005	CAF < GBR p=0.03
CAb	2.88 6,19	0.03	<i>NIC > VEH p=0.003</i> <i>NIC+HAL > VEH p=0.01</i> NIC > GBR p=0.03 NIC > HAL p=0.01 <i>NIC+HAL > HAL p=0.04</i>	<i>NIC > VEH p=0.02</i>
SAb	4,26 6,19	0.007	<i>GBR > VEH p=0.04</i> <i>NIC > VEH p=0.0007</i> <i>NIC+HAL > VEH p=0.006</i> NIC > GBR p=0.05 NIC > HAL p=0.002 <i>NIC+HAL > HAL p=0.02</i>	<i>NIC > VEH p=0.005</i> <i>NIC+HAL > VEH p=0.04</i> NIC > HAL p=0.01

Table 10.

Table 10. Summarization of statistical data for *Homer1b* mRNA expression analysis. In this table, we provided statistical data outputs after quantification of relativized signal intensity of *Homer1b* mRNA expression in ISHH. Data have been listed for Regions of Interest as effect size (F), degrees of freedom (df), and two-tailed p level. In case of significant ANOVA, results of group pair's comparisons at the Student-Newman-Keuls post-hoc test have been reported. Also, significant differences surviving Bonferroni's correction were reported. Significant differences vs. vehicle have been given in italics, for clarity.

Vehicle+vehicle (NaCl 0.9%, VEH); vehicle+haloperidol 0.8mg/kg (HAL); vehicle+GBR-12909 30mg/kg (GBR); vehicle+caffeine 40mg/kg (CAF); vehicle+nicotine 1.5mg/kg (NIC); caffeine 40mg/kg+haloperidol 0.8mg/kg (CAF+HAL); nicotine 1.5mg/kg+haloperidol 0.8mg/kg (NIC+HAL).

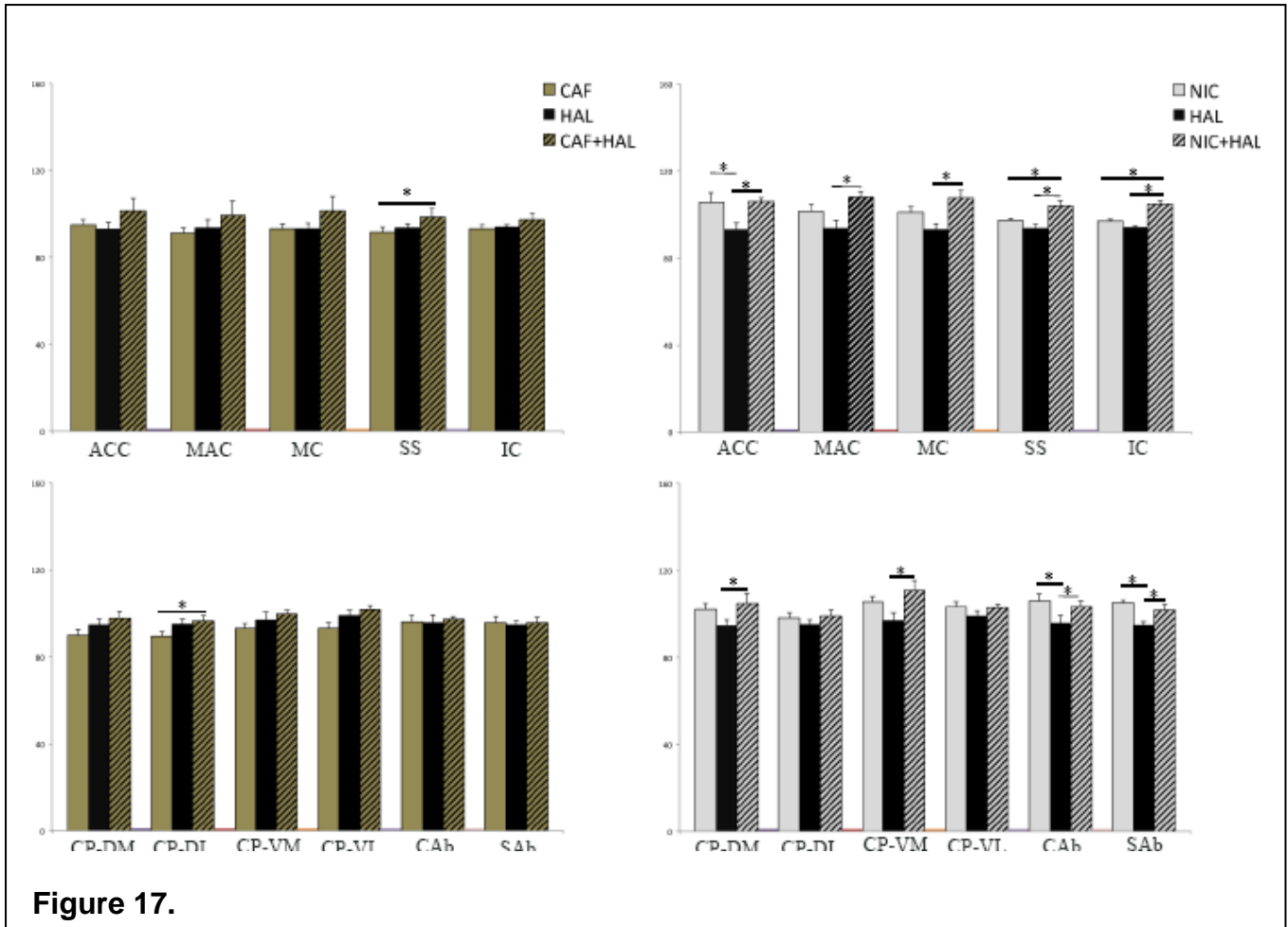


Figure 17. Intergroup differences in *Homer1b* mRNA expression among haloperidol, caffeine, and caffeine+haloperidol (left side) and among haloperidol, nicotine, nicotine+haloperidol (right side) in cortical (upper side) and striatal (lower side) ROIs. Data were reported in relative d.p.m. as mean±S.E.M. Lines connected groups whose mean mRNA expression was significantly different. * = significant differences at the Student-Newman-Keuls post-hoc test (p<0.05).

2.2. Protein Levels Analysis in Striatum

Homer1a protein levels were significantly increased compared to basal levels by nicotine, alone or in association with haloperidol, and by caffeine plus haloperidol (Figure 18.). Protein levels by nicotine were also significantly higher than levels by GBR-12909 or haloperidol (SNK: p=0.0009 and p=0.002, respectively). Caffeine or nicotine addition to haloperidol significantly increased protein levels compared to haloperidol alone (SNK: p<0.0001 and p=0.004, respectively).

Nicotine, alone or in association with haloperidol, and caffeine plus haloperidol were found to significantly increase Arc protein levels over basal ones (Figure 18.). Again, caffeine addition to haloperidol significantly increased protein levels compared to haloperidol alone (SNK: p=0.007).

Homer1b protein levels were unaffected (Figure 18.).

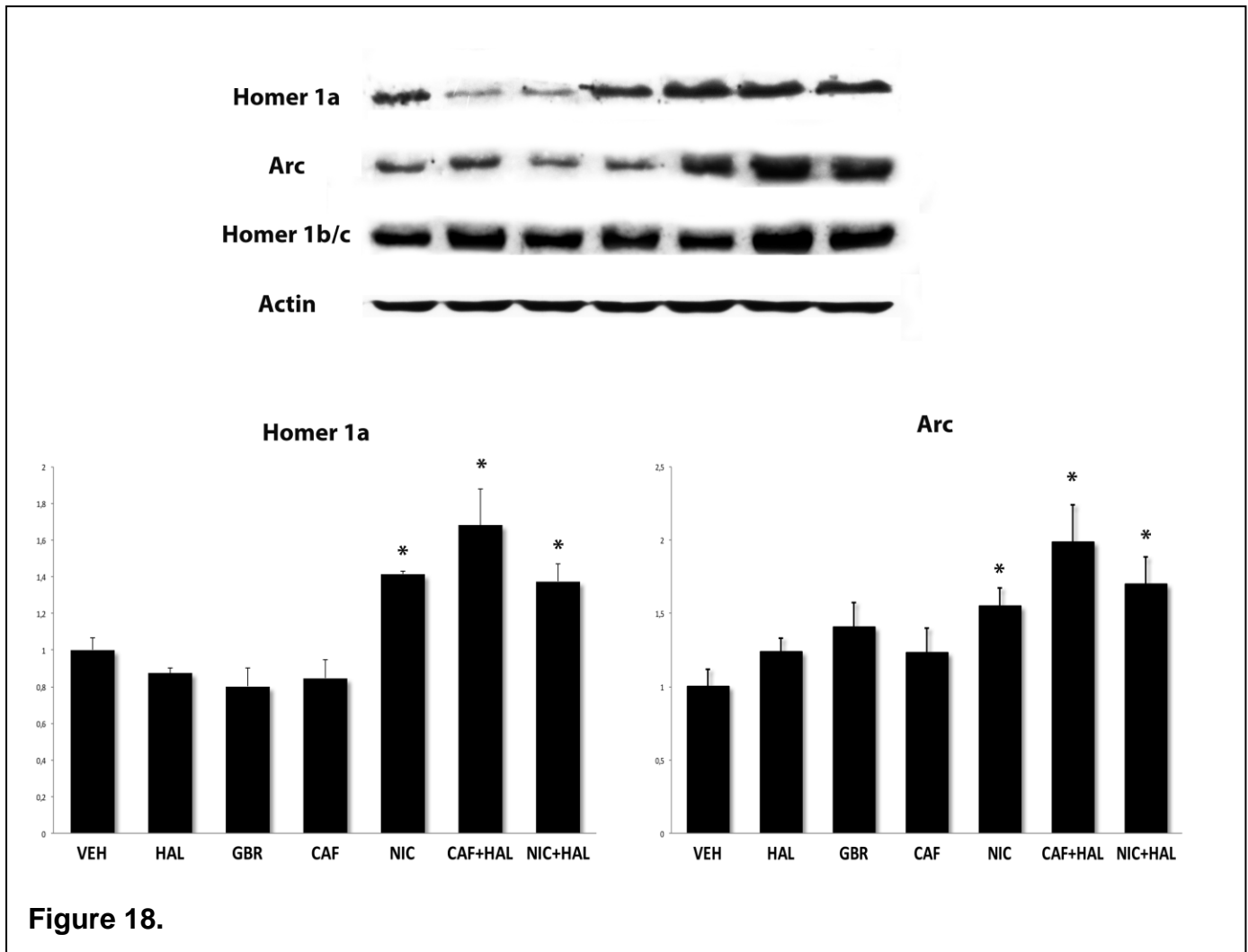


Figure 18. Measurements of Homer1a (left side) and Arc (right side) protein expression by Western Blot quantitation. Data are reported in relative intensity as means \pm S.E.M. Student-Newman-Keuls post hoc test: * = vs. VEH ($p < 0.05$). Homer1b protein levels were not depicted as they were not significantly different among groups. Vehicle+vehicle (NaCl 0.9%, VEH); vehicle+haloperidol 0.8mg/kg (HAL); vehicle+GBR-12909 30mg/kg (GBR); vehicle+caffeine 40mg/kg (CAF); vehicle+nicotine 1.5mg/kg (NIC); caffeine 40mg/kg+haloperidol 0.8mg/kg (CAF+HAL); nicotine 1.5mg/kg+haloperidol 0.8mg/kg (NIC+HAL).

3. Behavioral Analysis

In order to avoid possible biases induced in gene expression by novel environment stimuli, after the second injection each rat was re-placed, for 20 minutes before the locomotion assessment, in the same cage and with the same other animals with which it was allowed to become familiar during the housing and adaptation period, as well as during all the experiment procedures.

Locomotor activity was significantly increased by GBR-12909 and decreased by haloperidol compared to vehicle-treated rats, as expected (Figure 6). Nicotine significantly reduced locomotion compared to vehicle, either when given alone or in addition to haloperidol (Figure 19.). Notably, locomotor activity by nicotine plus haloperidol was significantly lower than by nicotine alone (SNK:

p=0.01), suggesting a reinforcing effect of haloperidol on nicotine as regard to impaired locomotion (Figure 19.). Caffeine did not reduce locomotor activity *per se*, however it did when given in addition to haloperidol (Figure 19.). Both nicotine and caffeine-mediated locomotor activity was significantly lower compared to that elicited by GBR-12909 (SNK: p<0.0001 either). On the contrary, caffeine-mediated locomotor activity was significantly higher than that by haloperidol (SNK: p=0.005).

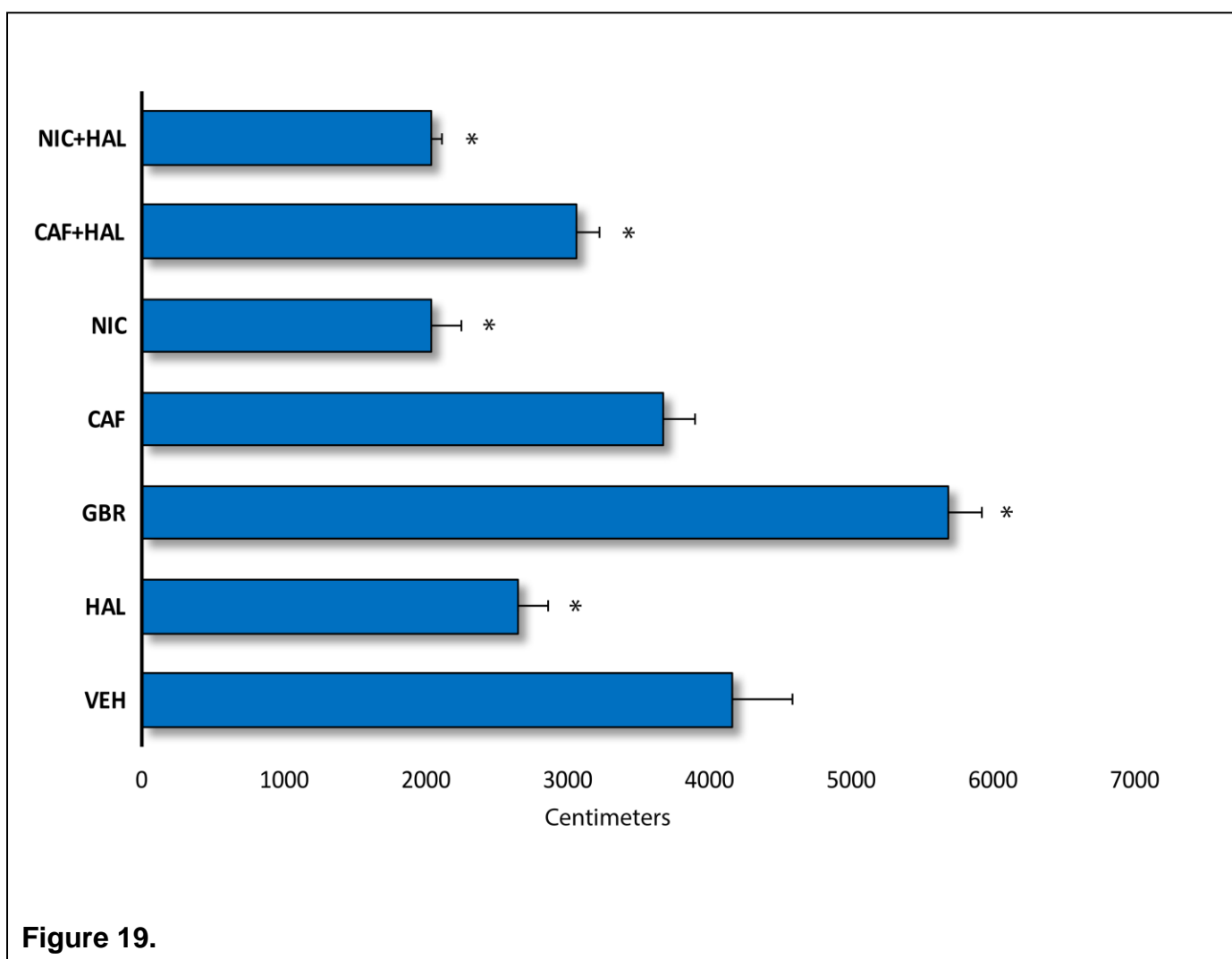


Figure 19. Locomotor activity measurement following each treatment. Data are reported in centimeters measuring the distance walked as means ± S.E.M. Student-Newman-Keuls post hoc test: * = vs. VEH (p<0.05).
 Vehicle+vehicle (NaCl 0.9%, VEH); vehicle+haloperidol 0.8mg/kg (HAL); vehicle+GBR-12909 30mg/kg (GBR); vehicle+caffeine 40mg/kg (CAF); vehicle+nicotine 1.5mg/kg (NIC); caffeine 40mg/kg+haloperidol 0.8mg/kg (CAF+HAL); nicotine 1.5mg/kg+haloperidol 0.8mg/kg (NIC+HAL).

CHAPTER 7

Postsynaptic density protein transcripts are differentially modulated by minocycline alone or in add-on to haloperidol.

1.Rationale

Existing antipsychotics are only partially effective towards negative symptoms and cognitive deficits of schizophrenia (Dunlop and Brandon, 2015; Karam et al., 2010; Pratt et al., 2012; Stroup et al., 2016). These data rise the issue of the urgent need of pro-cognitive therapeutic strategies.

Interestingly, several case reports and clinical trials have reported therapeutic improvement in psychotic, negative, and cognitive symptoms by add-on therapies to antipsychotics with minocycline (Chaudhry et al., 2012; Chaves et al., 2010; Chaves et al., 2015; Ghanizadeh et al., 2014; Kelly et al., 2011; Oya et al., 2014). Therefore, minocycline has been proposed among the potential augmentation strategies in the treatment of poor responder and TRS patients (Kelly et al., 2015; Qurashi et al., 2014). Nevertheless, preclinical studies on the molecular effects of minocycline administration on brain plasticity are still lacking. Indeed, animal studies to date have only explored the behavioral effects of minocycline administration. For example, in mice and monkeys it has been shown that, in either dopaminergic or glutamatergic pharmacological models of psychosis-like behavior, minocycline administration could improve locomotor and behavioral abnormalities (Mizoguchi et al., 2008; Zhang et al., 2006a; Zhang et al., 2006b). Furthermore, minocycline has been found to revert cognitive visuo-spatial memory deficits and changes in sensorimotor gating in rats administered with the non-competitive NMDA receptor antagonist dizocilpine maleate (MK-801) (Levkovitz et al., 2007).

On the basis of the translational value of the research, we therefore investigated whether minocycline add-on to haloperidol may affect the expression of PSD transcripts known to play a relevant role in synaptic regulation, i.e. *Homer1a*, *Homer1b* and *Arc* (details for oligodeoxyribonucleotide probes have been listed in Table 11.).

Probe	cDNA length (bp)	cDNA position	mRNA	Gen-Bank#
Homer1a	48	2527–2574	<i>Homer1a</i>	U92079
Homer1b/c	48	1306–1353	<i>Homer1b/c</i>	AF093268
Arc	45	789-833	<i>Arc</i>	NM019361

Table 11.

Table 11. Probes for in situ hybridization histochemistry.

The experimental paradigm comprised originally two groups of animals receiving a pre-treatment of vehicle (VEH; NaCl 0.9%) or ketamine (KET; 30 mg/kg), in order to evaluate gene expression under physiological conditions and after the manipulation of the glutamatergic system. Specifically, the rationale of the pre-treatment stemmed from the idea of mimicking an acute “glutamatergic” psychosis compared to a “naturalistic” condition, and ketamine was chosen among the other NMDA receptor antagonists since it has been widely used in pharmacological models of psychotic-like behaviors in preclinical studies (Lipska and Weinberger, 2000). Subsequently, animals (n=28 for each pre-treatment group) underwent the treatment step, where a second compound was administered. In the treatment step, animals were randomly subdivided in four subgroups in each pre-treatment arm (n=7 for each treatment group), and the evaluation of gene expression was obtained after the administration of haloperidol (HAL), minocycline (MIN), or the combination of the two compounds (HAL+MIN) as compared with controls (VEH). An i.p. injection 30 min after the pre-treatment was performed for the administration of the second compound and animals were sacrificed 90 min after the last injection. In the VEH pre-treatment arm, the following treatment groups were obtained: (a) VEH+VEH (NaCl 0.9%, VEH+VEH); (b) VEH+HAL 0.8 mg/kg (VEH+HAL); (c) VEH+MIN 45 mg/kg (VEH+MIN); (d) VEH+HAL 0.8 mg/kg+MIN 45 mg/kg (VEH+HAL+MIN). In the KET pre-treatment arm, the following treatment groups were obtained: (a) KET+VEH; (b) KET+HAL 0.8 mg/kg (KET+HAL); (c) KET+MIN 45 mg/kg (KET+MIN); (d) KET+HAL 0.8 mg/kg+MIN 45 mg/kg (KET+HAL+MIN).

Ketamine was administered at a sub-anaesthetic and sub-convulsant dose considered to mimic an animal model of acute psychosis (Lipska and Weinberger, 2000). Haloperidol was given at behaviourally active doses, known to elicit gene expression (Ambesi-Impiombato et al., 2007). Finally, minocycline was given at a dose reported to have neuroprotective effects according to previous published works (Adembri et al., 2014; Bye et al., 2007).

Repeated measures ANOVA was used to analyze the individual contribution of each of the categorization factors on the outcome of gene expression that was considered the dependent variable. Pre-treatment and treatment effects and their interaction were investigated by between-subjects analysis, while within-subjects analysis investigated the ROI effect. Analyses of ROIs interaction with pre-treatment, treatment, and pre-treatment×treatment effects were also carried out (Table..). The SNK *post-hoc* test with the Bonferroni correction was used for groups' comparison. *Post-hoc* comparisons were carried out at each individual ROI level, for clarity, and separately among groups pre-treated by VEH and among groups pre-treated by KET. In case of significant between-subjects pre-treatment×treatment interaction, we also carried out comparisons among groups pre-treated by VEH vs groups pre-treated by KET. In all tests, significance was set at $p < 0.05$ (two-tailed). The statistical analyses were performed using JMP9.0.1 and SPSS softwares.

2.Results

We observed that the expression of the IEGs *Homer1a* and *Arc* was significantly and differentially modulated by the psychoactive treatments administered. The major result obtained was that minocycline add-on to haloperidol blunted the haloperidol-mediated expression of *Arc* gene, and specifically the add-on treatment significantly modified *Arc* mRNA expression in the cortex, while haloperidol *per se* did not significantly affect gene expression in this area.

The second result was that *Homer1a* transcript expression underwent a significant treatment effect with also a significant region- dependent effect, as a confirmation of the observations reported in previous studies.

Results are listed as gene expression changes observed for each transcript taken into account (*Homer1a*, *Homer1b* and *Arc*, respectively).

2.1.Homer1a

At the between-subjects analysis, only treatment administration showed a significant effect on *Homer1a* gene expression levels, while no significant effects of pre-treatment or of the pre-treatment×treatment interaction were observed (Table 12.). At the within-subjects analysis, the consideration of the ROIs showed a significant effect on *Homer1a* mRNA expression levels (Table 12.). Significant treatment×ROI and pre-treatment×treatment×ROI effects were found, while no pre-treatment×ROI effect was found (Table 12.).

Among the VEH pre-treated groups, *Homer1a* expression levels were significantly higher in the VEH+HAL group as compared with VEH+VEH in the MC region of the cortex and in the entire caudate putamen (Figure20.; Table 13.). On the other side, no significant differences were observed between the VEH+MIN and VEH+VEH groups (Figure 20.), suggesting that MIN *per se* did not impact *Homer1a* mRNA levels. Finally, *Homer1a* was found significantly induced by VEH+HAL+MIN compared with VEH+VEH in the majority of the caudate putamen regions (Figure 20.).

Among the KET pre-treated groups, few significant differences were found, that substantially matched those found in the VEH pre-treated groups (Figure 20.).

<i>Homer1a</i>			<i>Homer1b/c</i>			<i>Arc</i>		
Between-Subjects Effects			Between-Subjects Effects			Between-Subjects Effects		
Effect	<i>p</i> -value	<i>F</i> -value _{df}	Effect	<i>p</i> -value	<i>F</i> -value _{df}	Effect	<i>p</i> -value	<i>F</i> -value _{df}
Pre-treatment	0.64	0.22 ₁	Pre-treatment	0.53	0.41 ₁	Pre-treatment	0.95	0.01 ₁
Treatment	0.003	6.23 ₃	Treatment	0.31	1.24 ₃	Treatment	<0.0001	40.69 ₃
Pre-treatment* Treatment	0.62	0.60 ₃	Pre-treatment* Treatment	0.51	0.79 ₃	Pre-treatment* Treatment	0.03	3.20 ₃
Within-Subjects Effects			Within-Subjects Effects			Within-Subjects Effects		
Effect	<i>p</i> -value	<i>F</i> -value _{df}	Effect	<i>p</i> -value	<i>F</i> -value _{df}	Effect	<i>p</i> -value	<i>F</i> -value _{df}
ROI	<0.0001	8.66 ₁₀	ROI	<0.0001	22.09 ₁₀	ROI	<0.0001	46.05 ₁₀

Table 12.

Table 12. This table summarizes the outputs of repeated measures ANOVA for *Homer1a*, *Homer1b/c*, and *Arc* gene transcripts. Between-subjects effects were pre-treatment (either vehicle or ketamine). Within-subjects effects were regions of interest (ROIs; see Figure 2.). Significant values ($p < 0.05$, two-tailed) are reported in bold. HAL: haloperidol; KET: ketamine; MIN: minocycline.

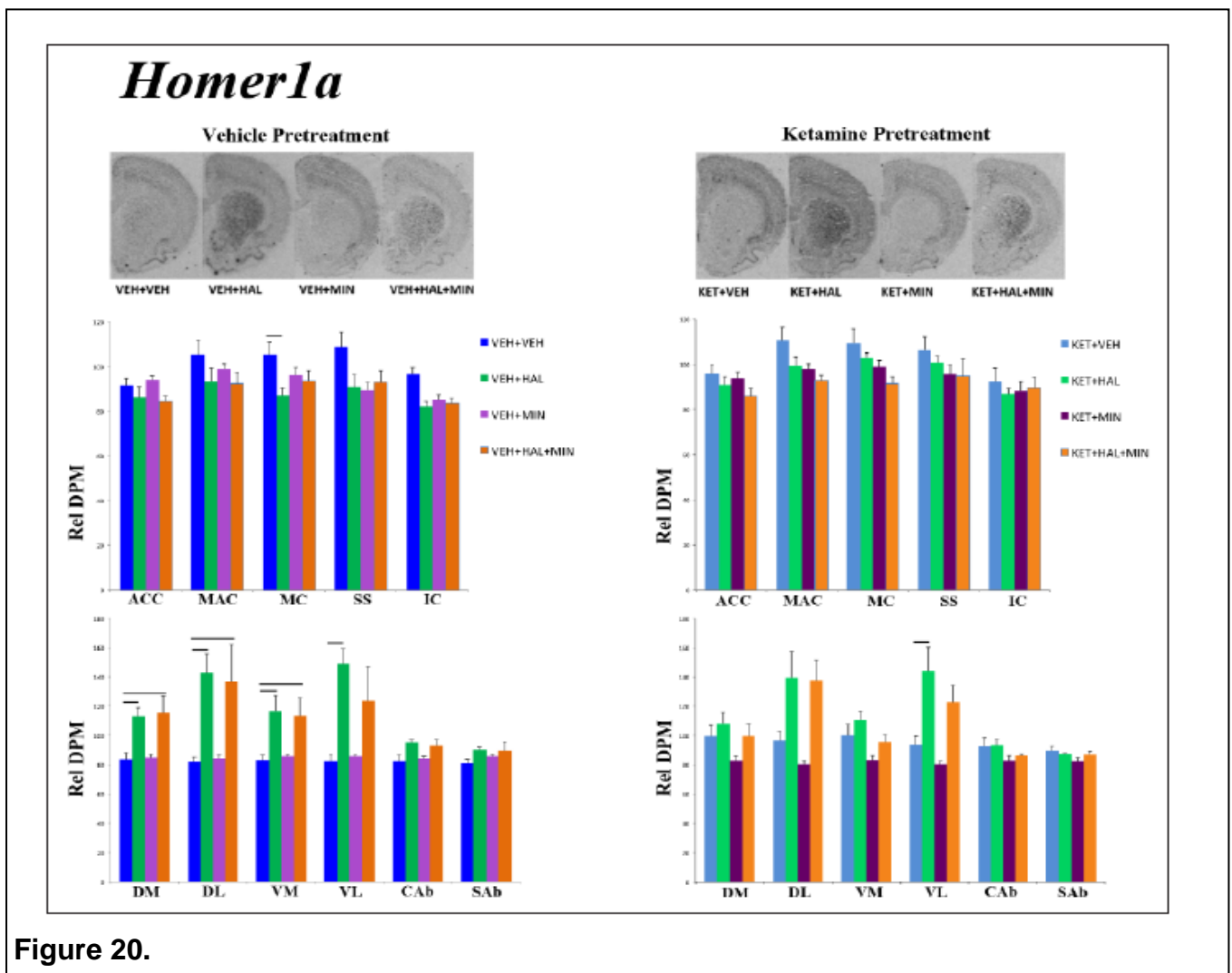


Figure 20.

Figure 20. Autoradiograms of *Homer1a* expression and illustrative histograms of gene expression throughout cortical and striatal subregions. Upper panel: illustrative autoradiograms of *Homer1a* expression in cortico-striatal regions. Lower panels: levels of *Homer1a* mRNA expression (in relative dpm) for each cortical (upper side) and striatal (lower side) subregion. Histogram bars illustrate means±standard error of the mean (SEM). Significant inter-group differences have been depicted by solid lines connecting significantly different groups. ACC: anterior cingulate cortex; CAb: core of the nucleus accumbens; DL: dorsolateral caudate-putamen; DM: dorsomedial caudate-putamen; HAL: haloperidol; IC: insular cortex; KET: ketamine; MAC: medial agranular cortex; MC: motor cortex; MIN: minocycline; SAb: shell of the nucleus accumbens; SS: somatosensory cortex; VEH: vehicle; VL: ventrolateral caudate-putamen; VM: ventromedial caudate-putamen.

Pre-Treatment	VEHICLE							
Group Comparison	HAL vs. VEH		MIN vs. VEH		HAL+MIN vs. VEH		HAL+MIN vs. HAL	
<i>p</i> -value	SNK	Bonferroni	SNK	Bonferroni	SNK	Bonferroni	SNK	Bonferroni
ACC	>.05	>.05	>.05	>.05	>.05	>.05	>.05	>.05
MAC	>.05	>.05	>.05	>.05	>.05	>.05	>.05	>.05
MC	.01	.03	>.05	>.05	>.05	>.05	>.05	>.05
SS	.03	>.05	.02	>.05	>.05	>.05	>.05	>.05
IC	.001	<i>.06</i>	.004	>.05	.003	>.05	>.05	>.05
DM	.005	.03	>.05	>.05	.004	.002	>.05	>.05
DL	.003	.01	>.05	>.05	.01	.04	>.05	>.05
VM	.006	.009	>.05	>.05	.01	.04	>.05	>.05
VL	.0009	.001	>.05	>.05	.02	>.05	>.05	>.05
CAb	.01	<i>.06</i>	>.05	>.05	.03	>.05	>.05	>.05
SAb	.04	>.05	>.05	>.05	>.05	>.05	>.05	>.05

Pre-Treatment	KETAMINE							
Group Comparison	HAL vs. VEH		MIN vs. VEH		HAL+MIN vs. VEH		HAL+MIN vs. HAL	
<i>p</i> -value	SNK	Bonferroni	SNK	Bonferroni	SNK	Bonferroni	SNK	Bonferroni
ACC	>.05	>.05	>.05	>.05	>.05	>.05	>.05	>.05
MAC	>.05	>.05	.03	>.05	.005	<i>.06</i>	>.05	>.05
MC	>.05	>.05	>.05	>.05	.006	>.05	>.05	>.05
SS	>.05	>.05	>.05	>.05	>.05	>.05	>.05	>.05
IC	>.05	>.05	>.05	>.05	>.05	>.05	>.05	>.05
DM	>.05	>.05	>.05	>.05	>.05	>.05	>.05	>.05
DL	.03	>.05	>.05	>.05	.03	>.05	>.05	>.05
VM	>.05	>.05	.04	>.05	>.05	>.05	>.05	>.05
VL	.007	.05	>.05	>.05	>.05	>.05	>.05	>.05
CAb	>.05	>.05	>.05	>.05	>.05	>.05	>.05	>.05
SAb	>.05	>.05	.04	>.05	>.05	>.05	>.05	>.05

Table 13.

Table 13. Treatment group comparisons of *Homer1a* transcript expression. ACC: anterior cingulate cortex; CAb: core of the nucleus accumbens; DL: dorsolateral caudate-putamen; DM: dorsomedial caudate-putamen; HAL: haloperidol; IC: insular cortex; KET: ketamine; MAC: medial agranular cortex; MC: motor cortex; MIN: minocycline; SAb: shell of the nucleus accumbens; SNK: Student-Newman-Keuls; SS: somatosensory cortex; VEH: vehicle; VL: ventrolateral caudate-putamen; VM: ventromedial caudate-putamen. In this table are reported the *p*-values of the comparison among treatment groups (in order: HAL; VEH; MIN; HAL+MIN) throughout cortical and striatal regions of interest (ROIs). Comparisons were carried out by SNK with Bonferroni correction, separately among groups pre-treated with VEH and groups pre-treated with KET. Significant *p*-values ($p < 0.05$, two-tailed) after Bonferroni correction are given in bold. In italics are provided *p*-values that show a trend toward significance.

2.2. *Homer1b*

At the between-subjects analysis, no significant effects of pre-treatment or treatment were observed on *Homer1b* gene expression levels (Table 12.) and no pre-treatment×treatment effect was found. At the within-subjects analysis, a significant ROI effect on *Homer1b* transcript expression values was found (Table 12.). Comparisons carried out, by SNK with Bonferroni correction, separately among groups pre-treated with VEH and groups pre-treated with KET did not show significant p-values (Table 14.; Figure 21.).

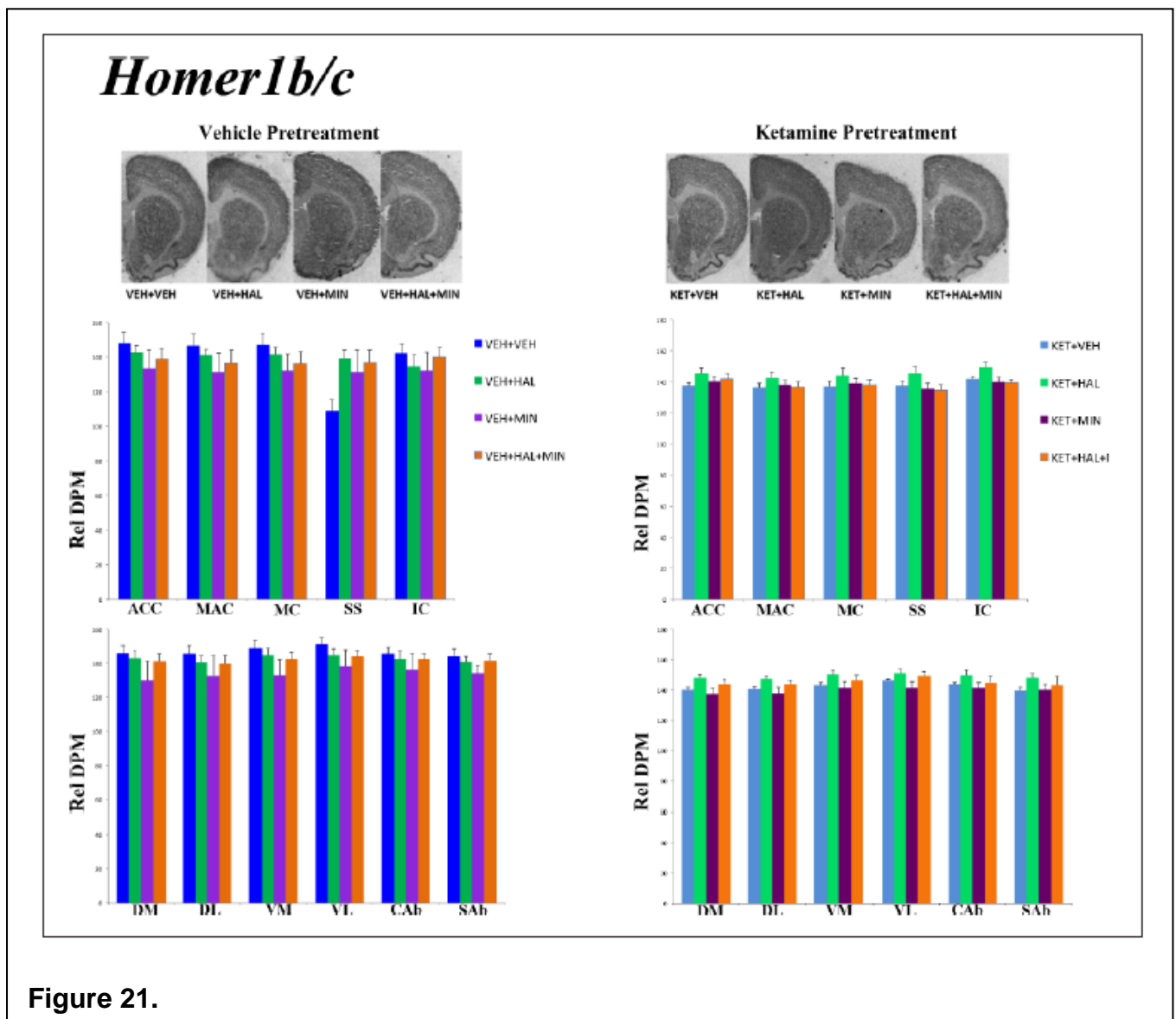


Figure 21. Autoradiograms of *Homer1b/c* expression and illustrative histograms of gene expression throughout cortical and striatal subregions. Upper panel: illustrative autoradiograms of *Homer1b/c* expression in corticostriatal regions. Lower panels: levels of *Homer1b/c* mRNA expression (in relative dpm) for each cortical (upper side) and striatal (lower side) subregion. Histogram bars illustrate means±standard error of the mean (SEM). ACC:

anterior cingulate cortex; CAb: core of the nucleus accumbens; DL: dorsolateral caudate-putamen; DM: dorsomedial caudate-putamen; HAL: haloperidol; IC: insular cortex; KET: ketamine; MAC: medial agranular cortex; MC: motor cortex; MIN: minocycline; SAb: shell of the nucleus accumbens; SS: somatosensory cortex; VEH: vehicle; VL: ventrolateral caudate-putamen; VM: ventromedial caudate-putamen.

Pre-Treatment	VEHICLE							
Group Comparison	HAL vs. VEH		MIN vs. VEH		HAL+MIN vs. VEH		HAL+MIN vs. HAL	
<i>p</i> -value	SNK	Bonferroni	SNK	Bonferroni	SNK	Bonferroni	SNK	Bonferroni
ACC	>.05	>.05	>.05	>.05	>.05	>.05	>.05	>.05
MAC	>.05	>.05	>.05	>.05	>.05	>.05	>.05	>.05
MC	>.05	>.05	>.05	>.05	>.05	>.05	>.05	>.05
SS	>.05	>.05	>.05	>.05	>.05	>.05	>.05	>.05
IC	>.05	>.05	>.05	>.05	>.05	>.05	>.05	>.05
DM	>.05	>.05	>.05	>.05	>.05	>.05	>.05	>.05
DL	>.05	>.05	>.05	>.05	>.05	>.05	>.05	>.05
VM	>.05	>.05	>.05	>.05	>.05	>.05	>.05	>.05
VL	>.05	>.05	>.05	>.05	>.05	>.05	>.05	>.05
CAb	>.05	>.05	>.05	>.05	>.05	>.05	>.05	>.05
SAb	>.05	>.05	>.05	>.05	>.05	>.05	>.05	>.05
Pre-Treatment	KETAMINE							
Group Comparison	HAL vs. VEH		MIN vs. VEH		HAL+MIN vs. VEH		HAL+MIN vs. HAL	
<i>p</i> -value	SNK	Bonferroni	SNK	Bonferroni	SNK	Bonferroni	SNK	Bonferroni
ACC	>.05	>.05	>.05	>.05	>.05	>.05	>.05	>.05
MAC	>.05	>.05	>.05	>.05	>.05	>.05	>.05	>.05
MC	>.05	>.05	>.05	>.05	>.05	>.05	>.05	>.05
SS	>.05	>.05	>.05	>.05	>.05	>.05	.02	>.05
IC	>.05	>.05	>.05	>.05	>.05	>.05	.02	>.05
DM	>.05	>.05	>.05	>.05	>.05	>.05	>.05	>.05
DL	>.05	>.05	>.05	>.05	>.05	>.05	>.05	>.05
VM	>.05	>.05	>.05	>.05	>.05	>.05	>.05	>.05
VL	>.05	>.05	>.05	>.05	>.05	>.05	>.05	>.05
CAb	>.05	>.05	>.05	>.05	>.05	>.05	>.05	>.05
SAb	>.05	>.05	>.05	>.05	>.05	>.05	>.05	>.05

Table 14.

Table 14. Treatment group comparisons of *Homer1b/c* transcript expression. ACC: anterior cingulate cortex; CAb: core of the nucleus accumbens; DL: dorsolateral caudate-putamen; DM: dorsomedial caudate-putamen; HAL: haloperidol; IC: insular cortex; KET: ketamine; MAC: medial agranular cortex; MC: motor cortex; MIN: minocycline; SAb: shell of the nucleus accumbens; SNK: Student-Newman-Keuls; SS: somatosensory cortex; VEH: vehicle; VL: ventrolateral caudate-putamen; VM: ventromedial caudate-putamen.

In this table are reported the *p*-values of the comparison among treatment groups (in order: HAL; VEH; MIN; HAL+MIN) throughout cortical or striatal regions of interest. Comparisons were carried out, by SNK with Bonferroni correction, separately among groups pre-treated with VEH and groups pre-treated with KET. To note: no significant *p*-values were found.

2.3. Arc

At the between-subjects analysis, the treatment effect was statistically significant, but no pre-treatment effect was observed (Table 12.). However, a significant pre-treatment×treatment effect was

found. At the within-subjects analysis, a significant ROI effect on *Arc* mRNA expression levels was observed (Table 12.). Finally, a significant treatment×ROI interaction was also observed (Table 12.), with comparisons carried out separately in each ROI.

Among the VEH pre-treated groups, VEH+HAL treatment significantly induced *Arc* mRNA expression compared with VEH+VEH in all striatal regions (Figure 22.). Conversely, in the same regions, *Arc* mRNA expression was significantly reduced by VEH+MIN compared with VEH+VEH (Figure 22.). Notably, *Arc* mRNA expression was significantly lower in rats treated with VEH+HAL+MIN compared with the VEH+VEH and the VEH+HAL groups in almost all cortical regions and in almost all caudate putamen regions taken into account (Figure 22., Table 15.).

Among the KET pre-treated groups, significant changes in *Arc* mRNA expression substantially matched the changes observed in VEH pre-treated groups (Table 4). However, no significant differences between KET+HAL+MIN and KET+HAL were observed (Table 15.).

As in the case of *Arc* transcript a significant pre-treatment effect was found, differentially from *Homer1a* and *Homer1b*, a comparison between the groups pretreated with VEH and those pre-treated with KET was also carried out (Table 16.; for clarity, only corresponding treatments were compared). *Arc* mRNA expression was significantly lower in KET+HAL treated rats compared with VEH+HAL treated ones in the majority of the caudate putamen regions considered (Table 16.).

Arc

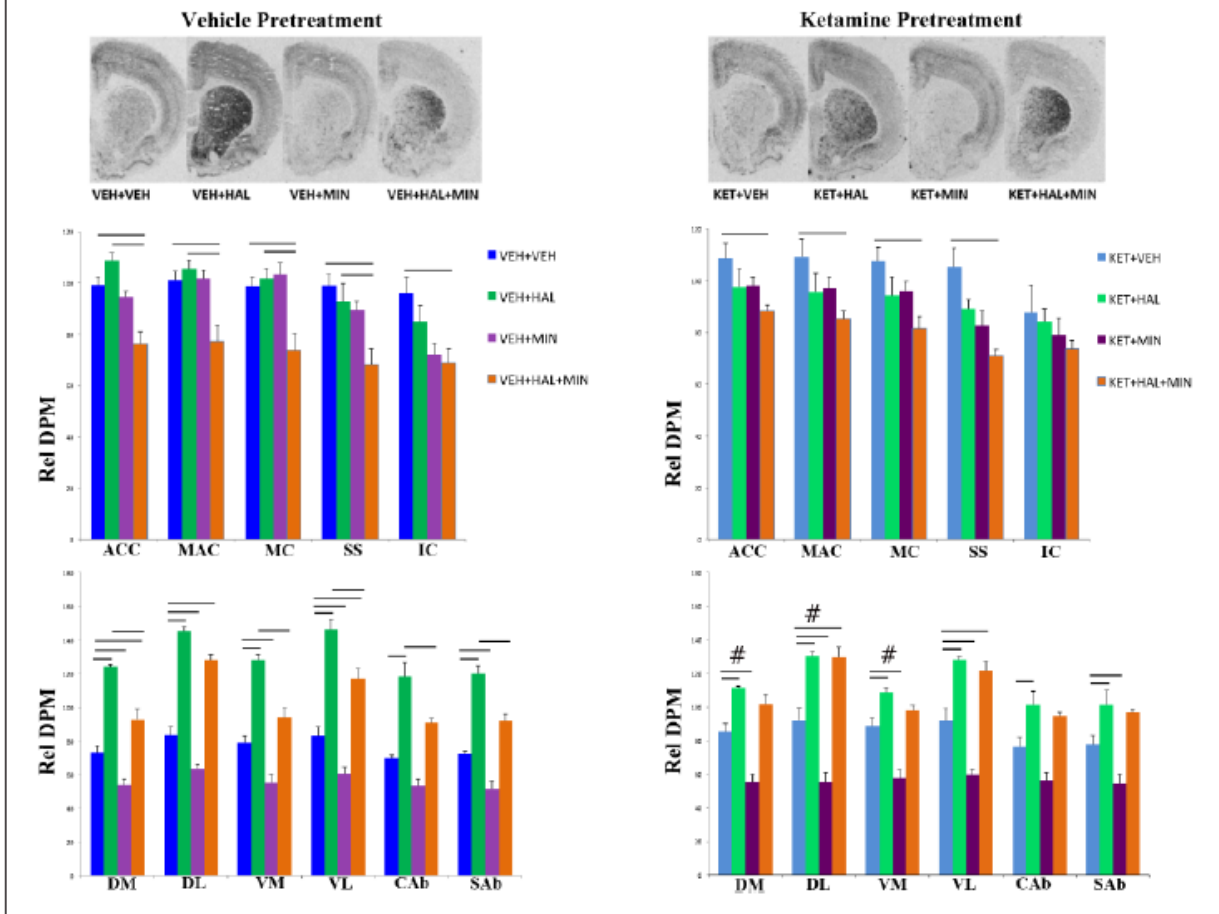


Figure 22.

Figure 22. Autoradiograms of *Arc* expression and illustrative histograms of gene expression throughout cortical and striatal subregions. Upper panel: illustrative autoradiograms of *Arc* expression in corticostriatal regions. Lower panels: levels of *Arc* mRNA expression (in relative dpm) for each cortical (upper side) and striatal (lower side) subregion. Histogram bars illustrate means±standard error of the mean (SEM). Significant inter-group differences have been depicted by solid lines connecting significantly different groups. #: significantly different from the corresponding group that received vehicle as the pre-treatment. ACC: anterior cingulate cortex; CAb: core of the nucleus accumbens; DL: dorsolateral caudate-putamen; DM: dorsomedial caudate-putamen; HAL: haloperidol; IC: insular cortex; KET: ketamine; MAC: medial agranular cortex; MC: motor cortex; MIN: minocycline; SAb: shell of the nucleus accumbens; SS: somatosensory cortex; VEH: vehicle; VL: ventrolateral caudate-putamen; VM: ventromedial caudate-putamen.

Pre-Treatment	VEHICLE							
Group Comparison	HAL vs. VEH		MIN vs. VEH		HAL+MIN vs. VEH		HAL+MIN vs. HAL	
<i>p-value</i>	SNK	Bonferroni	SNK	Bonferroni	SNK	Bonferroni	SNK	Bonferroni
ACC	>.05	>.05	>.05	>.05	.0003	.006	<.0001	.001
MAC	>.05	>.05	>.05	>.05	.001	.02	.0003	.003
MC	>.05	>.05	>.05	>.05	.003	.02	.001	.005
SS	>.05	>.05	>.05	>.05	.002	.005	.007	.02
IC	>.05	>.05	.01	>.05	.007	.05	>.05	>.05
DM	<.0001	.001	.004	.02	.004	.03	<.0001	.001
DL	<.0001	.001	.0007	.04	<.0001	.001	.001	>.05
VM	<.0001	.001	.002	.005	.04	>.05	<.0001	.001
VL	<.0001	.001	.009	.03	.0008	.001	.001	.004
CAb	<.0001	.001	.04	>.05	.01	>.05	.002	.009
SAb	<.0001	.001	.003	.04	.005	.07	.0003	.002

Pre-Treatment	KETAMINE							
Group Comparison	HAL vs. VEH		MIN vs. VEH		HAL+MIN vs. VEH		HAL+MIN vs. HAL	
<i>p-value</i>	SNK	Bonferroni	SNK	Bonferroni	SNK	Bonferroni	SNK	Bonferroni
ACC	>.05	>.05	>.05	>.05	.008	.01	>.05	>.05
MAC	>.05	>.05	>.05	>.05	.007	.01	>.05	>.05
MC	>.05	>.05	>.05	>.05	.003	.01	>.05	>.05
SS	.04	>.05	.007	.07	.0002	.001	.01	>.05
IC	>.05	>.05	>.05	>.05	>.05	>.05	>.05	>.05
DM	.001	.002	.0004	.001	.01	.08	>.05	>.05
DL	.0004	.001	.0006	.001	.0003	.001	>.05	>.05
VM	.004	.03	.0002	.002	>.05	>.05	>.05	>.05
VL	.0002	.001	.0004	.001	.0005	.003	>.05	>.05
CAb	.005	.03	.01	>.05	.03	>.05	>.05	>.05
SAb	.008	.02	.009	.02	.02	.07	>.05	>.05

Table 15.

Table 15. Treatment group comparisons of *Arc* transcript expression. ACC: anterior cingulate cortex; CAb: core of the nucleus accumbens; DL: dorsolateral caudate-putamen; DM: dorsomedial caudate-putamen; HAL: haloperidol; IC: insular cortex; KET: ketamine; MAC: medial agranular cortex; MC: motor cortex; MIN: minocycline; SAb: shell of the nucleus accumbens; SNK: Student-Newman-Keuls; SS: somatosensory cortex; VEH: vehicle; VL: ventrolateral caudate-putamen; VM: ventromedial caudate-putamen. In this table are reported the *p*-values of the comparison among treatment groups (in order: HAL; VEH; MIN; HAL+MIN) throughout cortical or striatal regions of interest. Comparisons were carried out by SNK with Bonferroni correction, separately among groups pre-treated with VEH and groups pre-treated with KET. Significant *p*-values (*p*<0.05, two-tailed) after Bonferroni correction are given in bold. In italics are provided *p*-values that show a trend toward significance.

Group Comparisons	VEH+VEH vs. KET+VEH		VEH+HAL vs. KET+HAL		VEH+MIN vs. KET+MIN		VEH+HAL+MIN vs. KET+HAL+MIN		
	p-value	SNK	Bonferroni	SNK	Bonferroni	SNK	Bonferroni	SNK	Bonferroni
ACC	>.05	>.05	>.05	>.05	>.05	>.05	>.05	>.05	>.05
MAC	>.05	>.05	>.05	>.05	>.05	>.05	>.05	>.05	>.05
MC	>.05	>.05	>.05	>.05	>.05	>.05	>.05	>.05	>.05
SS	>.05	>.05	>.05	>.05	>.05	>.05	>.05	>.05	>.05
IC	>.05	>.05	>.05	>.05	>.05	>.05	>.05	>.05	>.05
DM	>.05	>.05	<.0001	.001	>.05	>.05	>.05	>.05	>.05
DL	>.05	>.05	.005	.02	>.05	>.05	>.05	>.05	>.05
VM	>.05	>.05	.03	.01	>.05	>.05	>.05	>.05	>.05
VL	>.05	>.05	.03	>.05	>.05	>.05	>.05	>.05	>.05
CAB	>.05	>.05	>.05	>.05	>.05	>.05	>.05	>.05	>.05
SAb	>.05	>.05	>.05	>.05	>.05	>.05	>.05	>.05	>.05

Table 16.

Table 16. Pre-treatment effect in *Arc* transcript expression. ACC: anterior cingulate cortex; CAB: core of the nucleus accumbens; DL: dorsolateral caudate-putamen; DM: dorsomedial caudate-putamen; HAL: haloperidol; IC: insular cortex; KET: ketamine; MAC: medial agranular cortex; MC: motor cortex; MIN: minocycline; SAb: shell of the nucleus accumbens; SNK: Student-Newman-Keuls; SS: somatosensory cortex; VEH: vehicle; VL: ventrolateral caudate-putamen; VM: ventromedial caudate-putamen. This table summarizes the results of the comparison between groups pre-treated with VEH and groups pre-treated with KET. Only corresponding groups were compared. Statistical analysis was carried out by SNK with Bonferroni correction. Significant *p*-values after Bonferroni correction are given in bold. In italics are provided *p*-values that show a trend toward significance.

CHAPTER 8

1. Discussion

In the first research protocol studied herein, we aimed to gain knowledge into the antipsychotic-induced PSD transcripts changes after chronic treatments with first and second generation antipsychotics (namely, haloperidol and olanzapine) compared to the multitargeting agent asenapine. The choice of the set of PSD molecules was based on the fact that they have all been reported to be responsive to antipsychotic treatments ((de Bartolomeis et al., 2013b; Iasevoli et al., 2011a; Iasevoli et al., 2011b), as well as found to directly or indirectly interact with each other mainly mediating postsynaptic mGluR5-dependent signaling (Bertaso et al., 2010; Tu et al., 1999; Zhang and Lisman, 2012).

Specifically, the IEG *Homer1a*, which expression is linked to neuronal depolarization (Shiraishi-Yamaguchi and Furuichi, 2007; Wang et al., 2015), was found significantly reduced by haloperidol (mostly at the 0.8 mg/kg dose) in multiple cortical regions, possibly mirroring a reduced neuronal activation. Interestingly, both asenapine and olanzapine induced *Homer1a* at a significant higher extent when compared to haloperidol (Buonaguro et al., 2017a). To note, asenapine and olanzapine share a strong action on serotonergic receptor (Scheidemantel et al., 2015) and their receptor-binding profile may tackle the dopamine-glutamate-mediated neurotransmission in the cortex differentially from haloperidol. Therefore, the different cortical expression patterns of *Homer1a* could reflect on a molecular level a broader receptor-binding profile and therefore a different action on the glutamatergic cortical neurotransmission of olanzapine and mostly of asenapine. On the other hand, in accordance with previous published results, haloperidol exerted the highest and asenapine the least induction of *Homer1a* in the striatum, where the gene expression has been reported to be strongly dependent on D2 receptors antagonism (de Bartolomeis et al., 2016; Iasevoli et al., 2011b; Iasevoli et al., 2010a).

Almost all chronic antipsychotics tested herein reduced the IEG *Arc* in the cortex (Buonaguro et al., 2017a). This result may suggest that lowering *Arc* expression may be a mechanism to increase post-synaptic neuronal activation, given that the IEG expression has been related to glutamate-mediated neuronal activation (Kumar et al., 2012) and agonism at serotonin 5-HT_{2A} receptors (Li et al., 2015).

Accordingly, *Arc* mRNA expression was particularly reduced by the highest dose of asenapine and by olanzapine, with both compounds being antagonists at 5-HT_{2A} receptors (Bymaster et al., 1996; Tarazi and Neill, 2013; Xiberas et al., 2001). Indeed, asenapine, which is the most potent 5-HT_{2A} antagonist among the three compounds, produced significantly higher *Arc* mRNA cortical levels than both olanzapine and haloperidol. On the other hand, in the striatum the IEG seemed to be under the regulation of potent D₂ receptor blockade, since haloperidol significantly induced *Arc* gene at a higher extent compared to both asenapine and olanzapine.

For what concerns the constitutive genes *Homer1b*, *PSD-95*, and *Shank1*, which are all implicated in synaptic architecture and plasticity, there is a lack of information in the literature concerning their modulation by different antipsychotics chronically administered. In the present study, they were found substantially reduced after chronic antipsychotic treatments (Buonaguro et al., 2017a). It could be suggested that a reduced expression of these transcripts may implicate that chronic antipsychotics mediate a re-arrangement of synaptic architecture in post-glutamatergic neurons, as previously observed for the case of PSD-95 protein levels after antipsychotic treatment (Fumagalli et al., 2008). Specifically, when considering inter-group differences among the antipsychotics tested herein, *Homer1b* and *PSD-95* expression was significantly increased by olanzapine and asenapine compared to haloperidol in all brain regions, while *Shank1* expression by antipsychotics followed another pattern. In this latter case, no gross significant differences among antipsychotics were found in the cortex, while in striatum, differently from the other two constitutive genes, haloperidol and olanzapine significantly increased gene expression compared to the lowest dose of asenapine. To note, the expression of the constitutive genes was found affected by the different haloperidol and asenapine doses tested herein, confirming the hypothesis that the modulation of synaptic plasticity could be differentially tuned based on the dose of the compound (de Bartolomeis et al., 2015).

Finally, with the evaluation of the relative ratio of *Homer1a/Homer1b* expression, we aimed at addressing the question of whether different receptor profile and different doses of the same antipsychotic may change the relative ratio of the two Homer1 isomers. In cortical regions, haloperidol

was found to significantly shift the ratio toward *Homer1b* expression, and the shift toward the expression of *Homer1b* progressively grew in more cortical regions as the dose went from the lowest to the highest administered. Conversely, in the striatum all antipsychotics shifted the ratio at various degrees toward the expression of *Homer1a*. Therefore, it could be suggested that the different modulation by the antipsychotics studied herein of the inducible vs. the constitutive *Homer1* isoforms may mirror a differential impact on postsynaptic plasticity, exerting *Homer1a* and *Homer1b* opposite actions (Kammermeier, 2008).

Intriguingly, the IEGs tested herein appeared to be mostly regulated by the 0.5 mg/kg haloperidol and by the 0.05 mg/kg asenapine over the other doses of the respective compounds. This is in contrast with what observed in a previous acute paradigm of the same set antipsychotic given at the same dose-ranges (de Bartolomeis et al., 2015). Indeed, the acute paradigm previously realized showed that the expression of early and constitutive genes was significantly increased in cortical and sub-cortical regions by all antipsychotics used and at each dose. We therefore specifically investigated the expression pattern of the IEG *Homer1a* comparing acutely *versus* chronically treated groups of animals.

The results of the comparison suggested that the biological effects of antipsychotics may be attenuated after prolonged treatments and that the maximum modulation of gene expression may be obtained by the chronic administration of high doses of these compounds. Indeed, as the dose of the antipsychotic tested increased in both paradigms of administration, a progressive recruitment of more striatal and cortical regions was observed. Specifically, we found that increasing doses of haloperidol resulted in significant differences in acute *versus* chronic paradigms in a major number of cortical regions, while increasing doses of asenapine triggered differences in gene expression in a progressive major number of striatal regions. This final observation could be of particular translational meaning, since it could be speculated that chronic treatments exert very different effects when compared to acute ones, particularly topographically tackling distinct areas of the brain depending on the dose administered.

The third set of experiments aimed at the characterization of the molecular and behavioral effects of caffeine and nicotine in addition to haloperidol. The major results were that caffeine and nicotine *per se* were found not to widely affect mRNA expression at the PSD, while the scenario dramatically changed when their administration was followed by haloperidol. In the case of caffeine, the expression of the two IEGs *Homer1a* and *Arc* was significantly reduced when its administration was followed by haloperidol compared to haloperidol alone, while protein levels were significantly increased compared to both basal and haloperidol-induced levels. These results may be explained on the basis of caffeine's complex receptor interactions. It has been reported that at the presynaptic level, caffeine may preferentially block A2ARs over A1Rs on glutamatergic terminals (Ciruela et al., 2006), which may increase glutamate release. At the postsynaptic level, caffeine antagonist action on A2ARs may reduce mGluR5 (Fuxe et al., 2003), which may increase D2 receptors activation. In our paradigm, D2 receptors activation may be prevented by haloperidol blockade. The combined effect of glutamatergic activation and loss of D2 receptor-mediated inhibitory effect may explain why the combination of caffeine and haloperidol increased protein levels significantly more than caffeine or haloperidol alone, which did not increase *Homer1a* and *Arc* proteins compared to basal levels. On the other hand, the observed reduction of mRNA expression may represent a feedback mechanism consequent to protein amount elevation or may depend on the blockade of post-receptor signaling cascades leading to *Homer1a* and *Arc* expression. Notably, it has been observed that A1Rs mediate *Homer1a* mRNA expression, at least in cortical areas (Serchov et al., 2015), where A1Rs are more abundant than A2ARs (Ferre and Sebastiao, 2016). Therefore, the significant reduction of *Homer1a* expression by caffeine addition to haloperidol in comparison to both basal levels and haloperidol-induced levels may depend, at least in cortical areas, by caffeine antagonist action on A1Rs. This same mechanism may also account for increased *Homer1b* expression by caffeine plus haloperidol in cortical areas.

In the case of nicotine, gene expression was increased by nicotine in association to haloperidol. This effect may be mediated by a reinforcing action of haloperidol, which may boost the known dopamine and glutamate activation by nicotine (Sulzer, 2011). On the protein level, nicotine was found to increase protein levels for example of Homer1a, and this results was observed also by other researches (Rezvani et al., 2007). Notably, Homer1a is known to counteract excessive NMDA receptor activation (Wang et al., 2015), and its increase may represent a neuronal feedback mechanism to prevent over-activation.

Intriguingly, in all treatments where there was found an increase of Homer1a protein levels, a concomitant reduction of locomotor behavior was observed. In a previously published study, transgenic mice overexpressing Homer1a protein in striatum were associated to decreased locomotor activity in the open field test compared to wild-type littermates (Tappe and Kuner, 2006).. Notably, caffeine- and nicotine-induced locomotion was significantly higher than that induced by haloperidol alone, mostly as a result of the hypokinetic effects of haloperidol, rather than to a combined effect of the associations.

Taken together, these data showed that caffeine and nicotine *per se* exert minor molecular effects on PSD molecules implicated in synaptic plasticity, schizophrenia pathophysiology, and antipsychotic treatment. However, these substances strongly affect haloperidol-mediated effects on these same molecules, with putative relevant pharmacological and clinical consequences potentially affecting treatment response and resistance to antipsychotics.

In the final set of experiments, the expression profile of the two IEGs *Homer1a* and *Arc*, together with the constitutive gene *Homer1b*, were evaluated in the context of a newly proposed pharmacologic treatment consisting of minocycline add-on to antipsychotics in a preclinical model. In this study, two pre-treatment groups were tested: drug-naïve (i.e. vehicle-pre-treated) rats *versus* ketamine-pre-treated rats. Indeed, ketamine has been reported to induce behavioral and

neurochemical outcomes reminiscent of psychosis (Iasevoli et al., 2014a; Krystal et al., 1994; Newcomer et al., 1999) and according to previously published reports, acute ketamine administration can be regarded as a valuable and heuristic preclinical model of psychosis (Lipska and Weinberger, 2000).

The main findings of this set of experiments was that the above mentioned IEGs were significantly and differentially modulated by the psychoactive treatments administered, while no effects of the different pharmacological manipulations were observed in regards to the constitutive *Homer1b* gene (Buonaguro et al., 2017b).

Particularly, it was observed that minocycline add-on to haloperidol blunted the haloperidol-mediated expression of *Arc* gene in both cortical and subcortical regions. These results could suggest that minocycline add-on to haloperidol could impact the glutamate signaling pathway through the modulation of *Arc* gene expression. Indeed, *Arc* has been found to promote the endocytosis of AMPA receptors (Chowdhury et al., 2006; Shepherd and Bear, 2011), while the compound tested herein has been found to increase membrane localization and phosphorylation of AMPA receptor (Imbesi et al., 2008), which turns in an increase of glutamatergic activity and modulation of neuroplasticity (Wang et al., 2005). Since *Arc* expression was reduced by minocycline when the compound was given as an add-on, the combination with antipsychotics may potentiate minocycline-mediated effects on AMPA-dependent glutamate signaling. To note, mice lacking GluR1 AMPA receptors have been reported to exhibit schizophrenia-like behaviors (Wiedholz et al., 2008), and drugs that act as positive modulators of these receptors have been reported to show precognitive effects and have been proposed as therapeutic strategies for schizophrenia (de Bartolomeis et al., 2012; Woolley et al., 2009). These observations may be regarded as a putative molecular rationale for the reported pro-cognitive action of minocycline when given as an add-on to antipsychotics (Levkovitz et al., 2010).

Conversely, in the case of *Homer1a*, the administration of minocycline as an add-on to haloperidol

did not shown to impact *Homer1a* mRNA levels differentially from the administration of haloperidol alone. As already stated before, *Homer1a* expression has been found to be elicited by glutamatergic and dopaminergic stimuli with a key role in synaptic downscaling and reduction of neural excitability (Hu et al., 2010; Li et al., 2013; Siddoway et al., 2014). Nevertheless, it could be speculated that that the antibiotic tested herein alone and in combination with a first-generation antipsychotic impacts the architecture of the synapse more likely acting on *Arc* signaling pathway rather than on the Homer family of transcripts. Indeed, the results of the present study show that *Homer1b* mRNA levels were not modulated by the treatments tested herein.

These results may represent the first step in elucidating potential changes of postsynaptic molecules after minocycline treatment in naïve and ketamine pre-treated animals (Buonaguro et al., 2017b). Minocycline may exert complex molecular actions on glutamate receptors and their post-synaptic effectors. In general, minocycline has been reported to reduce NMDA receptors-mediated transmission and may reinforce AMPA receptors- and possibly mGluR-mediated signaling, which may have a 'recovering' effect on the glutamatergic synapse, in conditions of excitotoxicity or NMDA receptor blockade, respectively. These effects could be mirrored by the activation of specific intracellular signaling pathways, as that of *Arc*, and the modulatory action of minocycline on glutamatergic transmission may support, from a molecular point of view, its use in combination with conventional antidopaminergic compounds in TRS patients (Kelly et al., 2015; Oya et al., 2014; Qurashi et al., 2014).

2. Concluding remarks

With respect to the pathogenesis and treatment, schizophrenia and psychoses in general still remain 'the big enigma of psychiatry' (O'Tuathaigh et al., 2017; Pull, 1981). Among the different methodologies possibly being applied to the study of the biological aspects of the disease, research on PSD molecules modifications may represent one possibility to elucidate synaptic remodeling

processes at least after psychotropic drugs administration. PSD are placed at crucial crossroads for multiple receptor signaling involved in the mechanisms of action of the most frequently used psychopharmacologic drugs and their close intermingling receives, elaborates, and converges multiple signals to the appropriate nuclear targets, in order to finely modulate synaptic rearrangements in response to neural activity. However, PSD molecular mechanisms are so sophisticated and complex that their knowledge is only partial at the moment.

In the present work, we have pointed out that dose and duration of antipsychotics administration impact differentially the level and topography of these molecules expression, further reinforcing the concept of an essential role of PSD molecules in dendritic spines morphologic changes induced by long-term antipsychotic treatment (Buonaguro et al., 2017a; Buonaguro et al., 2017b). The administration of substances such as caffeine and nicotine together with the well-characterized first generation antipsychotic haloperidol also gave interesting results in terms of differential quantitative and spatial modulation of key PSD transcripts and proteins, with also different effects on behavioral outcomes. Moreover, the evaluation of the pattern of expression of PSD molecules has also been suggested to provide information on augmentation or association strategies. Indeed, we have shown that *Arc* expression is differentially modulated by haloperidol alone, or in association with minocycline, the synthetic second-generation tetracycline recently proposed as an adjunctive treatment mostly for negative symptoms of schizophrenia.

Overall, these reports suggest that PSD molecules are key actors in the mechanisms of action of psychotropic agents and their modulation may represent one of the ultimate biological steps responsible of pharmacological effects of these drugs. In these terms, PSD molecule modulation may characterize other recently proposed therapeutic agents (for example, the ones that act on glutamatergic transmission, such as: agonists at group 2/3 metabotropic glutamate receptors; positive allosteric modulators of type 5 metabotropic glutamate receptors; NMDA receptor modulators; AMPAkinases; or glycine transporter inhibitors). Notably, despite multiple technical concerns, some

recent clinical and preclinical studies have investigated the efficacy of cell permeable peptides (CPP) and small peptide inhibitors (SPI), which may specifically interact with PSD proteins, such as PSD-95 (Bach et al., 2012; Cook et al., 2012).

Thanks to the observations obtained so far on PSD molecules 'role in dopamine-glutamate interplay and their modulation after current therapeutics and other psychotropic drugs, further studies will putatively permit the development of "synapse-targeting" pharmacological strategies, which could finally and possibly target the resistant symptoms domains poorly impacted by available psychopharmacologic treatment.

BIBLIOGRAPHY

- Abi-Dargham, A., Moore, H., 2003. Prefrontal DA transmission at D1 receptors and the pathology of schizophrenia. *Neuroscientist* 9(5), 404-416.
- Acuna-Lizama, M.M., Bata-Garcia, J.L., Alvarez-Cervera, F.J., Gongora-Alfaro, J.L., 2013. Caffeine has greater potency and efficacy than theophylline to reverse the motor impairment caused by chronic but not acute interruption of striatal dopaminergic transmission in rats. *Neuropharmacology* 70, 51-62.
- Adembri, C., Selmi, V., Vitali, L., Tani, A., Margheri, M., Loriga, B., Carlucci, M., Nosi, D., Formigli, L., De Gaudio, A.R., 2014. Minocycline but not tigecycline is neuroprotective and reduces the neuroinflammatory response induced by the superimposition of sepsis upon traumatic brain injury. *Crit Care Med* 42(8), e570-582.
- Alberati, D., Moreau, J.L., Lengyel, J., Hauser, N., Mory, R., Borroni, E., Pinard, E., Knoflach, F., Schlotterbeck, G., Hainzl, D., Wettstein, J.G., 2012. Glycine reuptake inhibitor RG1678: a pharmacologic characterization of an investigational agent for the treatment of schizophrenia. *Neuropharmacology* 62(2), 1152-1161.
- Ambesi-Impiombato, A., D'Urso, G., Muscettola, G., de Bartolomeis, A., 2003. Method for quantitative in situ hybridization histochemistry and image analysis applied for Homer1a gene expression in rat brain. *Brain Res Brain Res Protoc* 11(3), 189-196.
- Ambesi-Impiombato, A., Panariello, F., Dell'aversano, C., Tomasetti, C., Muscettola, G., de Bartolomeis, A., 2007. Differential expression of Homer 1 gene by acute and chronic administration of antipsychotics and dopamine transporter inhibitors in the rat forebrain. *Synapse* 61(6), 429-439.
- Bach, A., Clausen, B.H., Moller, M., Vestergaard, B., Chi, C.N., Round, A., Sorensen, P.L., Nissen, K.B., Kastrup, J.S., Gajhede, M., Jemth, P., Kristensen, A.S., Lundstrom, P., Lambertsen, K.L., Stromgaard, K., 2012. A high-affinity, dimeric inhibitor of PSD-95 bivalently interacts with PDZ1-2 and protects against ischemic brain damage. *Proc Natl Acad Sci U S A* 109(9), 3317-3322.
- Bayes, A., van de Lagemaat, L.N., Collins, M.O., Croning, M.D., Whittle, I.R., Choudhary, J.S., Grant, S.G., 2011. Characterization of the proteome, diseases and evolution of the human postsynaptic density. *Nat Neurosci* 14(1), 19-21.
- Beaulieu, J.M., Gainetdinov, R.R., 2011. The physiology, signaling, and pharmacology of dopamine receptors. *Pharmacol Rev* 63(1), 182-217.
- Beneyto, M., Kristiansen, L.V., Oni-Orisan, A., McCullumsmith, R.E., Meador-Woodruff, J.H., 2007. Abnormal glutamate receptor expression in the medial temporal lobe in schizophrenia and mood disorders. *Neuropsychopharmacology* 32(9), 1888-1902.
- Beneyto, M., Meador-Woodruff, J.H., 2008. Lamina-specific abnormalities of NMDA receptor-associated postsynaptic protein transcripts in the prefrontal cortex in schizophrenia and bipolar disorder. *Neuropsychopharmacology* 33(9), 2175-2186.
- Bertaso, F., Roussignol, G., Worley, P., Bockaert, J., Fagni, L., Ango, F., 2010. Homer1a-dependent crosstalk between NMDA and metabotropic glutamate receptors in mouse neurons. *PLoS One* 5(3), e9755.
- Bloomer, W.A., VanDongen, H.M., VanDongen, A.M., 2007. Activity-regulated cytoskeleton-associated protein Arc/Arg3.1 binds to spectrin and associates with nuclear promyelocytic leukemia (PML) bodies. *Brain Res* 1153, 20-33.
- Boeckers, T.M., Bockmann, J., Kreutz, M.R., Gundelfinger, E.D., 2002. ProSAP/Shank proteins - a family of higher order organizing molecules of the postsynaptic density with an emerging role in human neurological disease. *J Neurochem* 81(5), 903-910.

Bottai, D., Guzowski, J.F., Schwarz, M.K., Kang, S.H., Xiao, B., Lanahan, A., Worley, P.F., Seeburg, P.H., 2002. Synaptic activity-induced conversion of intronic to exonic sequence in Homer 1 immediate early gene expression. *J Neurosci* 22(1), 167-175.

Buonaguro, E.F., Iasevoli, F., Marmo, F., Eramo, A., Latte, G., Avagliano, C., Tomasetti, C., de Bartolomeis, A., 2017a. Re-arrangements of gene transcripts at glutamatergic synapses after prolonged treatments with antipsychotics: A putative link with synaptic remodeling. *Prog Neuropsychopharmacol Biol Psychiatry* 76, 29-41.

Buonaguro, E.F., Tomasetti, C., Chiodini, P., Marmo, F., Latte, G., Rossi, R., Avvisati, L., Iasevoli, F., de Bartolomeis, A., 2017b. Postsynaptic density protein transcripts are differentially modulated by minocycline alone or in add-on to haloperidol: Implications for treatment resistant schizophrenia. *J Psychopharmacol* 31(4), 406-417.

Bye, N., Habgood, M.D., Callaway, J.K., Malakooti, N., Potter, A., Kossmann, T., Morganti-Kossmann, M.C., 2007. Transient neuroprotection by minocycline following traumatic brain injury is associated with attenuated microglial activation but no changes in cell apoptosis or neutrophil infiltration. *Exp Neurol* 204(1), 220-233.

Bymaster, F.P., Calligaro, D.O., Falcone, J.F., Marsh, R.D., Moore, N.A., Tye, N.C., Seeman, P., Wong, D.T., 1996. Radioreceptor binding profile of the atypical antipsychotic olanzapine. *Neuropsychopharmacology* 14(2), 87-96.

Chaki, S., Hikichi, H., 2011. Targeting of metabotropic glutamate receptors for the treatment of schizophrenia. *Curr Pharm Des* 17(2), 94-102.

Chaudhry, I.B., Hallak, J., Husain, N., Minhas, F., Stirling, J., Richardson, P., Dursun, S., Dunn, G., Deakin, B., 2012. Minocycline benefits negative symptoms in early schizophrenia: a randomised double-blind placebo-controlled clinical trial in patients on standard treatment. *J Psychopharmacol* 26(9), 1185-1193.

Chaves, C., de Marque, C.R., Wichert-Ana, L., Maia-de-Oliveira, J.P., Itikawa, E.N., Crippa, J.A., Zuardi, A.W., Todd, K.G., Baker, G.B., Dursun, S.M., Hallak, J.E., 2010. Functional neuroimaging of minocycline's effect in a patient with schizophrenia. *Prog Neuropsychopharmacol Biol Psychiatry* 34(3), 550-552.

Chaves, C., Marque, C.R., Maia-de-Oliveira, J.P., Wichert-Ana, L., Ferrari, T.B., Santos, A.C., Araujo, D., Machado-de-Sousa, J.P., Bressan, R.A., Elkis, H., Crippa, J.A., Guimaraes, F.S., Zuardi, A.W., Baker, G.B., Dursun, S.M., Hallak, J.E., 2015. Effects of minocycline add-on treatment on brain morphometry and cerebral perfusion in recent-onset schizophrenia. *Schizophr Res* 161(2-3), 439-445.

Chen, J.F., Moratalla, R., Impagnatiello, F., Grandy, D.K., Cuellar, B., Rubinstein, M., Beilstein, M.A., Hackett, E., Fink, J.S., Low, M.J., Ongini, E., Schwarzschild, M.A., 2001. The role of the D(2) dopamine receptor (D(2)R) in A(2A) adenosine receptor (A(2A)R)-mediated behavioral and cellular responses as revealed by A(2A) and D(2) receptor knockout mice. *Proc Natl Acad Sci U S A* 98(4), 1970-1975.

Cheng, M.C., Lu, C.L., Luu, S.U., Tsai, H.M., Hsu, S.H., Chen, T.T., Chen, C.H., 2010. Genetic and functional analysis of the DLG4 gene encoding the post-synaptic density protein 95 in schizophrenia. *PLoS One* 5(12), e15107.

Chowdhury, S., Shepherd, J.D., Okuno, H., Lyford, G., Petralia, R.S., Plath, N., Kuhl, D., Huganir, R.L., Worley, P.F., 2006. Arc/Arg3.1 interacts with the endocytic machinery to regulate AMPA receptor trafficking. *Neuron* 52(3), 445-459.

Ciruela, F., Casado, V., Rodrigues, R.J., Lujan, R., Burgueno, J., Canals, M., Borycz, J., Rebola, N., Goldberg, S.R., Mallol, J., Cortes, A., Canela, E.I., Lopez-Gimenez, J.F., Milligan, G., Lluís, C., Cunha, R.A., Ferre, S., Franco, R., 2006. Presynaptic control of striatal glutamatergic neurotransmission by adenosine A1-A2A receptor heteromers. *J Neurosci* 26(7), 2080-2087.

Clinton, S.M., Haroutunian, V., Davis, K.L., Meador-Woodruff, J.H., 2003. Altered transcript expression of NMDA receptor-associated postsynaptic proteins in the thalamus of subjects with schizophrenia. *Am J Psychiatry* 160(6), 1100-1109.

Cohen, A., George, O., 2013. Animal models of nicotine exposure: relevance to second-hand smoking, electronic cigarette use, and compulsive smoking. *Front Psychiatry* 4, 41.

Collins, M.O., Husi, H., Yu, L., Brandon, J.M., Anderson, C.N., Blackstock, W.P., Choudhary, J.S., Grant, S.G., 2006. Molecular characterization and comparison of the components and multiprotein complexes in the postsynaptic proteome. *J Neurochem* 97 Suppl 1, 16-23.

Cook, D.J., Teves, L., Tymianski, M., 2012. Treatment of stroke with a PSD-95 inhibitor in the gyrencephalic primate brain. *Nature* 483(7388), 213-217.

Cope, Z.A., Powell, S.B., Young, J.W., 2016. Modeling neurodevelopmental cognitive deficits in tasks with cross-species translational validity. *Genes Brain Behav* 15(1), 27-44.

Corbett, R., Camacho, F., Woods, A.T., Kerman, L.L., Fishkin, R.J., Brooks, K., Dunn, R.W., 1995. Antipsychotic agents antagonize non-competitive N-methyl-D-aspartate antagonist-induced behaviors. *Psychopharmacology (Berl)* 120(1), 67-74.

Correll, C.U., 2010. From receptor pharmacology to improved outcomes: individualising the selection, dosing, and switching of antipsychotics. *Eur Psychiatry* 25 Suppl 2, S12-21.

Corti, C., Crepaldi, L., Mion, S., Roth, A.L., Xuereb, J.H., Ferraguti, F., 2007. Altered dimerization of metabotropic glutamate receptor 3 in schizophrenia. *Biol Psychiatry* 62(7), 747-755.

Coyle, J.T., Basu, A., Benneyworth, M., Balu, D., Konopaske, G., 2012. Glutamatergic synaptic dysregulation in schizophrenia: therapeutic implications. *Handb Exp Pharmacol*(213), 267-295.

Dani, J.A., Bertrand, D., 2007. Nicotinic acetylcholine receptors and nicotinic cholinergic mechanisms of the central nervous system. *Annu Rev Pharmacol Toxicol* 47, 699-729.

Dassesse, D., Vanderwinden, J.M., Goldberg, I., Vanderhaeghen, J.J., Schiffmann, S.N., 1999. Caffeine-mediated induction of c-fos, zif-268 and arc expression through A1 receptors in the striatum: different interactions with the dopaminergic system. *Eur J Neurosci* 11(9), 3101-3114.

de Bartolomeis, A., Aloj, L., Ambesi-Impiombato, A., Bravi, D., Caraco, C., Muscettola, G., Barone, P., 2002. Acute administration of antipsychotics modulates Homer striatal gene expression differentially. *Brain Res Mol Brain Res* 98(1-2), 124-129.

de Bartolomeis, A., Balletta, R., Giordano, S., Buonaguro, E.F., Latte, G., Iasevoli, F., 2013a. Differential cognitive performances between schizophrenic responders and non-responders to antipsychotics: correlation with course of the illness, psychopathology, attitude to the treatment and antipsychotics doses. *Psychiatry Res* 210(2), 387-395.

de Bartolomeis, A., Buonaguro, E.F., Iasevoli, F., Tomasetti, C., 2014. The emerging role of dopamine-glutamate interaction and of the postsynaptic density in bipolar disorder pathophysiology: Implications for treatment. *J Psychopharmacol* 28(6), 505-526.

de Bartolomeis, A., Fiore, G., Iasevoli, F., 2005. Dopamine-glutamate interaction and antipsychotics mechanism of action: implication for new pharmacological strategies in psychosis. *Curr Pharm Des* 11(27), 3561-3594.

de Bartolomeis, A., Iasevoli, F., 2003. The Homer family and the signal transduction system at glutamatergic postsynaptic density: potential role in behavior and pharmacotherapy. *Psychopharmacol Bull* 37(3), 51-83.

de Bartolomeis, A., Iasevoli, F., Marmo, F., Buonaguro, E.F., Eramo, A., Rossi, R., Avvisati, L., Latte, G., Tomasetti, C., 2015. Progressive recruitment of cortical and striatal regions by inducible postsynaptic density transcripts after increasing doses of antipsychotics with different receptor profiles: insights for psychosis treatment. *Eur Neuropsychopharmacol* 25(4), 566-582.

de Bartolomeis, A., Marmo, F., Buonaguro, E.F., Latte, G., Tomasetti, C., Iasevoli, F., 2016. Switching antipsychotics: Imaging the differential effect on the topography of postsynaptic density transcripts in antipsychotic-naive vs. antipsychotic-exposed rats. *Prog Neuropsychopharmacol Biol Psychiatry* 70, 24-38.

de Bartolomeis, A., Marmo, F., Buonaguro, E.F., Rossi, R., Tomasetti, C., Iasevoli, F., 2013b. Imaging brain gene expression profiles by antipsychotics: region-specific action of amisulpride on postsynaptic density transcripts compared to haloperidol. *Eur Neuropsychopharmacol* 23(11), 1516-1529.

de Bartolomeis, A., Sarappa, C., Buonaguro, E.F., Marmo, F., Eramo, A., Tomasetti, C., Iasevoli, F., 2013c. Different effects of the NMDA receptor antagonists ketamine, MK-801, and memantine on postsynaptic density transcripts and their topography: role of Homer signaling, and implications for novel antipsychotic and pro-cognitive targets in psychosis. *Prog Neuropsychopharmacol Biol Psychiatry* 46, 1-12.

de Bartolomeis, A., Sarappa, C., Magara, S., Iasevoli, F., 2012. Targeting glutamate system for novel antipsychotic approaches: relevance for residual psychotic symptoms and treatment resistant schizophrenia. *Eur J Pharmacol* 682(1-3), 1-11.

Dosemeci, A., Makusky, A.J., Jankowska-Stephens, E., Yang, X., Slotta, D.J., Markey, S.P., 2007. Composition of the synaptic PSD-95 complex. *Mol Cell Proteomics* 6(10), 1749-1760.

Dunlop, J., Brandon, N.J., 2015. Schizophrenia drug discovery and development in an evolving era: are new drug targets fulfilling expectations? *J Psychopharmacol* 29(2), 230-238.

Fatemi, S.H., Reutiman, T.J., Folsom, T.D., Bell, C., Nos, L., Fried, P., Pearce, D.A., Singh, S., Siderovski, D.P., Willard, F.S., Fukuda, M., 2006. Chronic olanzapine treatment causes differential expression of genes in frontal cortex of rats as revealed by DNA microarray technique. *Neuropsychopharmacology* 31(9), 1888-1899.

Featherstone, R.E., Siegel, S.J., 2015. The Role of Nicotine in Schizophrenia. *Int Rev Neurobiol* 124, 23-78.

Ferre, S., 2016. Mechanisms of the psychostimulant effects of caffeine: implications for substance use disorders. *Psychopharmacology (Berl)* 233(10), 1963-1979.

Ferre, S., Sebastiao, A.M., 2016. Dissecting striatal adenosine-cannabinoid receptor interactions. New clues from rats over-expressing adenosine A2A receptors. *J Neurochem* 136(5), 897-899.

Franberg, O., Marcus, M.M., Ivanov, V., Schilstrom, B., Shahid, M., Svensson, T.H., 2009. Asenapine elevates cortical dopamine, noradrenaline and serotonin release. Evidence for activation of cortical and subcortical dopamine systems by different mechanisms. *Psychopharmacology (Berl)* 204(2), 251-264.

Franberg, O., Wiker, C., Marcus, M.M., Konradsson, A., Jardemark, K., Schilstrom, B., Shahid, M., Wong, E.H., Svensson, T.H., 2008. Asenapine, a novel psychopharmacologic agent: preclinical evidence for clinical effects in schizophrenia. *Psychopharmacology (Berl)* 196(3), 417-429.

Fumagalli, F., Frasca, A., Racagni, G., Riva, M.A., 2008. Dynamic regulation of glutamatergic postsynaptic activity in rat prefrontal cortex by repeated administration of antipsychotic drugs. *Mol Pharmacol* 73(5), 1484-1490.

Fuxe, K., Agnati, L.F., Jacobsen, K., Hillion, J., Canals, M., Torvinen, M., Tinner-Staines, B., Staines, W., Rosin, D., Terasmaa, A., Popoli, P., Leo, G., Vergoni, V., Lluís, C., Ciruela, F., Franco, R., Ferre, S., 2003. Receptor heteromerization in adenosine A2A receptor signaling: relevance for striatal function and Parkinson's disease. *Neurology* 61(11 Suppl 6), S19-23.

Gardoni, F., Marcello, E., Di Luca, M., 2009. Postsynaptic density-membrane associated guanylate kinase proteins (PSD-MAGUKs) and their role in CNS disorders. *Neuroscience* 158(1), 324-333.

Gaspar, P.A., Bustamante, M.L., Rojo, L.E., Martinez, A., 2012. From glutamatergic dysfunction to cognitive impairment: boundaries in the therapeutic of the schizophrenia. *Curr Pharm Biotechnol* 13(8), 1543-1548.

Ghanizadeh, A., Dehbozorgi, S., OmraniSigaroodi, M., Rezaei, Z., 2014. Minocycline as add-on treatment decreases the negative symptoms of schizophrenia; a randomized placebo-controlled clinical trial. *Recent Pat Inflamm Allergy Drug Discov* 8(3), 211-215.

Gold, M.G., 2012. A frontier in the understanding of synaptic plasticity: solving the structure of the postsynaptic density. *Bioessays* 34(7), 599-608.

- Green, M.F., 2006. Cognitive impairment and functional outcome in schizophrenia and bipolar disorder. *J Clin Psychiatry* 67 Suppl 9, 3-8; discussion 36-42.
- Gu, W.H., Yang, S., Shi, W.X., Jin, G.Z., Zhen, X.C., 2007. Requirement of PSD-95 for dopamine D1 receptor modulating glutamate NR1a/NR2B receptor function. *Acta Pharmacol Sin* 28(6), 756-762.
- Gupta, D.S., McCullumsmith, R.E., Beneyto, M., Haroutunian, V., Davis, K.L., Meador-Woodruff, J.H., 2005. Metabotropic glutamate receptor protein expression in the prefrontal cortex and striatum in schizophrenia. *Synapse* 57(3), 123-131.
- Hallett, P.J., Spoelgen, R., Hyman, B.T., Standaert, D.G., Dunah, A.W., 2006. Dopamine D1 activation potentiates striatal NMDA receptors by tyrosine phosphorylation-dependent subunit trafficking. *J Neurosci* 26(17), 4690-4700.
- Halperin, R., Guerin, J.J., Jr., Davis, K.L., 1983. Chronic administration of three neuroleptics: effects of behavioral supersensitivity mediated by two different brain regions in the rat. *Life Sci* 33(6), 585-592.
- Hayashi, M.K., Tang, C., Verpelli, C., Narayanan, R., Stearns, M.H., Xu, R.M., Li, H., Sala, C., Hayashi, Y., 2009. The postsynaptic density proteins Homer and Shank form a polymeric network structure. *Cell* 137(1), 159-171.
- Ho, B.C., Andreasen, N.C., Ziebell, S., Pierson, R., Magnotta, V., 2011. Long-term antipsychotic treatment and brain volumes: a longitudinal study of first-episode schizophrenia. *Arch Gen Psychiatry* 68(2), 128-137.
- Hong, Q., Yang, L., Zhang, M., Pan, X.Q., Guo, M., Fei, L., Tong, M.L., Chen, R.H., Guo, X.R., Chi, X., 2013. Increased locomotor activity and non-selective attention and impaired learning ability in SD rats after lentiviral vector-mediated RNA interference of Homer 1a in the brain. *Int J Med Sci* 10(1), 90-102.
- Howes, O.D., Kapur, S., 2009. The dopamine hypothesis of schizophrenia: version III--the final common pathway. *Schizophr Bull* 35(3), 549-562.
- Howes, O.D., McCutcheon, R., Agid, O., de Bartolomeis, A., van Beveren, N.J., Birnbaum, M.L., Bloomfield, M.A., Bressan, R.A., Buchanan, R.W., Carpenter, W.T., Castle, D.J., Citrome, L., Daskalakis, Z.J., Davidson, M., Drake, R.J., Dursun, S., Ebdrup, B.H., Elkis, H., Falkai, P., Fleischacker, W.W., Gadelha, A., Gaughran, F., Glenthøj, B.Y., Graff-Guerrero, A., Hallak, J.E., Honer, W.G., Kennedy, J., Kinon, B.J., Lawrie, S.M., Lee, J., Leweke, F.M., MacCabe, J.H., McNabb, C.B., Meltzer, H., Moller, H.J., Nakajima, S., Pantelis, C., Reis Marques, T., Remington, G., Rossell, S.L., Russell, B.R., Siu, C.O., Suzuki, T., Sommer, I.E., Taylor, D., Thomas, N., Ukok, A., Umbricht, D., Walters, J.T., Kane, J., Correll, C.U., 2017. Treatment-Resistant Schizophrenia: Treatment Response and Resistance in Psychosis (TRRIP) Working Group Consensus Guidelines on Diagnosis and Terminology. *Am J Psychiatry* 174(3), 216-229.
- Hu, J.H., Park, J.M., Park, S., Xiao, B., Dehoff, M.H., Kim, S., Hayashi, T., Schwarz, M.K., Haganir, R.L., Seeburg, P.H., Linden, D.J., Worley, P.F., 2010. Homeostatic scaling requires group I mGluR activation mediated by Homer1a. *Neuron* 68(6), 1128-1142.
- Huang, M., Li, Z., Dai, J., Shahid, M., Wong, E.H., Meltzer, H.Y., 2008. Asenapine increases dopamine, norepinephrine, and acetylcholine efflux in the rat medial prefrontal cortex and hippocampus. *Neuropsychopharmacology* 33(12), 2934-2945.
- Hung, A.Y., Futai, K., Sala, C., Valtschanoff, J.G., Ryu, J., Woodworth, M.A., Kidd, F.L., Sung, C.C., Miyakawa, T., Bear, M.F., Weinberg, R.J., Sheng, M., 2008. Smaller dendritic spines, weaker synaptic transmission, but enhanced spatial learning in mice lacking Shank1. *J Neurosci* 28(7), 1697-1708.
- Iasevoli, F., Ambesi-Impiombato, A., Fiore, G., Panariello, F., Muscettola, G., de Bartolomeis, A., 2011a. Pattern of acute induction of Homer1a gene is preserved after chronic treatment with first- and second-generation antipsychotics: effect of short-term drug discontinuation and comparison with Homer1a-interacting genes. *J Psychopharmacol* 25(7), 875-887.

Iasevoli, F., Balletta, R., Gilardi, V., Giordano, S., de Bartolomeis, A., 2013a. Tobacco smoking in treatment-resistant schizophrenia patients is associated with impaired cognitive functioning, more severe negative symptoms, and poorer social adjustment. *Neuropsychiatr Dis Treat* 9, 1113-1120.

Iasevoli, F., Buonaguro, E.F., Sarappa, C., Marmo, F., Latte, G., Rossi, R., Eramo, A., Tomasetti, C., de Bartolomeis, A., 2014a. Regulation of postsynaptic plasticity genes' expression and topography by sustained dopamine perturbation and modulation by acute memantine: relevance to schizophrenia. *Prog Neuropsychopharmacol Biol Psychiatry* 54, 299-314.

Iasevoli, F., Cicale, M., Abbott, L.C., de Bartolomeis, A., 2011b. Striatal expression of Homer1a is affected by genotype but not dystonic phenotype of tottering mice: a model of spontaneously occurring motor disturbances. *Neurosci Lett* 503(3), 176-180.

Iasevoli, F., Fiore, G., Cicale, M., Muscettola, G., de Bartolomeis, A., 2010a. Haloperidol induces higher Homer1a expression than risperidone, olanzapine and sulpiride in striatal sub-regions. *Psychiatry Res* 177(1-2), 255-260.

Iasevoli, F., Polese, D., Ambesi-Impiombato, A., Muscettola, G., de Bartolomeis, A., 2007. Ketamine-related expression of glutamatergic postsynaptic density genes: possible implications in psychosis. *Neurosci Lett* 416(1), 1-5.

Iasevoli, F., Tomasetti, C., Buonaguro, E.F., de Bartolomeis, A., 2014b. The glutamatergic aspects of schizophrenia molecular pathophysiology: role of the postsynaptic density, and implications for treatment. *Curr Neuropharmacol* 12(3), 219-238.

Iasevoli, F., Tomasetti, C., de Bartolomeis, A., 2013b. Scaffolding proteins of the post-synaptic density contribute to synaptic plasticity by regulating receptor localization and distribution: relevance for neuropsychiatric diseases. *Neurochem Res* 38(1), 1-22.

Iasevoli, F., Tomasetti, C., Marmo, F., Bravi, D., Arnt, J., de Bartolomeis, A., 2010b. Divergent acute and chronic modulation of glutamatergic postsynaptic density genes expression by the antipsychotics haloperidol and sertindole. *Psychopharmacology (Berl)* 212(3), 329-344.

Imbesi, M., Uz, T., Manev, R., Sharma, R.P., Manev, H., 2008. Minocycline increases phosphorylation and membrane insertion of neuronal GluR1 receptors. *Neurosci Lett* 447(2-3), 134-137.

Javitt, D.C., 1987. Negative schizophrenic symptomatology and the PCP (phencyclidine) model of schizophrenia. *Hillside J Clin Psychiatry* 9(1), 12-35.

Javitt, D.C., 2010. Glutamatergic theories of schizophrenia. *Isr J Psychiatry Relat Sci* 47(1), 4-16.

Javitt, D.C., Zukin, S.R., 1991. Recent advances in the phencyclidine model of schizophrenia. *Am J Psychiatry* 148(10), 1301-1308.

Jentsch, J.D., Taylor, J.R., Roth, R.H., 1998. Subchronic phencyclidine administration increases mesolimbic dopaminergic system responsivity and augments stress- and psychostimulant-induced hyperlocomotion. *Neuropsychopharmacology* 19(2), 105-113.

Johansson, C., Jackson, D.M., Svensson, L., 1994. The atypical antipsychotic, remoxipride, blocks phencyclidine-induced disruption of prepulse inhibition in the rat. *Psychopharmacology (Berl)* 116(4), 437-442.

Kammermeier, P.J., 2008. Endogenous homer proteins regulate metabotropic glutamate receptor signaling in neurons. *J Neurosci* 28(34), 8560-8567.

Kapur, S., 2004. How antipsychotics become anti-"psychotic"--from dopamine to salience to psychosis. *Trends Pharmacol Sci* 25(8), 402-406.

Kapur, S., Barsoum, S.C., Seeman, P., 2000. Dopamine D(2) receptor blockade by haloperidol. (3)H-raclopride reveals much higher occupancy than EEDQ. *Neuropsychopharmacology* 23(5), 595-598.

Karam, C.S., Ballon, J.S., Bivens, N.M., Freyberg, Z., Girgis, R.R., Lizardi-Ortiz, J.E., Markx, S., Lieberman, J.A., Javitch, J.A., 2010. Signaling pathways in schizophrenia: emerging targets and therapeutic strategies. *Trends Pharmacol Sci* 31(8), 381-390.

Kelly, D.L., Sullivan, K.M., McEvoy, J.P., McMahan, R.P., Wehring, H.J., Gold, J.M., Liu, F., Warfel, D., Vyas, G., Richardson, C.M., Fischer, B.A., Keller, W.R., Koola, M.M., Feldman, S.M.,

Russ, J.C., Keefe, R.S., Osing, J., Hubzin, L., August, S., Walker, T.M., Buchanan, R.W., 2015. Adjunctive Minocycline in Clozapine-Treated Schizophrenia Patients With Persistent Symptoms. *J Clin Psychopharmacol* 35(4), 374-381.

Kelly, D.L., Vyas, G., Richardson, C.M., Koola, M., McMahon, R.P., Buchanan, R.W., Wehring, H.J., 2011. Adjunct minocycline to clozapine treated patients with persistent schizophrenia symptoms. *Schizophr Res* 133(1-3), 257-258.

Kesner, R.P., Hardy, J.D., Calder, L.D., 1981. Phencyclidine and behavior: I. Sensory-motor function, activity level, taste aversion and water intake. *Pharmacol Biochem Behav* 15(1), 7-13.

Kim, E., Sheng, M., 2004. PDZ domain proteins of synapses. *Nat Rev Neurosci* 5(10), 771-781.

Kim, J.S., Kornhuber, H.H., Brand, U., Menge, H.G., 1981. Effects of chronic amphetamine treatment on the glutamate concentration in cerebrospinal fluid and brain: implications for a theory of schizophrenia. *Neurosci Lett* 24(1), 93-96.

Konradi, C., Heckers, S., 2003. Molecular aspects of glutamate dysregulation: implications for schizophrenia and its treatment. *Pharmacol Ther* 97(2), 153-179.

Kontkanen, O., Lakso, M., Wong, G., Castren, E., 2002. Chronic antipsychotic drug treatment induces long-lasting expression of fos and jun family genes and activator protein 1 complex in the rat prefrontal cortex. *Neuropsychopharmacology* 27(2), 152-162.

Krystal, J.H., D'Souza, D.C., Mathalon, D., Perry, E., Belger, A., Hoffman, R., 2003. NMDA receptor antagonist effects, cortical glutamatergic function, and schizophrenia: toward a paradigm shift in medication development. *Psychopharmacology (Berl)* 169(3-4), 215-233.

Krystal, J.H., Karper, L.P., Seibyl, J.P., Freeman, G.K., Delaney, R., Bremner, J.D., Heninger, G.R., Bowers, M.B., Jr., Charney, D.S., 1994. Subanesthetic effects of the noncompetitive NMDA antagonist, ketamine, in humans. Psychotomimetic, perceptual, cognitive, and neuroendocrine responses. *Arch Gen Psychiatry* 51(3), 199-214.

Kumar, V., Fahey, P.G., Jong, Y.J., Ramanan, N., O'Malley, K.L., 2012. Activation of intracellular metabotropic glutamate receptor 5 in striatal neurons leads to up-regulation of genes associated with sustained synaptic transmission including Arc/Arg3.1 protein. *J Biol Chem* 287(8), 5412-5425.

Lahti, A.C., Holcomb, H.H., Medoff, D.R., Tamminga, C.A., 1995. Ketamine activates psychosis and alters limbic blood flow in schizophrenia. *Neuroreport* 6(6), 869-872.

Lahti, A.C., Weiler, M.A., Tamara Michaelidis, B.A., Parwani, A., Tamminga, C.A., 2001. Effects of ketamine in normal and schizophrenic volunteers. *Neuropsychopharmacology* 25(4), 455-467.

Lane, R.F., Blaha, C.D., 1987. Chronic haloperidol decreases dopamine release in striatum and nucleus accumbens in vivo: depolarization block as a possible mechanism of action. *Brain Res Bull* 18(1), 135-138.

Laruelle, M., Kegeles, L.S., Abi-Dargham, A., 2003. Glutamate, dopamine, and schizophrenia: from pathophysiology to treatment. *Ann N Y Acad Sci* 1003, 138-158.

Lee, F.J., Xue, S., Pei, L., Vukusic, B., Chery, N., Wang, Y., Wang, Y.T., Niznik, H.B., Yu, X.M., Liu, F., 2002. Dual regulation of NMDA receptor functions by direct protein-protein interactions with the dopamine D1 receptor. *Cell* 111(2), 219-230.

Lennertz, L., Wagner, M., Wolwer, W., Schuhmacher, A., Frommann, I., Berning, J., Schulze-Rauschenbach, S., Landsberg, M.W., Steinbrecher, A., Alexander, M., Franke, P.E., Pukrop, R., Ruhrmann, S., Bechdolf, A., Gaebel, W., Klosterkötter, J., Hafner, H., Maier, W., Mossner, R., 2012. A promoter variant of SHANK1 affects auditory working memory in schizophrenia patients and in subjects clinically at risk for psychosis. *Eur Arch Psychiatry Clin Neurosci* 262(2), 117-124.

Levkovitz, Y., Levi, U., Braw, Y., Cohen, H., 2007. Minocycline, a second-generation tetracycline, as a neuroprotective agent in an animal model of schizophrenia. *Brain Res* 1154, 154-162.

Levkovitz, Y., Mendlovich, S., Riwkes, S., Braw, Y., Levkovitch-Verbin, H., Gal, G., Fennig, S., Treves, I., Kron, S., 2010. A double-blind, randomized study of minocycline for the treatment of negative and cognitive symptoms in early-phase schizophrenia. *J Clin Psychiatry* 71(2), 138-149.

Li, Y., Abdourahman, A., Tamm, J.A., Pehrson, A.L., Sanchez, C., Gulinello, M., 2015. Reversal of age-associated cognitive deficits is accompanied by increased plasticity-related gene expression after chronic antidepressant administration in middle-aged mice. *Pharmacol Biochem Behav* 135, 70-82.

Li, Y., Popko, J., Krogh, K.A., Thayer, S.A., 2013. Epileptiform stimulus increases Homer 1a expression to modulate synapse number and activity in hippocampal cultures. *J Neurophysiol* 109(6), 1494-1504.

Lindenmayer, J.P., Khan, A., 2004. Pharmacological treatment strategies for schizophrenia. *Expert Rev Neurother* 4(4), 705-723.

Lipska, B.K., Weinberger, D.R., 2000. To model a psychiatric disorder in animals: schizophrenia as a reality test. *Neuropsychopharmacology* 23(3), 223-239.

Lominac, K.D., Oleson, E.B., Pava, M., Klugmann, M., Schwarz, M.K., Seeburg, P.H., Doring, M.J., Worley, P.F., Kalivas, P.W., Szumlanski, K.K., 2005. Distinct roles for different Homer1 isoforms in behaviors and associated prefrontal cortex function. *J Neurosci* 25(50), 11586-11594.

Lyddon, R., Navarrett, S., Dracheva, S., 2012. Ionotropic glutamate receptor mRNA editing in the prefrontal cortex: no alterations in schizophrenia or bipolar disorder. *J Psychiatry Neurosci* 37(4), 267-272.

Malhotra, A.K., Pinals, D.A., Adler, C.M., Elman, I., Clifton, A., Pickar, D., Breier, A., 1997. Ketamine-induced exacerbation of psychotic symptoms and cognitive impairment in neuroleptic-free schizophrenics. *Neuropsychopharmacology* 17(3), 141-150.

Mamo, D., Kapur, S., Shammi, C.M., Papatheodorou, G., Mann, S., Therrien, F., Remington, G., 2004. A PET study of dopamine D2 and serotonin 5-HT2 receptor occupancy in patients with schizophrenia treated with therapeutic doses of ziprasidone. *Am J Psychiatry* 161(5), 818-825.

Manago, F., Mereu, M., Mastwal, S., Mastrogiacomo, R., Scheggia, D., Emanuele, M., De Luca, M.A., Weinberger, D.R., Wang, K.H., Papaleo, F., 2016. Genetic Disruption of Arc/Arg3.1 in Mice Causes Alterations in Dopamine and Neurobehavioral Phenotypes Related to Schizophrenia. *Cell Rep* 16(8), 2116-2128.

Marcus, M.M., Bjorkholm, C., Malmerfelt, A., Moller, A., Pahlsson, N., Konradsson-Geuken, A., Feltmann, K., Jardemark, K., Schilström, B., Svensson, T.H., 2016. Alpha7 nicotinic acetylcholine receptor agonists and PAMs as adjunctive treatment in schizophrenia. An experimental study. *Eur Neuropsychopharmacol* 26(9), 1401-1411.

Marston, H.M., Young, J.W., Martin, F.D., Serpa, K.A., Moore, C.L., Wong, E.H., Gold, L., Meltzer, L.T., Azar, M.R., Geyer, M.A., Shahid, M., 2009. Asenapine effects in animal models of psychosis and cognitive function. *Psychopharmacology (Berl)* 206(4), 699-714.

McCullumsmith, R.E., Kristiansen, L.V., Beneyto, M., Scarr, E., Dean, B., Meador-Woodruff, J.H., 2007. Decreased NR1, NR2A, and SAP102 transcript expression in the hippocampus in bipolar disorder. *Brain Res* 1127(1), 108-118.

McIntyre, C.K., Miyashita, T., Setlow, B., Marjon, K.D., Steward, O., Guzowski, J.F., McGaugh, J.L., 2005. Memory-influencing intra-basolateral amygdala drug infusions modulate expression of Arc protein in the hippocampus. *Proc Natl Acad Sci U S A* 102(30), 10718-10723.

Meisenzahl, E.M., Schmitt, G., Grunder, G., Dresel, S., Frodl, T., la Fougere, C., Scheuerecker, J., Schwarz, M., Boerner, R., Stauss, J., Hahn, K., Moller, H.J., 2008. Striatal D2/D3 receptor occupancy, clinical response and side effects with amisulpride: an iodine-123-iodobenzamide SPET study. *Pharmacopsychiatry* 41(5), 169-175.

Misiak, B., Kiejna, A., Frydecka, D., 2015. Assessment of cigarette smoking status with respect to symptomatic manifestation in first-episode schizophrenia patients. *Compr Psychiatry* 58, 146-151.

Mizoguchi, H., Takuma, K., Fukakusa, A., Ito, Y., Nakatani, A., Ibi, D., Kim, H.C., Yamada, K., 2008. Improvement by minocycline of methamphetamine-induced impairment of recognition memory in mice. *Psychopharmacology (Berl)* 196(2), 233-241.

Montanaro, N., Dall'Olio, R., Gandolfi, O., Vaccheri, A., 1982. Differential enhancement of behavioral sensitivity to apomorphine following chronic treatment of rats with (-)-sulpiride and haloperidol. *Eur J Pharmacol* 81(1), 1-9.

Moreau, A.W., Kullmann, D.M., 2013. NMDA receptor-dependent function and plasticity in inhibitory circuits. *Neuropharmacology* 74, 23-31.

Newcomer, J.W., Farber, N.B., Jevtovic-Todorovic, V., Selke, G., Melson, A.K., Hershey, T., Craft, S., Olney, J.W., 1999. Ketamine-induced NMDA receptor hypofunction as a model of memory impairment and psychosis. *Neuropsychopharmacology* 20(2), 106-118.

Nunez, C., Stephan-Otto, C., Cuevas-Esteban, J., Maria Haro, J., Huerta-Ramos, E., Ochoa, S., Usall, J., Brebion, G., 2015. Effects of caffeine intake and smoking on neurocognition in schizophrenia. *Psychiatry Res* 230(3), 924-931.

O'Connor, J.A., Hemby, S.E., 2007. Elevated GRIA1 mRNA expression in Layer II/III and V pyramidal cells of the DLPFC in schizophrenia. *Schizophr Res* 97(1-3), 277-288.

O'Connor, J.A., Muly, E.C., Arnold, S.E., Hemby, S.E., 2007. AMPA receptor subunit and splice variant expression in the DLPFC of schizophrenic subjects and rhesus monkeys chronically administered antipsychotic drugs. *Schizophr Res* 90(1-3), 28-40.

O'Tuathaigh, C.M.P., Moran, P.M., Zhen, X.C., Waddington, J.L., 2017. Translating advances in the molecular basis of schizophrenia into novel cognitive treatment strategies. *Br J Pharmacol* 174(19), 3173-3190.

Oertel, W., Schulz, J.B., 2016. Current and experimental treatments of Parkinson disease: A guide for neuroscientists. *J Neurochem* 139 Suppl 1, 325-337.

Ohnuma, T., Kato, H., Arai, H., Faull, R.L., McKenna, P.J., Emson, P.C., 2000. Gene expression of PSD95 in prefrontal cortex and hippocampus in schizophrenia. *Neuroreport* 11(14), 3133-3137.

Okabe, S., 2007. Molecular anatomy of the postsynaptic density. *Mol Cell Neurosci* 34(4), 503-518.

Olney, J.W., Farber, N.B., 1995. Glutamate receptor dysfunction and schizophrenia. *Arch Gen Psychiatry* 52(12), 998-1007.

Olney, J.W., Newcomer, J.W., Farber, N.B., 1999. NMDA receptor hypofunction model of schizophrenia. *J Psychiatr Res* 33(6), 523-533.

Oya, K., Kishi, T., Iwata, N., 2014. Efficacy and tolerability of minocycline augmentation therapy in schizophrenia: a systematic review and meta-analysis of randomized controlled trials. *Hum Psychopharmacol* 29(5), 483-491.

Paxinos, G., Watson, C., 1997. *The rat brain, in stereotaxic coordinates*, Compact 3rd ed. Academic Press, San Diego.

Pechlivanova, D., Tchekalarova, J., Nikolov, R., Yakimova, K., 2010. Dose-dependent effects of caffeine on behavior and thermoregulation in a chronic unpredictable stress model of depression in rats. *Behav Brain Res* 209(2), 205-211.

Pidoplichko, V.I., DeBiasi, M., Williams, J.T., Dani, J.A., 1997. Nicotine activates and desensitizes midbrain dopamine neurons. *Nature* 390(6658), 401-404.

Polese, D., de Serpis, A.A., Ambesi-Impombato, A., Muscettola, G., de Bartolomeis, A., 2002. Homer 1a gene expression modulation by antipsychotic drugs: involvement of the glutamate metabotropic system and effects of D-cycloserine. *Neuropsychopharmacology* 27(6), 906-913.

Pratt, J., Winchester, C., Dawson, N., Morris, B., 2012. Advancing schizophrenia drug discovery: optimizing rodent models to bridge the translational gap. *Nat Rev Drug Discov* 11(7), 560-579.

Pull, C.B., 1981. [Depression and schizophrenia (author's transl)]. *Encephale* 7(4 Suppl), 343-346.

Qurashi, I., Collins, J.D., Chaudhry, I.B., Husain, N., 2014. Promising use of minocycline augmentation with clozapine in treatment-resistant schizophrenia. *J Psychopharmacol* 28(7), 707-708.

Rezvani, K., Teng, Y., Shim, D., De Biasi, M., 2007. Nicotine regulates multiple synaptic proteins by inhibiting proteasomal activity. *J Neurosci* 27(39), 10508-10519.

Rial, D., Lara, D.R., Cunha, R.A., 2014. The adenosine neuromodulation system in schizophrenia. *Int Rev Neurobiol* 119, 395-449.

Richardson-Burns, S.M., Haroutunian, V., Davis, K.L., Watson, S.J., Meador-Woodruff, J.H., 2000. Metabotropic glutamate receptor mRNA expression in the schizophrenic thalamus. *Biol Psychiatry* 47(1), 22-28.

Rosenbaum, G., Cohen, B.D., Luby, E.D., Gottlieb, J.S., Yelen, D., 1959. Comparison of sernyl with other drugs: simulation of schizophrenic performance with sernyl, LSD-25, and amobarbital (amytal) sodium; I. Attention, motor function, and proprioception. *AMA Arch Gen Psychiatry* 1, 651-656.

Roth, B.L., Hanizavareh, S.M., Blum, A.E., 2004. Serotonin receptors represent highly favorable molecular targets for cognitive enhancement in schizophrenia and other disorders. *Psychopharmacology (Berl)* 174(1), 17-24.

Sala, C., Futai, K., Yamamoto, K., Worley, P.F., Hayashi, Y., Sheng, M., 2003. Inhibition of dendritic spine morphogenesis and synaptic transmission by activity-inducible protein Homer1a. *J Neurosci* 23(15), 6327-6337.

Samaha, A.N., Seeman, P., Stewart, J., Rajabi, H., Kapur, S., 2007. "Breakthrough" dopamine supersensitivity during ongoing antipsychotic treatment leads to treatment failure over time. *J Neurosci* 27(11), 2979-2986.

Satow, A., Maehara, S., Ise, S., Hikichi, H., Fukushima, M., Suzuki, G., Kimura, T., Tanak, T., Ito, S., Kawamoto, H., Ohta, H., 2008. Pharmacological effects of the metabotropic glutamate receptor 1 antagonist compared with those of the metabotropic glutamate receptor 5 antagonist and metabotropic glutamate receptor 2/3 agonist in rodents: detailed investigations with a selective allosteric metabotropic glutamate receptor 1 antagonist, FTIDC [4-[1-(2-fluoropyridine-3-yl)-5-methyl-1H-1,2,3-triazol-4-yl]-N-isopropyl-N-methyl-1,3,6-dihydropyridine-1(2H)-carboxamide]. *J Pharmacol Exp Ther* 326(2), 577-586.

Scheidemantel, T., Korobkova, I., Rej, S., Sajatovic, M., 2015. Asenapine for bipolar disorder. *Neuropsychiatr Dis Treat* 11, 3007-3017.

Scott, L., Kruse, M.S., Forssberg, H., Brismar, H., Greengard, P., Aperia, A., 2002. Selective up-regulation of dopamine D1 receptors in dendritic spines by NMDA receptor activation. *Proc Natl Acad Sci U S A* 99(3), 1661-1664.

Seeman, P., 2009. Glutamate and dopamine components in schizophrenia. *J Psychiatry Neurosci* 34(2), 143-149.

Serchov, T., Clement, H.W., Schwarz, M.K., Iasevoli, F., Tosh, D.K., Idzko, M., Jacobson, K.A., de Bartolomeis, A., Normann, C., Biber, K., van Calker, D., 2015. Increased Signaling via Adenosine A1 Receptors, Sleep Deprivation, Imipramine, and Ketamine Inhibit Depressive-like Behavior via Induction of Homer1a. *Neuron* 87(3), 549-562.

Shahid, M., Walker, G.B., Zorn, S.H., Wong, E.H., 2009. Asenapine: a novel psychopharmacologic agent with a unique human receptor signature. *J Psychopharmacol* 23(1), 65-73.

Sheng, M., Hoogenraad, C.C., 2007. The postsynaptic architecture of excitatory synapses: a more quantitative view. *Annu Rev Biochem* 76, 823-847.

Shepherd, J.D., Bear, M.F., 2011. New views of Arc, a master regulator of synaptic plasticity. *Nat Neurosci* 14(3), 279-284.

Shiraishi-Yamaguchi, Y., Furuichi, T., 2007. The Homer family proteins. *Genome Biol* 8(2), 206.

Shiraishi, Y., Mizutani, A., Yuasa, S., Mikoshiba, K., Furuichi, T., 2003. Glutamate-induced declustering of post-synaptic adaptor protein Cupidin (Homer 2/vesl-2) in cultured cerebellar granule cells. *J Neurochem* 87(2), 364-376.

Siddoway, B., Hou, H., Xia, H., 2014. Molecular mechanisms of homeostatic synaptic downscaling. *Neuropharmacology* 78, 38-44.

Soloviev, M.M., Ciruela, F., Chan, W.Y., McIlhinney, R.A., 2000. Molecular characterisation of two structurally distinct groups of human homers, generated by extensive alternative splicing. *J Mol Biol* 295(5), 1185-1200.

Spellmann, I., Rujescu, D., Musil, R., Mayr, A., Giegling, I., Genius, J., Zill, P., Dehning, S., Opgen-Rhein, M., Cerovecki, A., Hartmann, A.M., Schafer, M., Bondy, B., Muller, N., Moller, H.J., Riedel, M., 2011. Homer-1 polymorphisms are associated with psychopathology and response to treatment in schizophrenic patients. *J Psychiatr Res* 45(2), 234-241.

Stroup, T.S., Gerhard, T., Crystal, S., Huang, C., Olfson, M., 2016. Comparative Effectiveness of Clozapine and Standard Antipsychotic Treatment in Adults With Schizophrenia. *Am J Psychiatry* 173(2), 166-173.

Sulzer, D., 2011. How addictive drugs disrupt presynaptic dopamine neurotransmission. *Neuron* 69(4), 628-649.

Szumliński, K.K., Kalivas, P.W., Worley, P.F., 2006. Homer proteins: implications for neuropsychiatric disorders. *Curr Opin Neurobiol* 16(3), 251-257.

Tandon, R., Nasrallah, H.A., Keshavan, M.S., 2009. Schizophrenia, "just the facts" 4. Clinical features and conceptualization. *Schizophr Res* 110(1-3), 1-23.

Tappe, A., Kuner, R., 2006. Regulation of motor performance and striatal function by synaptic scaffolding proteins of the Homer1 family. *Proc Natl Acad Sci U S A* 103(3), 774-779.

Tarazi, F.I., Moran-Gates, T., Wong, E.H., Henry, B., Shahid, M., 2008. Differential regional and dose-related effects of asenapine on dopamine receptor subtypes. *Psychopharmacology (Berl)* 198(1), 103-111.

Tarazi, F.I., Moran-Gates, T., Wong, E.H., Henry, B., Shahid, M., 2010. Asenapine induces differential regional effects on serotonin receptor subtypes. *J Psychopharmacol* 24(3), 341-348.

Tarazi, F.I., Neill, J.C., 2013. The preclinical profile of asenapine: clinical relevance for the treatment of schizophrenia and bipolar mania. *Expert Opin Drug Discov* 8(1), 93-103.

Thoma, P., Daum, I., 2013. Comorbid substance use disorder in schizophrenia: a selective overview of neurobiological and cognitive underpinnings. *Psychiatry Clin Neurosci* 67(6), 367-383.

Tomasetti, C., Dell'Aversano, C., Iasevoli, F., de Bartolomeis, A., 2007. Homer splice variants modulation within cortico-subcortical regions by dopamine D2 antagonists, a partial agonist, and an indirect agonist: implication for glutamatergic postsynaptic density in antipsychotics action. *Neuroscience* 150(1), 144-158.

Tomasetti, C., Dell'Aversano, C., Iasevoli, F., Marmo, F., de Bartolomeis, A., 2011. The acute and chronic effects of combined antipsychotic-mood stabilizing treatment on the expression of cortical and striatal postsynaptic density genes. *Prog Neuropsychopharmacol Biol Psychiatry* 35(1), 184-197.

Tricklebank, M.D., Singh, L., Oles, R.J., Preston, C., Iversen, S.D., 1989. The behavioural effects of MK-801: a comparison with antagonists acting non-competitively and competitively at the NMDA receptor. *Eur J Pharmacol* 167(1), 127-135.

Tsai, S.J., Hong, C.J., Cheng, C.Y., Liao, D.L., Liou, Y.J., 2007. Association study of polymorphisms in post-synaptic density protein 95 (PSD-95) with schizophrenia. *J Neural Transm (Vienna)* 114(4), 423-426.

Tu, J.C., Xiao, B., Naisbitt, S., Yuan, J.P., Petralia, R.S., Brakeman, P., Doan, A., Aakalu, V.K., Lanahan, A.A., Sheng, M., Worley, P.F., 1999. Coupling of mGluR/Homer and PSD-95 complexes by the Shank family of postsynaptic density proteins. *Neuron* 23(3), 583-592.

Tu, J.C., Xiao, B., Yuan, J.P., Lanahan, A.A., Leoffert, K., Li, M., Linden, D.J., Worley, P.F., 1998. Homer binds a novel proline-rich motif and links group 1 metabotropic glutamate receptors with IP3 receptors. *Neuron* 21(4), 717-726.

Turner, P.V., Brabb, T., Pekow, C., Vasbinder, M.A., 2011. Administration of substances to laboratory animals: routes of administration and factors to consider. *J Am Assoc Lab Anim Sci* 50(5), 600-613.

Verma, A., Moghaddam, B., 1996. NMDA receptor antagonists impair prefrontal cortex function as assessed via spatial delayed alternation performance in rats: modulation by dopamine. *J Neurosci* 16(1), 373-379.

Vessey, J.P., Karra, D., 2007. More than just synaptic building blocks: scaffolding proteins of the post-synaptic density regulate dendritic patterning. *J Neurochem* 102(2), 324-332.

Vita, A., De Peri, L., Deste, G., Barlati, S., Sacchetti, E., 2015. The Effect of Antipsychotic Treatment on Cortical Gray Matter Changes in Schizophrenia: Does the Class Matter? A Meta-analysis and Meta-regression of Longitudinal Magnetic Resonance Imaging Studies. *Biol Psychiatry* 78(6), 403-412.

Wang, A.L., Yu, A.C., Lau, L.T., Lee, C., Wu le, M., Zhu, X., Tso, M.O., 2005. Minocycline inhibits LPS-induced retinal microglia activation. *Neurochem Int* 47(1-2), 152-158.

Wang, Y., Rao, W., Zhang, C., Zhang, C., Liu, M.D., Han, F., Yao, L.B., Han, H., Luo, P., Su, N., Fei, Z., 2015. Scaffolding protein Homer1a protects against NMDA-induced neuronal injury. *Cell Death Dis* 6, e1843.

Weickert, C.S., Fung, S.J., Catts, V.S., Schofield, P.R., Allen, K.M., Moore, L.T., Newell, K.A., Pellen, D., Huang, X.F., Catts, S.V., Weickert, T.W., 2013. Molecular evidence of N-methyl-D-aspartate receptor hypofunction in schizophrenia. *Mol Psychiatry* 18(11), 1185-1192.

Weinberg, D., Lenroot, R., Jacomb, I., Allen, K., Bruggemann, J., Wells, R., Balzan, R., Liu, D., Galletly, C., Catts, S.V., Weickert, C.S., Weickert, T.W., 2016. Cognitive Subtypes of Schizophrenia Characterized by Differential Brain Volumetric Reductions and Cognitive Decline. *JAMA Psychiatry* 73(12), 1251-1259.

Weinberger, D.R., Harrison, P., 2011. *Schizophrenia*, 3rd Edition ed. Wiley-Blackwell.

Wiedholz, L.M., Owens, W.A., Horton, R.E., Feyder, M., Karlsson, R.M., Hefner, K., Sprengel, R., Celikel, T., Daws, L.C., Holmes, A., 2008. Mice lacking the AMPA GluR1 receptor exhibit striatal hyperdopaminergia and 'schizophrenia-related' behaviors. *Mol Psychiatry* 13(6), 631-640.

Wiescholleck, V., Manahan-Vaughan, D., 2013. Long-lasting changes in hippocampal synaptic plasticity and cognition in an animal model of NMDA receptor dysfunction in psychosis. *Neuropharmacology* 74, 48-58.

Willuhn, I., Sun, W., Steiner, H., 2003. Topography of cocaine-induced gene regulation in the rat striatum: relationship to cortical inputs and role of behavioural context. *Eur J Neurosci* 17(5), 1053-1066.

Wohr, M., Rouillet, F.I., Hung, A.Y., Sheng, M., Crawley, J.N., 2011. Communication impairments in mice lacking Shank1: reduced levels of ultrasonic vocalizations and scent marking behavior. *PLoS One* 6(6), e20631.

Woolley, M.L., Waters, K.A., Gartlon, J.E., Lacroix, L.P., Jennings, C., Shaughnessy, F., Ong, A., Pemberton, D.J., Harries, M.H., Southam, E., Jones, D.N., Dawson, L.A., 2009. Evaluation of the pro-cognitive effects of the AMPA receptor positive modulator, 5-(1-piperidinylcarbonyl)-2,1,3-benzoxadiazole (CX691), in the rat. *Psychopharmacology (Berl)* 202(1-3), 343-354.

Worley, P.F., Zeng, W., Huang, G., Kim, J.Y., Shin, D.M., Kim, M.S., Yuan, J.P., Kiselyov, K., Muallem, S., 2007. Homer proteins in Ca²⁺ signaling by excitable and non-excitable cells. *Cell Calcium* 42(4-5), 363-371.

Xiao, B., Tu, J.C., Petralia, R.S., Yuan, J.P., Doan, A., Breder, C.D., Ruggiero, A., Lanahan, A.A., Wenthold, R.J., Worley, P.F., 1998. Homer regulates the association of group 1 metabotropic glutamate receptors with multivalent complexes of homer-related, synaptic proteins. *Neuron* 21(4), 707-716.

Xiberas, X., Martinot, J.L., Mallet, L., Artiges, E., Loc, H.C., Maziere, B., Paillere-Martinot, M.L., 2001. Extrastriatal and striatal D(2) dopamine receptor blockade with haloperidol or new antipsychotic drugs in patients with schizophrenia. *Br J Psychiatry* 179, 503-508.

Xu, W., 2011. PSD-95-like membrane associated guanylate kinases (PSD-MAGUKs) and synaptic plasticity. *Curr Opin Neurobiol* 21(2), 306-312.

Yin, J., Barr, A.M., Ramos-Miguel, A., Procyshyn, R.M., 2017. Antipsychotic Induced Dopamine Supersensitivity Psychosis: A Comprehensive Review. *Curr Neuropharmacol* 15(1), 174-183.

- Zhang, J., Xu, T.X., Hallett, P.J., Watanabe, M., Grant, S.G., Isacson, O., Yao, W.D., 2009. PSD-95 uncouples dopamine-glutamate interaction in the D1/PSD-95/NMDA receptor complex. *J Neurosci* 29(9), 2948-2960.
- Zhang, L., Kitaichi, K., Fujimoto, Y., Nakayama, H., Shimizu, E., Iyo, M., Hashimoto, K., 2006a. Protective effects of minocycline on behavioral changes and neurotoxicity in mice after administration of methamphetamine. *Prog Neuropsychopharmacol Biol Psychiatry* 30(8), 1381-1393.
- Zhang, L., Shirayama, Y., Shimizu, E., Iyo, M., Hashimoto, K., 2006b. Protective effects of minocycline on 3,4-methylenedioxymethamphetamine-induced neurotoxicity in serotonergic and dopaminergic neurons of mouse brain. *Eur J Pharmacol* 544(1-3), 1-9.
- Zhang, P., Lisman, J.E., 2012. Activity-dependent regulation of synaptic strength by PSD-95 in CA1 neurons. *J Neurophysiol* 107(4), 1058-1066.